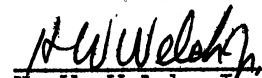ENGINEERING RESEARCH INSTITUTE
UNIVERSITY OF MICHIGAN
ANN ARBOR

INTERIM REPORT ON FERROELECTRIC MATERIALS AND THEIR APPLICATIONS

Technical Report No. 31
Electronic Defense Group
Department of Electrical Engineering

By: Howard Diamond
L. W. Orr

Approved by: _H. W. Welch, Jr._

Project 2262

TASK ORDER NO. EDG-4
CONTRACT NO. DA-36-039 sc-63203
SIGNAL CORPS, DEPARTMENT OF THE ARMY
DEPARTMENT OF ARMY PROJECT NO. 3-99-04-042
SIGNAL CORPS PROJECT NO. 194B

July, 1954

ensn

UMR1260

TABLE OF CONTENTS

LIST OF ILLUSTRATIONS

LIST OF ILLUSTRATIONS (Cont'd)

LIST OF TABLES

ABSTRACT

Results are given for a study of the basic properties
of ferroelectric materials and their applications to wide range
tuning devices. Data are presented on measurements of field
non-linearity of dielectric constant, hysteresis losses, high
frequency behavior, and the effect of electrode plating methods.
The results of quantitative measurements of the Barkhausen
noise in ferroelectric materials are also given.

Several local oscillator circuits employing dielectric
tuning are described and the results of tests made are tabulated.
Other applications discussed include a broadcast band dielectric
tuned receiver and an fm dielectric amplifier.

INTERIM REPORT ON FERROELECTRIC MATERIALS AND THEIR APPLICATIONS

1. INTRODUCTION

Ferroelectricity can be defined as that phenomenon, exhibited by certain materials, of having a permanent electric moment in the absence of an external electric field; that is, the phenomenon of ferroelectricity is the electric analog of ferromagnetism. It is found that all ferroelectric materials are piezoelectric but the converse is not necessarily true; quartz, for example, is piezoelectric but not ferroelectric. With the exception of the applications to dielectric amplifiers, the frequencies in which we are interested are much higher than those at which piezoelectric resonances are expected.

Anti-ferroelectricity can be defined as that property of certain materials of having a spontaneous polarization. However, in this case alternate lines of ions in the crystal lattice have opposite polarizations. These materials, in their anti-ferroelectric phase, do not exhibit hysteresis loops that are characteristic of ferroelectric materials. Certain perovskite materials, such as lead zirconate, are ferroelectric below a transition temperature and anti-ferroelectric above this transition, while at still higher temperatures the crystal becomes para electric (i.e. the crystal exhibits no spontaneous polarization).

Ferroelectric crystals fall into natural classes based upon their crystal structure and bond characteristics. These classes are:

a) Isomorphic hydrates such as rochelle salt. These have a complex crystal structure.

b) The potassium di-hydrogen phosphate type in which the crystal structure is also complex but the crystals are not hydrates.

c) Ionic type crystals such as barium titanate, which has the perovskite crystal structure.

Of the several classes of ferroelectric materials we have only used the third type. This has been examined both in the single crystal and ceramic forms. The ceramics have been supplied to us by several commercial manufacturers, with and without attached electrodes. The pure crystals of barium titanate were kindly furnished by the Bell Telephone Laboratories at Murray Hill, New Jersey.

Materials in the ferroelectric state show hysteresis loops and domain phenomena that are usually associated with ferromagnetism, and as in the magnetic case, the motion of the domains under an applied electric field gives rise to Barkhausen noise. The spontaneous polarization of barium titanate is of the order of 15 micro-coulombs per square centimeter. Barium titanate exists in three ferroelectric phases below its transition temperature. It is para-electric above the transition temperature.

During the period of work on materials of the barium-strontium titanate system, it was felt that as much information as possible should be gathered on ferroelectric materials outside of that system.

The characteristics of the barium-strontium titanate compositions have been fairly well investigated, and materials of these compostitions now find widespread use. Several manufacturers and investigators have recently turned their attention to ferroelectric compositions derived by replacing the barium or titanium in the barium titanate perovskite structure by other elements.

The published results of some of these experiments seem to indicate that there are mainly three points of view for developing these new materials.

1) The determination of lattice constants and phase behavior for theoretical considerations.

2) A program for developing high dielectric constant-low temperature coefficient or temperature compensating capacitors.

3) The development of transducer elements.

Unfortunately, very little has been published on the field non-linearity of dielectric constant for these materials, except what can be implied from published hysteresis loop data.

In mixed crystal ceramics such as barium-stronium titanate, there is no well-defined temperature at which the spontaneous polarization everywhere disappears. For the purpose of this report, the Curie temperature of mixed ceramics will therefore be defined as the temperature of maximum dielectric constant. The Curie temperatures of some typical ceramics that have been produced by several investigators are listed in Table I. Most of the listed compositions have been produced in order to study the phase behavior of the material rather than as non-linear dielectrics for specific applications.

Because of the large amount of active research in a rapidly expanding field and the rapid development of new ferroelectric materials, it must be pointed out that the conclusions drawn here must not be taken as final. Although the main objective of our research on ferroelectric materials is the application of these materials to electric tuning, we have, during this phase of our work, studied the basic properties of the materials in both the single crystal and ceramic form and in addition made several sample applications to other than tuned

TABLE I

RANGE OF CURIE TEMPERATURES FOR SOME FERROELECTRIC CERAMICS

Composition	Upper Curie Temperature[1]	Remarks
$BaTiO_3$ - $SrTiO_3$	120°C to -100°C	
$PbZrO_3$ - $PbTiO_3$	230°C to 500°C	The figure 500°C is for 10 mol per cent $PbZrO_3$. Below 10 per cent the composition is anti-ferroelectric.
$KNbO_3$ - $NaNbO_3$	435°C to 375°C	
$KNbO_3$ - $KTaO_3$	435°C to -268°C	Very similar to the Ba-Sr-TiO_3 system.
$BaZrO_3$ - $PbZrO_3$	?°C to 230°C	
$CdNbO_3$	160°C	Shows possibilities of replacing $BaTiO_3$ in transducers and for H.F. applications.
$EuTiO_3$	110°C	

[1]The upper Curie Temperatures are given for the respective end members of the system. As the composition is varied, the Curie Temperature changes monatonically between end member limits.

circuits. It was felt that this more general approach would be more desirable

than the specific one in dealing with the problems in a new field.

2. BASIC RESEARCH IN FERROELECTRIC MATERIALS

2.1 Electric Field Dependence of Capacity

The property of changing the incremental dielectric constant with an

applied biasing field, displayed by ferroelectric materials, allows their use

as a tuned element in frequency sensitive devices such as resonant tank circuits

and dielectric amplifiers. Therefore, in determining the applicability of ferro-

electric materials to wide range tuning of search receivers, it is necessary to

classify the presently available materials as to the degree of non-linearity.

2.1.1 Measuring Apparatus. Measurements were made of the incremental

dielectric constant or capacity as a function of a DC bias field.[1] The source

of the DC bias field was either a Dumont Model 263B ten kv power supply used

for the thick samples, or a battery stack used for thin samples. Measurements of

the incremental dielectric constant were made on the General Radio 650A impedance

bridge for 1000 cycles, on the Boonton 160A Q-meter for frequencies between 10 kc

and 50 mc, and on the Boonton 190A Q-meter for frequencies between 10 kc and

50 mc. Except for the measurements made with the high frequency Q-meter, all

samples were placed in an oil bath inside a Dewar flask in order to minimize the

errors due to temperature effects. The general set-up of the apparatus is shown

in Fig. 1.

---

[1]The measurements made by means of the equipment described in this section
were made by plotting the data point by point. A method for dynamic measurements
is described in Section 2.8, on Butterfly Loops, of this report.

FIG. 1
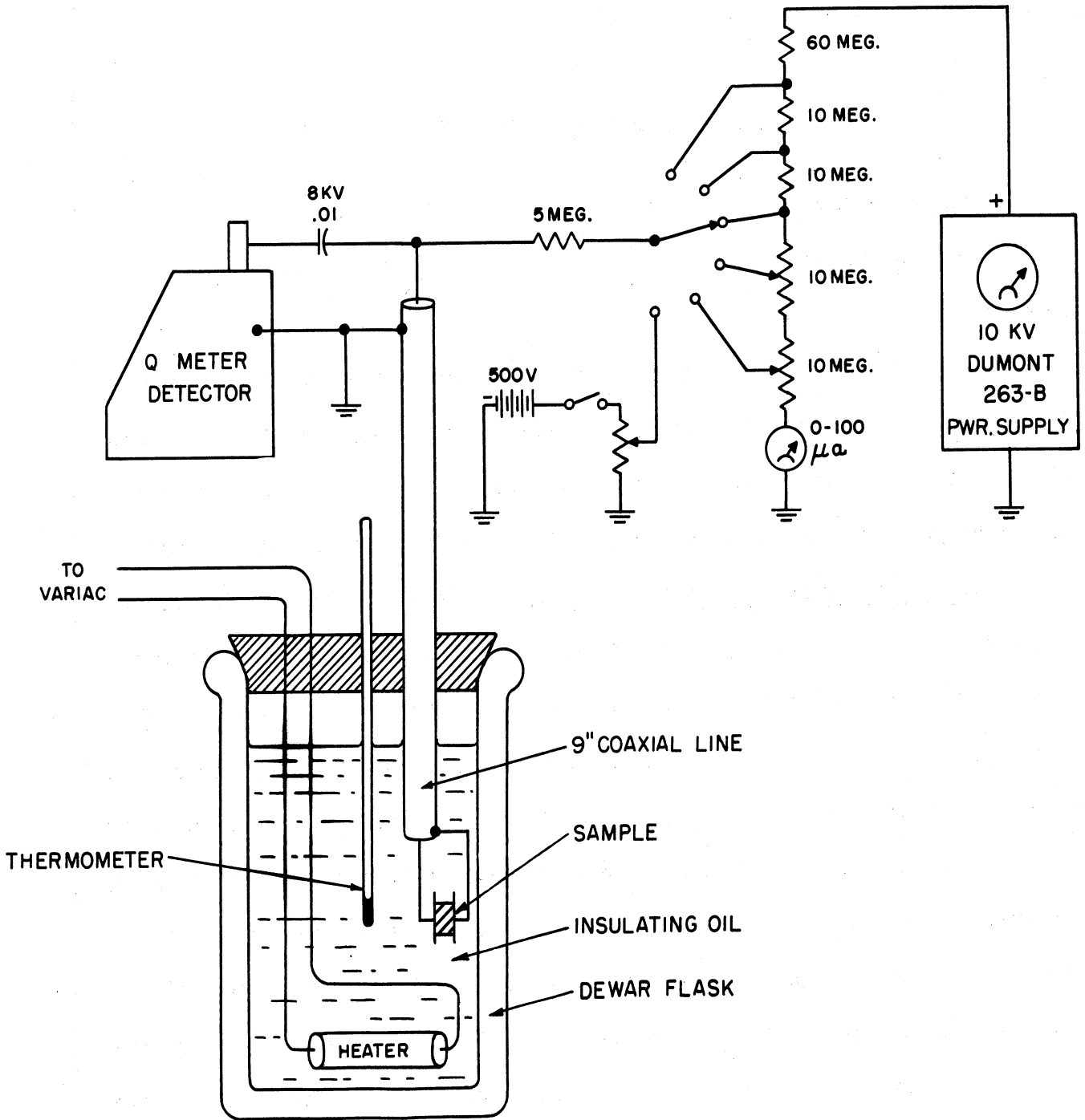
APPARATUS FOR MEASURING Q AND INCREMENTAL
DIELECTRIC CONSTANT, WITH VARYING D.C. BIAS FIELDS

6

2.1.2 Preparation of Samples. When extremely thin samples were being tested, a method that was found to be very satisfactory is to first plate the sample on both sides with silver electrodes using a vacuum evaporation process. The sheet is then fractured into small pieces. A suitable piece is chosen and the electrodes fitted with aluminum foil leads. These leads are attached with a silver conducting paint. The whole unit is "potted" in a small bead of polystyrene cement in order to provide mechanical strength and also to prevent an air-path arc at high fields. The finished unit, shown in Fig. 2b, is extremely small in size with a capacity of the order of $100\,\mu\mu f$. At the higher frequencies the inductance of the capacitor leads can result in considerable error in the capacity measurement, the more so, the greater the capacity to be measured. Thus it is necessary, using the described techniques, to mount the samples directly at the high frequency Q-meter terminals with only about one centimeter of total capacitor lead length. Moreover, it became necessary to construct some small low capacity condensers of the material being tested. The usual commercially prepared samples of the desired materials have a minimum capacity of about 200 $\mu\mu f$. It was desired to use a capacity of around $40\,\mu\mu f$ or less for the high frequency measurements. The low capacity units were constructed by chipping a titanate ceramic body which had been previously prepared with silvered electrodes. The chip is then provided with leads by "sweating" onto the silvered surfaces copper wires tinned with solder. The sides of the body are then ground with fine emery paper to the desired capacity. Figs. 2a and 2b show the construction of the completed test units for thick and thin materials respectively.

2.1.3 Results. The materials tested were commercially prepared titanate ceramic bodies. Figs. 3 and 4 show the ϵ_Δ - E curves for two typical

(a)

(b)
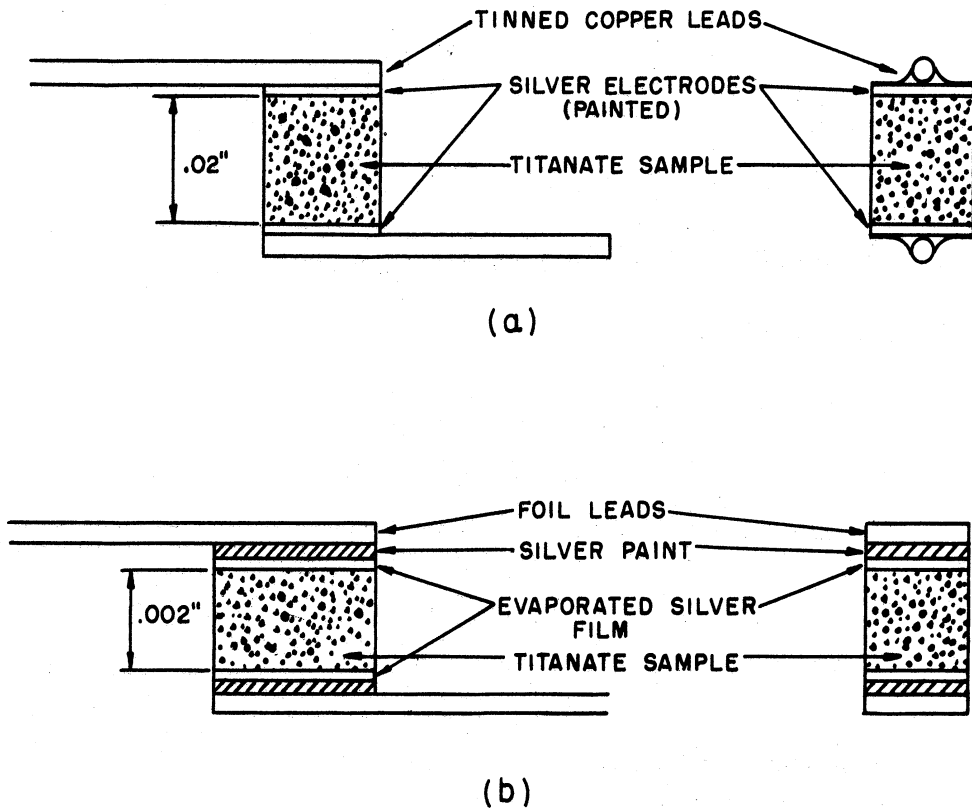
FIG. 2

CONSTRUCTION OF CAPACITORS USED
FOR HIGH FREQUENCY MEASUREMENTS.
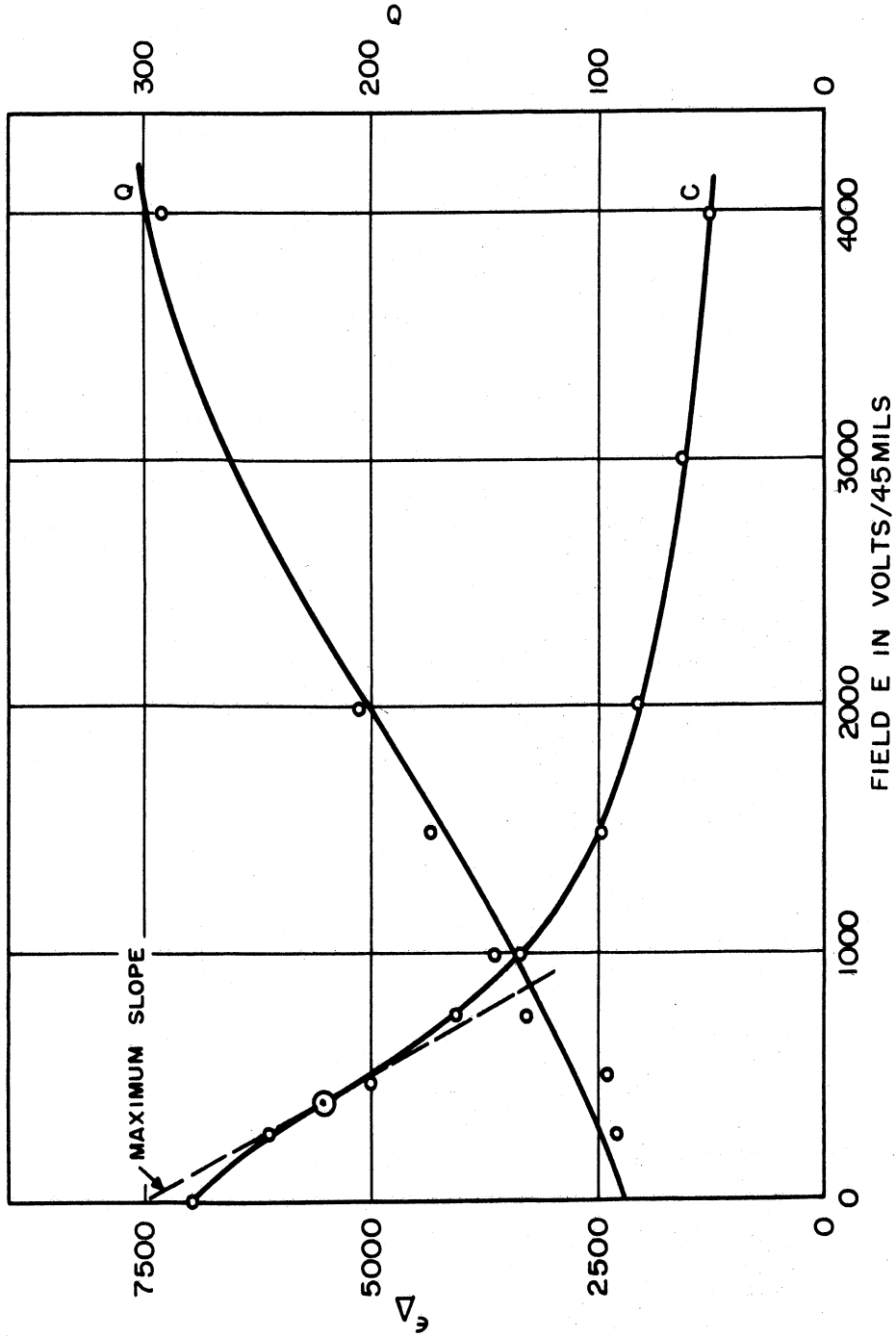
FIG. 3

A TYPICAL ϵ_Δ - E CURVE FOR AEROVOX BODY.
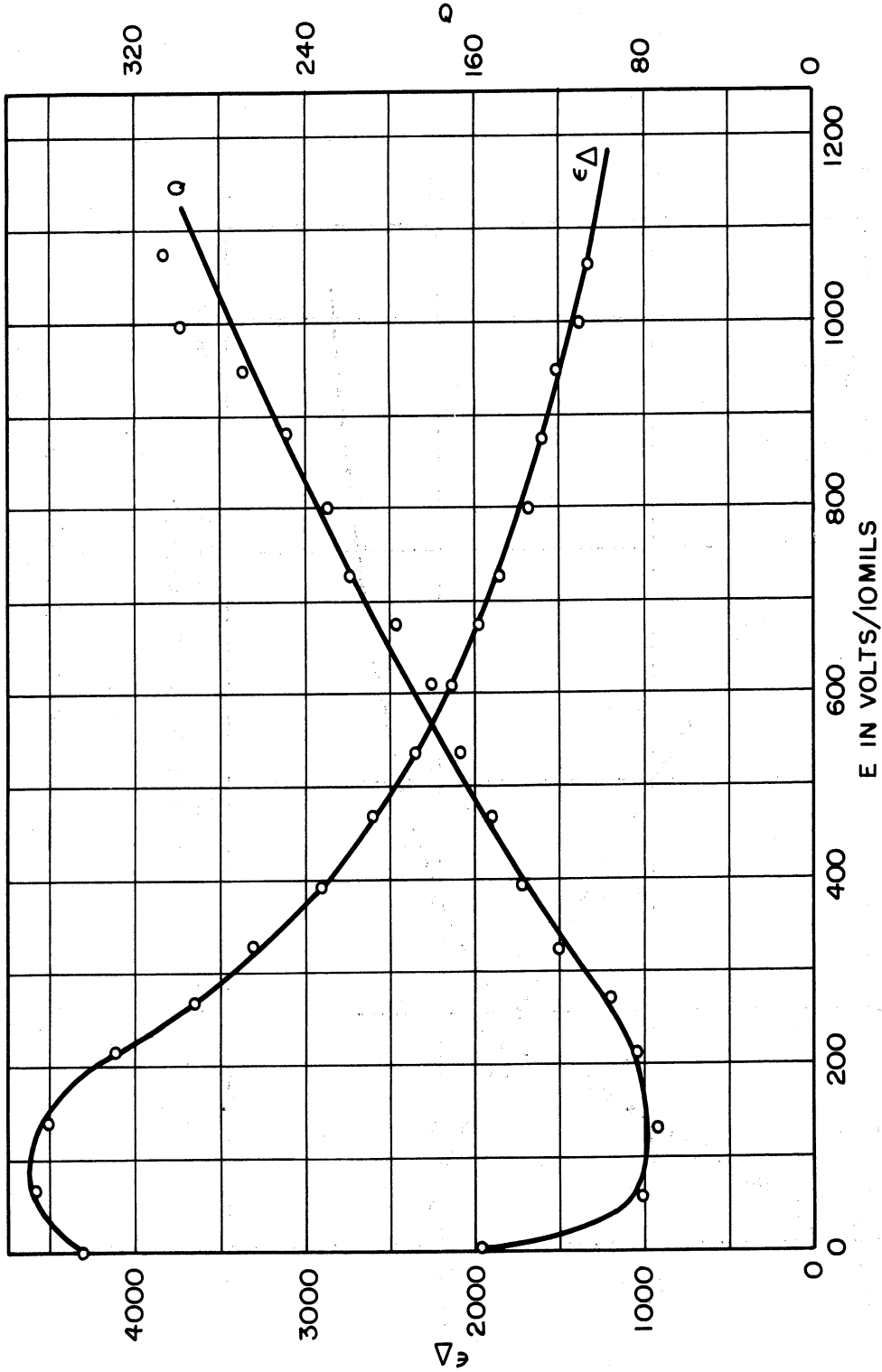
FIG. 4

ϵ_Δ-E CURVE FOR A CENTRALAB BODY D-31 CERAMIC.
A CASE IN WHICH THERE IS AN INITIAL RISE IN ϵ_Δ WITH E.

materials. An "S" or slope value is defined for the materials as the per centage change of the incremental capacity (or incremental dielectric constant) per unit change of field on the ϵ_Δ - E curve at the point of maximum slope. S has the units: "percent change per volt per mil." The point of maximum slope is shown in Fig. 3.

Thus:

$$S = \left[\frac{1}{\epsilon_\Delta} \cdot \frac{d\epsilon_\Delta}{dE} \right]_{max.} \tag{1}$$

We can define R as the ratio of maximum to minimum capacity with the minimum capacity being taken at the field of 100 volts per mil. Although the field of 100 volts per mil may seem rather severe it must be remembered that the titanate ceramics have extremely high dielectric strengths. With the proper precautions such as "potting" to prevent an air path breakdown, it is possible to use such fields in the applications. Table II shows the results for the materials checked. Note that the R and S values are correlated. It is also noted from data which will be shown in the next section, that the materials that have the greatest S values also are the most temperature sensitive. A good compromise between the desired field non-linearity of capacity and the undesired temperature effect is found in such bodies as the Glenco K-3300, which has a medium S value. Advantage may be taken of the materials with large R and S values if suitable thermostating or temperature compensation is employed. Thermostating should be very easily accomplished in a small package since the ferroelectric ceramic capacitors are typically very small for their values of capacity.

TABLE II

S AND R VALUES FOR COMMERCIAL CAPACITORS

Body and Mfg.	Plating	S in% Change/volt/mil	R
Sprague 200GA	Silk-screened conducting paint	-0.4	1.4
Glenco K-3300 3 mil stock	Hand painted	-0.6	2.
Centralab D-31	Vacuum deposited silver	-2.3	3.5
Sprague 120GA	Silk-screened conducting paint	-3.8	5.
Glenco K-3300	Silk-screened Conducting paint	-3.8	5.
Glenco K-3300 3 mil stock	Vacuum deposited silver	-2.4	4.5
Aerovox Hi-Q 41 *	Silk-screened conducting paint	-4.0	5.
Aerovox Hi-Q 40	Silk-screened conducting paint	-5.8	9.

*Some specimens of this ceramic failed at fields slightly greater than 50 volts per mil.

2.2 The Temperature Dependence of Capacity and Q

It is well known that the dielectric constant of ferroelectric ceramics is often very temperature sensitive. A ferroelectric material consisting of a single constituent shows extremely sharp peaks of dielectric constant as a function of temperature. An example of this is shown in Fig. 5, showing the variation in dielectric constant with temperature for a crystal of pure barium titanate. The peaks in the curve occur at temperatures where there is a phase transition in the crystal structure. Above 120°C the crystal lattice is cubic and no spontaneous polarization exists; the crystal in this state is non-ferro-electric. Between 5°C and 120°C the crystal lattice is tetragonal, as shown in Fig. 6, and has a spontaneous polarization. Between -70°C and 5°C it is orthorhombic and below -70°C the lattice is rhombohedral. Peaks in the dielectric constant come at these phase transitions. The upper transition is defined as the Curie point. Above the Curie temperature, the material is non-ferroelectric, and the dielectric constant falls off according to a Curie-Weiss Law,

$$\epsilon = \frac{K}{T - T_c} \qquad , \qquad (2)$$

where K is of the order of 10^5, and T_c is approximately 120°C.

In the case of ceramic materials, the addition of other constituents such as stronium titanate (having a Curie Temperature of about -100°C), and buffer materials has the effect of both suppressing and broadening the peak in the dielectric constant. This is shown in Fig. 7 for a typical barium-strontium titanate sample. The usual non-linear dielectric materials that are prepared by commercial manufacturers have their peak of dielectric constant with temperature ("Curie" Temperature) in the room temperature region; slightly below room
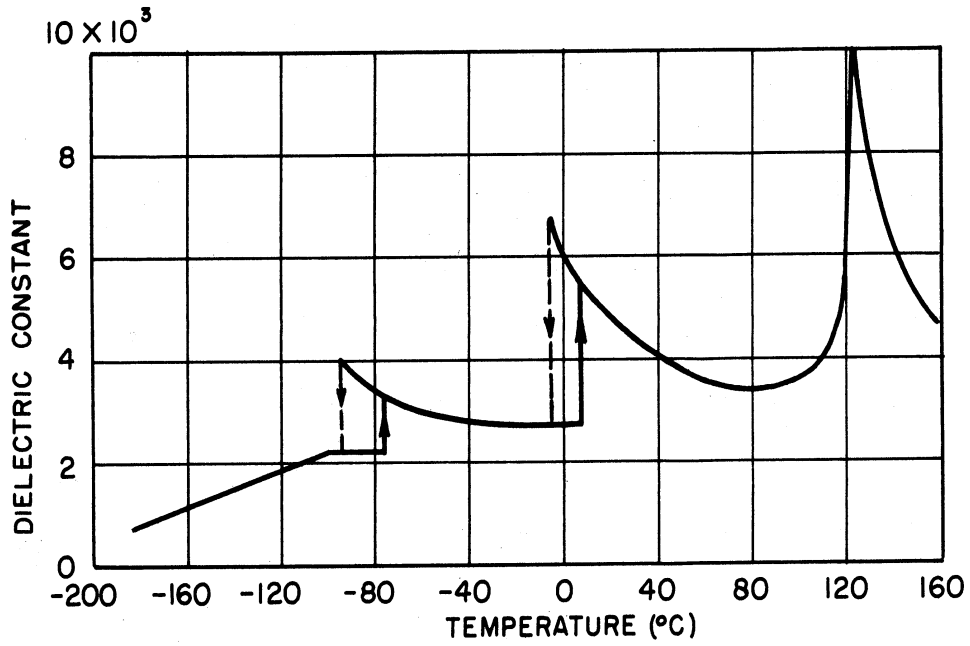
FIG. 5

INITIAL DIELECTRIC CONSTANTS OF BARIUM TITANATE
PERPENDICULAR TO THE DIRECTION OF SPONTANEOUS
POLARIZATION .

● Ti

○ Ba

⦿ OXYGEN
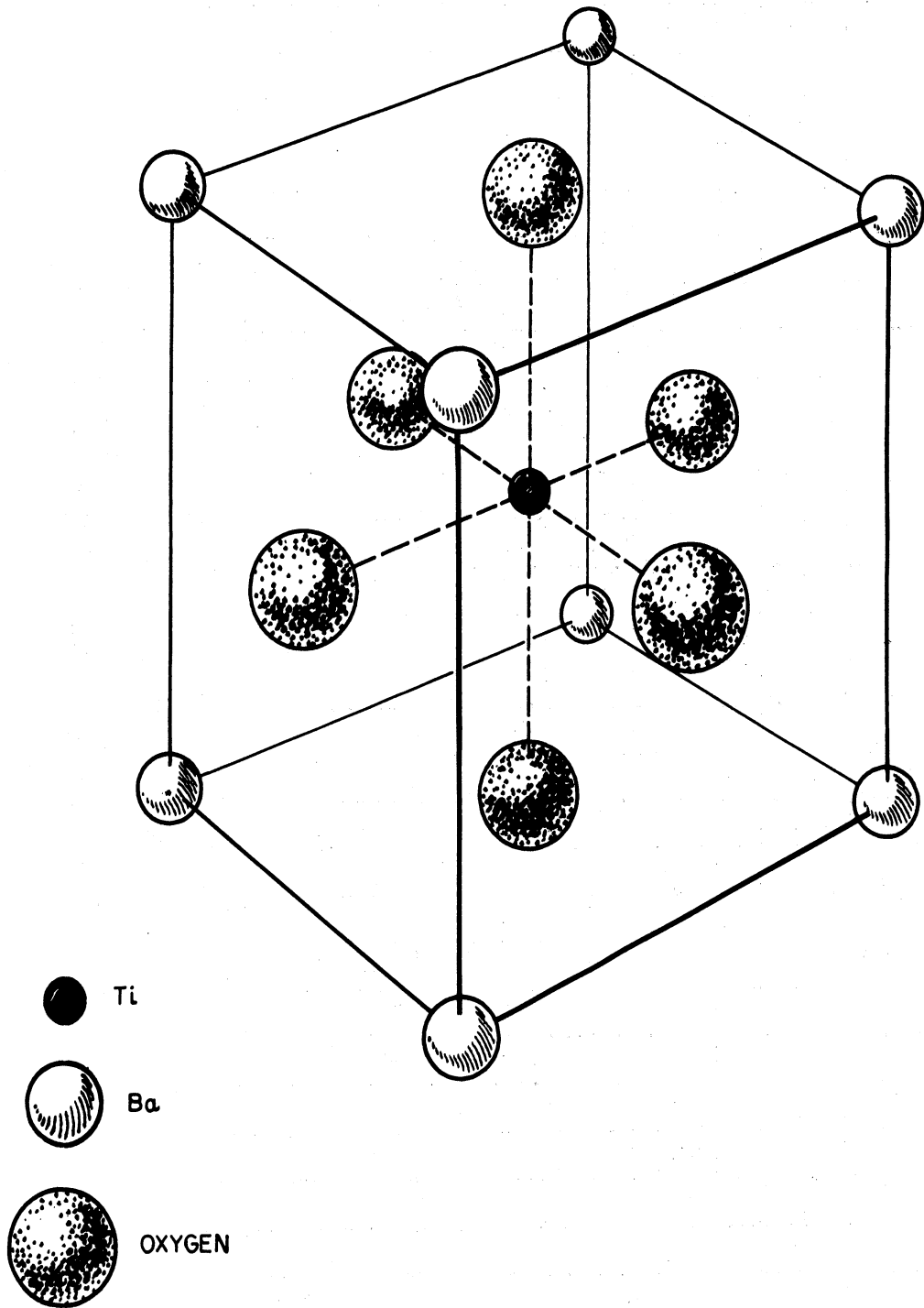
FIG. 6

THE PEROVSKITE CRYSTAL STRUCTURE
OF BARIUM TITANATE IN THE TETRA-
GONAL PHASE.

15
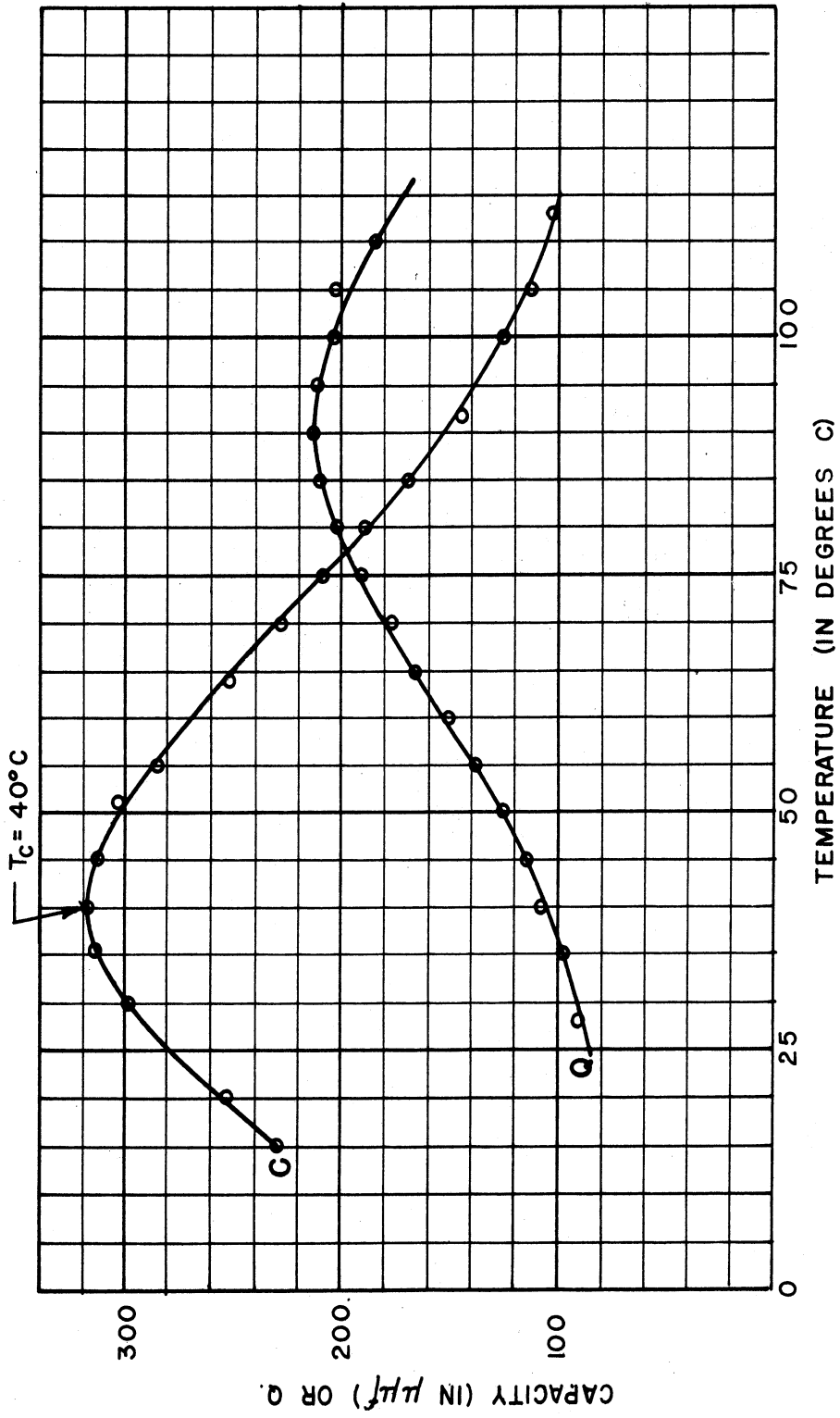
C & Q VS TEMPERATURE FOR ZERO FIELD
USING AEROVOX "HI Q" BODY NO 41

FIGURE 7

temperature if a negative temperature coefficient of capacity is desired or

slightly above room temperature for the positive temperature coefficient. In

most cases the manufacturers supplied the ϵ - T data with their samples, so that

our measurements of the ϵ - T curves are restricted to spot checks of given data.

Complete ϵ - T curves were obtained where the information was not supplied by

the manufacturer. For example, the effect of temperature on dielectric constant

and Q, was determined for zero DC field for the Aerovox Hi-Q body Nos. 40 and

41 and the Centralab body D-31, as representative materials. The measurements

are made with the equipment shown in Fig. 1. For the commercially prepared

barium-stronium titanate ceramics, the so called "Curie" temperature is not the

point of demarcation between the ferroelectric and non-ferroelectric phases as

in the case of the single crystals since it is seen from the hysteresis loops

that the material shows large remanent polarization at temperatures above this

point.

Another effect to be considered in the applications in the aging

effect after heating a ferroelectric ceramic and quenching it. Fig. 8 shows

the effect for the Aerovox body 41 after heating to 100°C and then quenching

in an oil bath at 25°C. Other ferroelectric ceramics tested behave similarly.

It can be readily seen that a sudden temperature shock may have serious conse-

quences, long after the shock has been applied, where the capacitor is used in

such services as tuning devices.

In Section 3 of this report, the effect of temperature variation on a

swept oscillator using ferroelectric ceramics is presented.
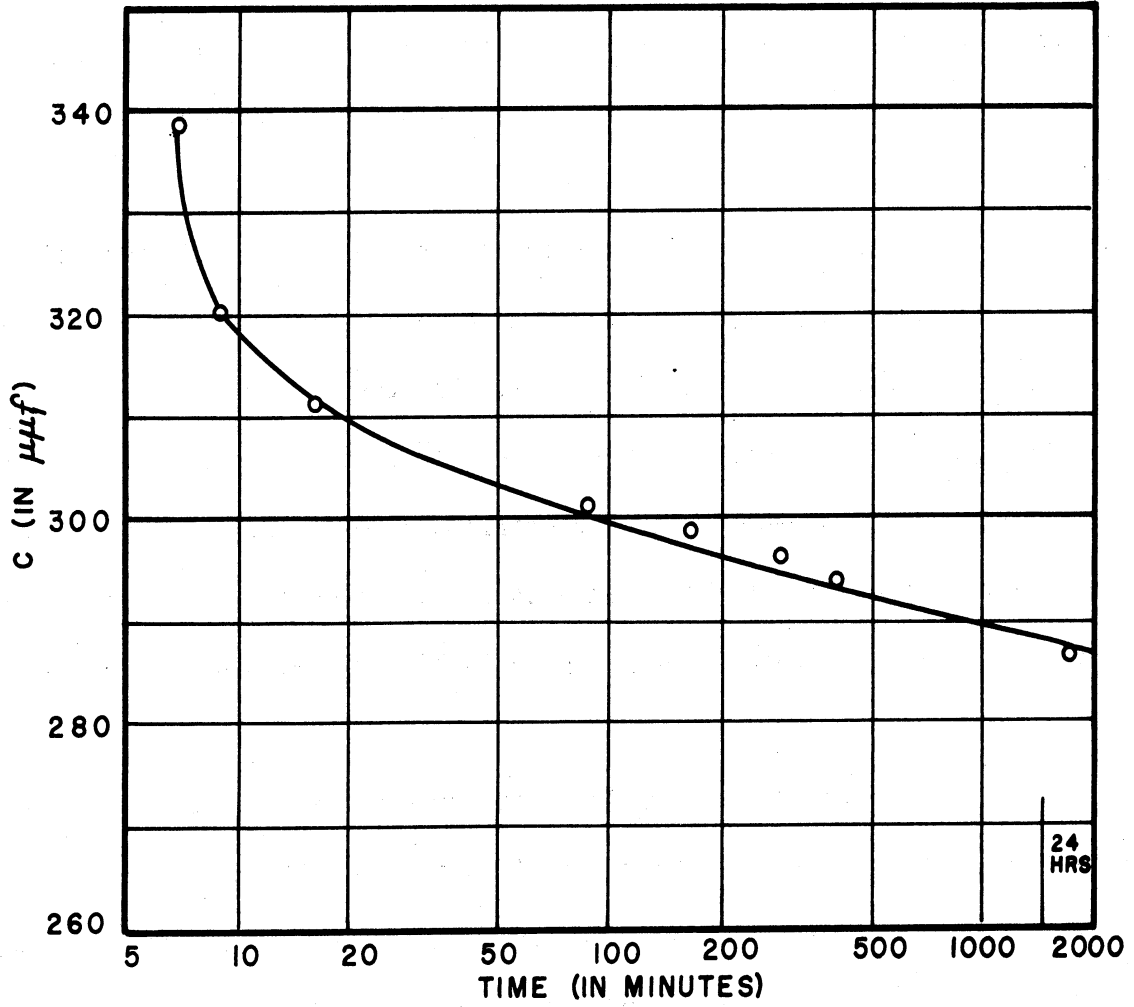
C VS TIME. AGING AFTER HEATING TO
100°C AND QUENCHING AT 25°C, AEROVOX
"HI-Q" BODY NO 41.

FIGURE 8

18

2.3 The Dependence of Dielectric Constant on Electric Field and Temperature

It has been reported that the application of a field to single crystals of barium titanate has the effect of shifting the Curie point to higher temperatures.[1] If this is true of single crystals, one might expect this for multi-crystalline samples of ferroelectric materials, and this has been indeed found, as discussed below.

In the applications both the temperature effect and the DC bias field dependence of capacity have to be considered. Such relationships can best be shown as a family of curves or as an epsilon-temperature surface as shown in Fig. 9.

Fig. 9 shows an isometric projection of the ϵ - T surface generated by a specimen of Aerovox Hi-Q 41 ceramic. The measuring frequency was 1 mc. and the applied rf voltage was about 1 volt r.m.s. The capacity measurements were made with a Boonton Q-meter with the DC field increasing slowly from zero through positive values and with the temperature held constant for each run. In Fig. 9, the curves of constant electric field show the variation of ϵ as the temperature varies. The point of maximum ϵ is shown on each such curve by a small circle. Thus, at zero field it is seen that the maximum ϵ occurs at about 43°C, while at a field of 20 Kv/cm. the maximum ϵ is at 67°C.

The ϵ - T surface for a particular material is a clear presentation of tuning capabilities and severity of temperature coefficients for a particular combination of field and temperature; it is very useful in comparing various

---

[1]M. E. Caspari and W. J. Merz, Phys. Rev., Vol. 80, p. 1082, (1950)
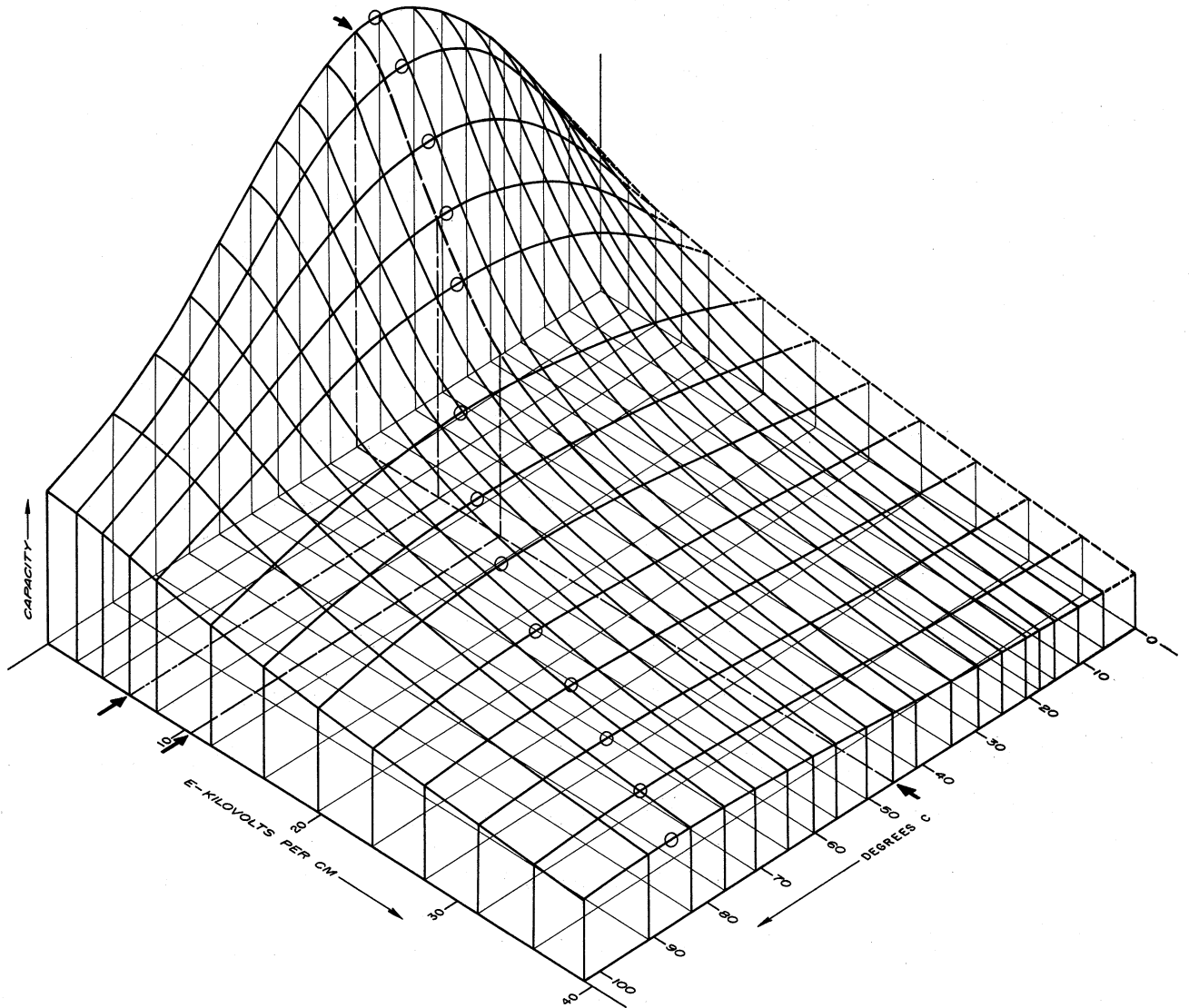
FIG. 9

EPSILON—TEMPERATURE SURFACE
FOR AEROVOX HI—Q 41.

20

materials for specific applications such as electric tuning.

Measurements have recently been made of the shift of the Curie temperature with field on single crystals of barium titanate, and it was found that the Curie shift was linear with field up to fields of 15 volts per mil. The measured shift is of the order of 0.5°C per volt per mil field.[1]

Good quantitative measurements of this effect are difficult to made in ceramic materials due to the broad Curie points. However, it can be seen from Fig. 9, that the Curie shift is not too pronounced for fields up to 6 kv. per cm. (15 volts per mil) and has a value of about 0.2°C per volt per mil.

In the next range of fields (i.e. between 15 and 40 volts per mil) the Curie shift has the rather large value of about 0.7°C per volt per mil, and finally for the very high field range (from about 40 to 150 volts per mil) the shift has again a value of about 0.2°C per volt per mil. Again it must be emphasized that these figures for the Curie shift are only approximate since it is readily seen from Fig. 9, that the point for maximum may be determined only approximately.

If a ferroelectric capacitor is used as a tuning unit in a swept receiver, and there is a Curie shift, the tuning curves for temperatures above and below the zero-field Curie temperature should cross. This is very nicely illustrated by the tuning curves for a Centralab K-6000 body which are shown in Fig.38 of this report. The Curie temperature for this body is about 45°C.

---

[1] After W. Mertz, Phys. Rev., Vol. 91, p. 514 (1953)

2.4 Hysteresis Loops in Ferroelectric Materials

    2.4.1 Hysteresis Loops in Ferroelectric Ceramics. If a ferroelectric material is subjected to an alternating field, and the polarization is measured, it is noticed that a hysteresis loop results. These loops are similar to the B-H loops of a ferromagnetic material. By means of the apparatus shown in Fig. 10, hysteresis loops of ferroelectric specimens at different temperatures may be displayed. The specimen is placed in a constant temperature bath of transformer oil and excited by a 60-cycle, 1000 v power transformer. The X input of the oscilloscope receives a suitable low voltage from the divider, R_1R_2, which is proportional to the electric field applied to the specimen.

    The polarizing current, i, which flows in the specimen, is integrated by the capacitor, C, to give a voltage, V, proportional to the polarization, P. This voltage is applied to the Y input of the oscilloscope. The display is thus a P-E loop for the specimen.

    If P is the polarization in coulombs per square centimeter, and A is the electrode area in square centimeters of the ferroelectric sample being tested, then we may write the current, i, in the form

$$i = A \frac{dP}{dt} \qquad ,$$

so that   (3)

$$P = \frac{1}{A} \int i \, dt \qquad .$$

    The voltage on the capacitor, C, is given by:

$$V = \frac{1}{C} \int i \, dt \qquad , \qquad\qquad\qquad (4)$$

THERMOMETER

TO VARIAC

VACUUM FLASK

TRANSFORMER OIL

TEST SPECIMEN

HEATER

1000V
XFMR

R3

R1
3X330K
2W

VARIAC

110V
60~

i

V

R2
33K
2W

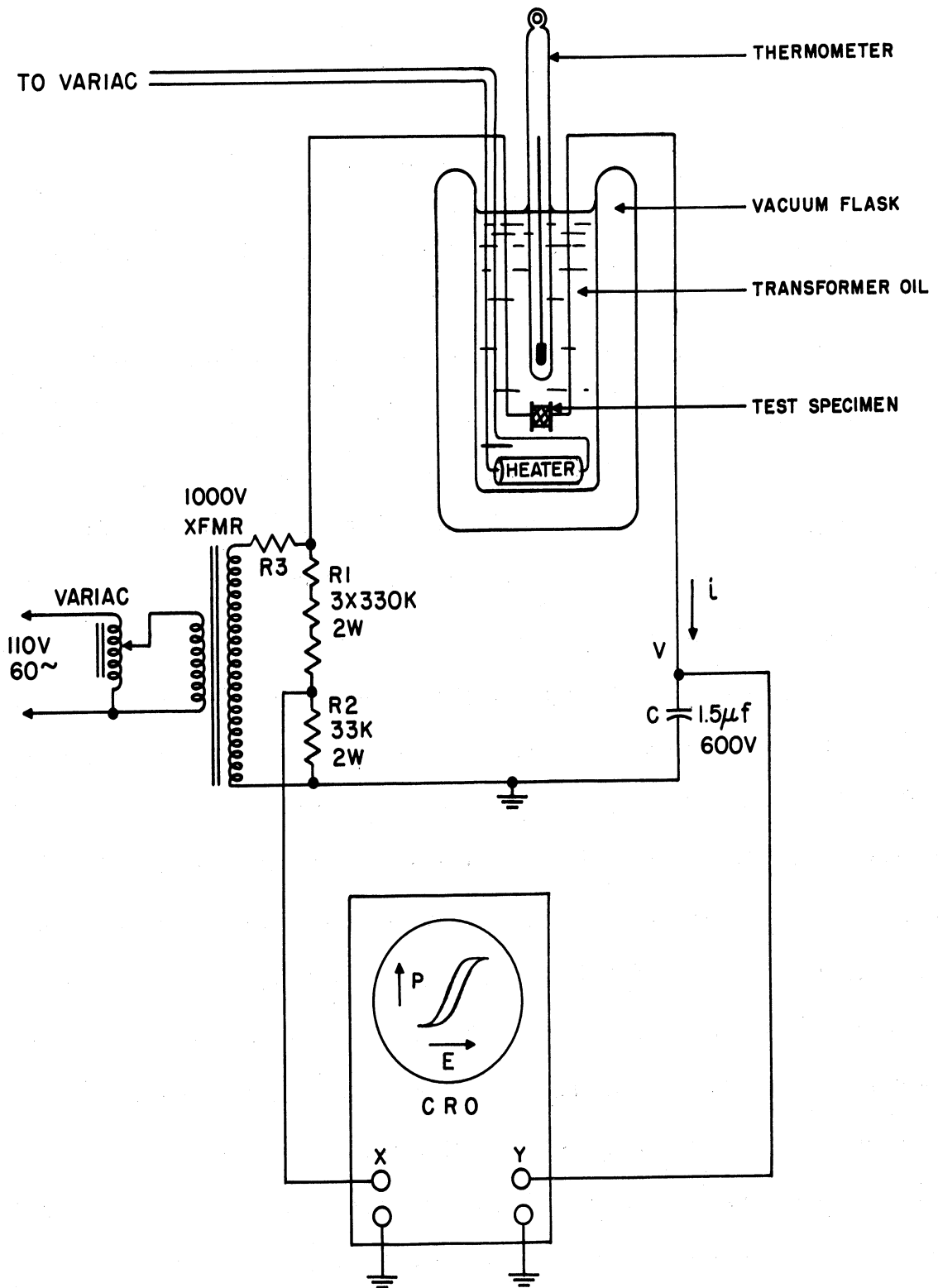C $=$ 1.5μf
600V

P

E

CRO

X   Y

FIG. 10. P-E LOOP PLOTTER.

so that

$$P = \frac{C}{A} V \qquad .$$ (5)

Using Eq. 5, we may easily calibrate the vertical co-ordinate of the oscillogram.

R_3 is placed in the circuit in order to limit the current to the specimen. This is especially important in the case where materials with steep-sided hysteresis loops are measured. Since the instantaneous current is given by $i = A \frac{dp}{dt}$, it is readily seen that a sudden jump in the polarization will result in a large current pulse. It was found that several specimens failed due to this large current pulse before R_3 was placed in the circuit.

Fig. 11 shows a typical series of P-E loops for ferroelectric ceramics at different temperatures. The series shown here is for a specimen of Aerovox Hi-Q 41. In each oscillogram the vertical calibration is one micro-coulomb per small square. These loops are for a peak field strength of 18 kv/cm, (about 50 volts per mil) representing the useful limit for the particular body and specimen thickness used (.020 inch). Similar specimens of this ceramic failed by voltage breakdown at field strengths slightly greater than 50 volts per mil, whereas the Aerovox Hi-Q 40 and the Glenco K-3300 bodies have been able to with-stand cyclic fields in excess of 100 volts per mil.

The oscillograms in Fig. 11 show that as the temperature is increased the area of the hysteresis loop is reduced. The hysteresis is reduced most rapidly in the range below the Curie temperature, (45°C). Above this temperature the hysteresis is reduced more gradually and vanishes at about 120°C -- the Curie temperature of pure barium titanate. Again note that for the ceramic materials,
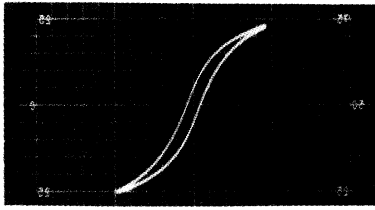
A. 0°C
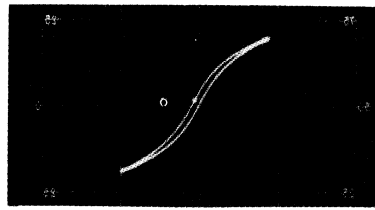
B. 40°C
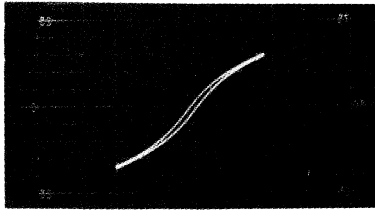
C. 60°C

D. 80°C
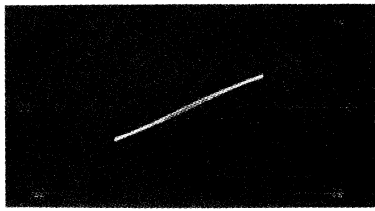
E. 100°C
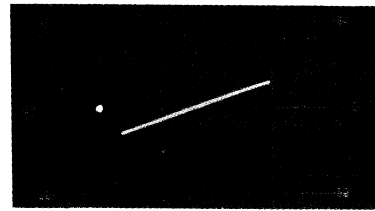
F. 120°C

FIG. II

P – E LOOPS

FOR AEROVOX HI – Q 41.

25

the Curie temperature has been defined as the temperature of maximum dielectric

constant and <u>not</u> the temperature at which a spontaneous electric moment dis-

appears. (In pure crystals these two points coincide.) Thus the material which

gave the loops in Fig. 11, shows a remanent polarization above its "Curie" temper-

ature.

2.4.2 Hysteresis Loops for Single Crystals of Barium Titanate.

Hysteresis loops were obtained from pure crystals of barium titanate using the

same equipment as shown in Fig. 10, with the exception that the sample is placed

in an oven rather than an oil bath. It was found that the oil bath tended to

load the crystal, and abnormally fat P-E loops resulted. When electrodes of

silver paint were used, mechanical loading again produced fattening of the P-E

loops. Best results were obtained with vacuum deposited silver electrodes. The

vacuum plating was done with equipment in the Randall Laboratory of Physics.

The connections to the electrodes were made with rather fine foil leads and these

leads were then attached to silver paint strips on a glass microscope slide as

shown in Fig. 12. Thus, the crystal was suspended from the fine leads and

allowed a minimum of mechanical loading. For convenience in handling and sorting,

this method of mounting samples was finally adopted for both single crystal

and ceramic samples. The connections to the external testing circuit are made

by clipping onto the silver-painted strips on the glass slide. Fig. 13 shows

the square hysteresis loops resulting from the application of increasing values

of field. The maximum field is 20 volts per mil.

The barium titanate crystals used for our measurements are in the form

of thin plates, about half a centimeter square and average about .2 or .3 mm

(about 10 mils) in thickness. The electrodes are plated on the crystals' flat

FERROELECTRIC
SPECIMEN

SILVER PAINTED
ELECTRODES

FOIL LEADS

VACUUM DEPOSITED
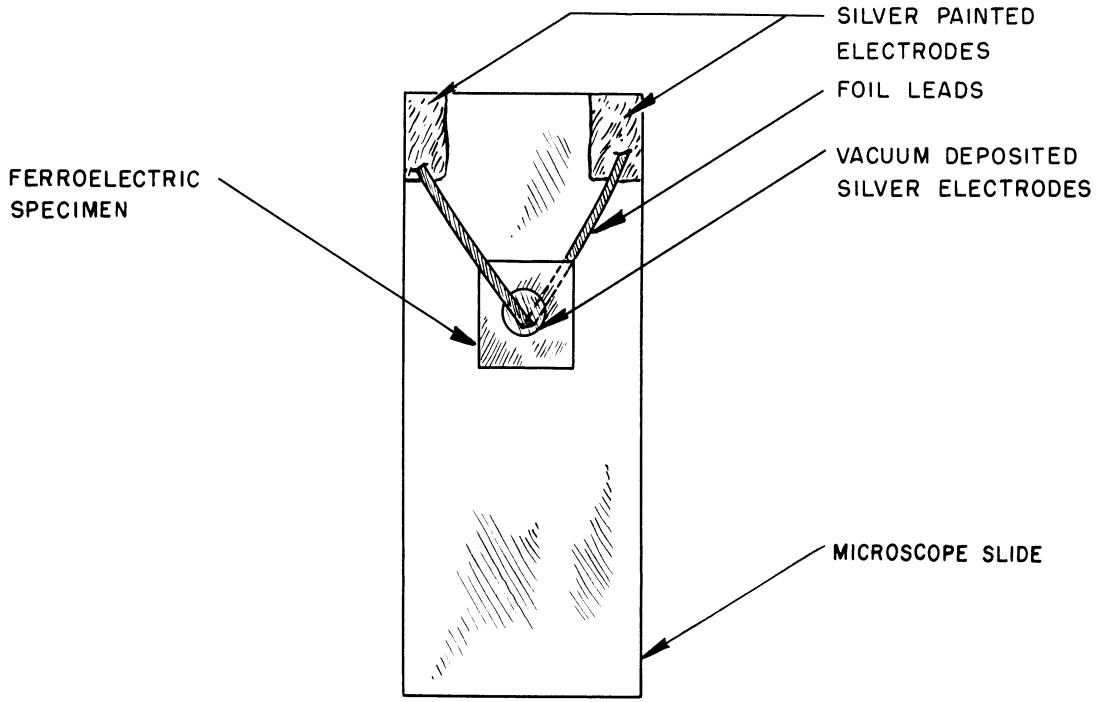SILVER ELECTRODES

MICROSCOPE SLIDE

FIG. 12

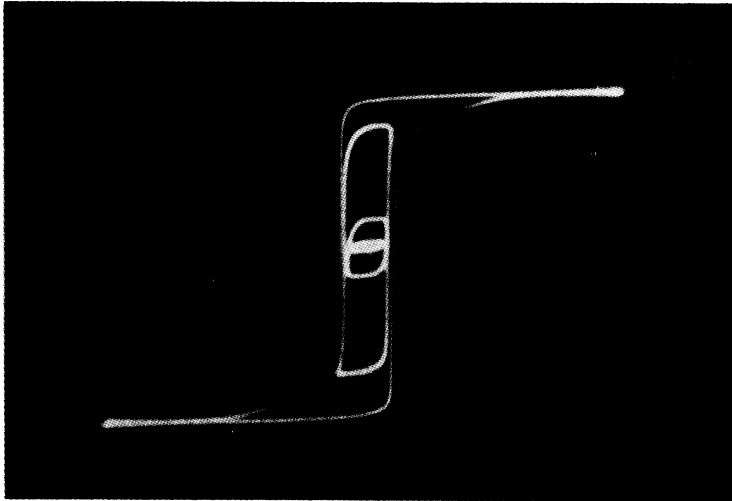METHOD OF MOUNTING FERROELECTRIC SAMPLES
FOR TESTING .

FIG. 13

HYSTERESIS LOOP OF BARIUM TITANATE FOR
VARIOUS VALUES OF MAXIMUM APPLIED FIELD

surfaces so that the domains that are aligned parallel and anti-parallel to the direction of the applied field are also perpendicular to the plane of the crystal, whereas those domains that are perpendicular to the applied field lie in the plane of the crystal.

For the single crystal of barium titanate it is found that the domains are switched easiest if they are aligned parallel and anti-parallel to the direction of the applied fields. The domains that are aligned perpendicularly to the applied field require larger fields in order to align the domain. This is seen from the outer most loop of Fig. 13, where the sample has both parallel and perpendicular domains. Here the anti-parallel domains are suddenly aligned at low value of field (the sharp, low-field corner) and the perpendicular domains require the higher fields (the rounded high field corner). Fig. 14 shows the case in which the material has only parallel and anti-parallel domains (i.e. a c-oriented crystal). Here all the corners of the loop are sharp and occur at low fields, indicating the fact that only parallel and anti-parallel domains are being alligned.

In contrast to the motion of the domains in the magnetic material where the favorably oriented domains grow at the expense of those unfavorably oriented by the movement of the domain walls, the motion of the domains in a ferroelectric crystal proceeds by a sudden appearance of many new thin, splinter-like favorably oriented domains within domains that are unfavorably oriented.

The hysteresis loop of the unoriented ceramic, which is composed of many crystals of the ferroelectric constituents, can be considered as a statistical smearing out of the loops for each crystalline particle. In the case of the hysteresis loops for the monocrystalline sample, Fig. 14, it is seen that a condition
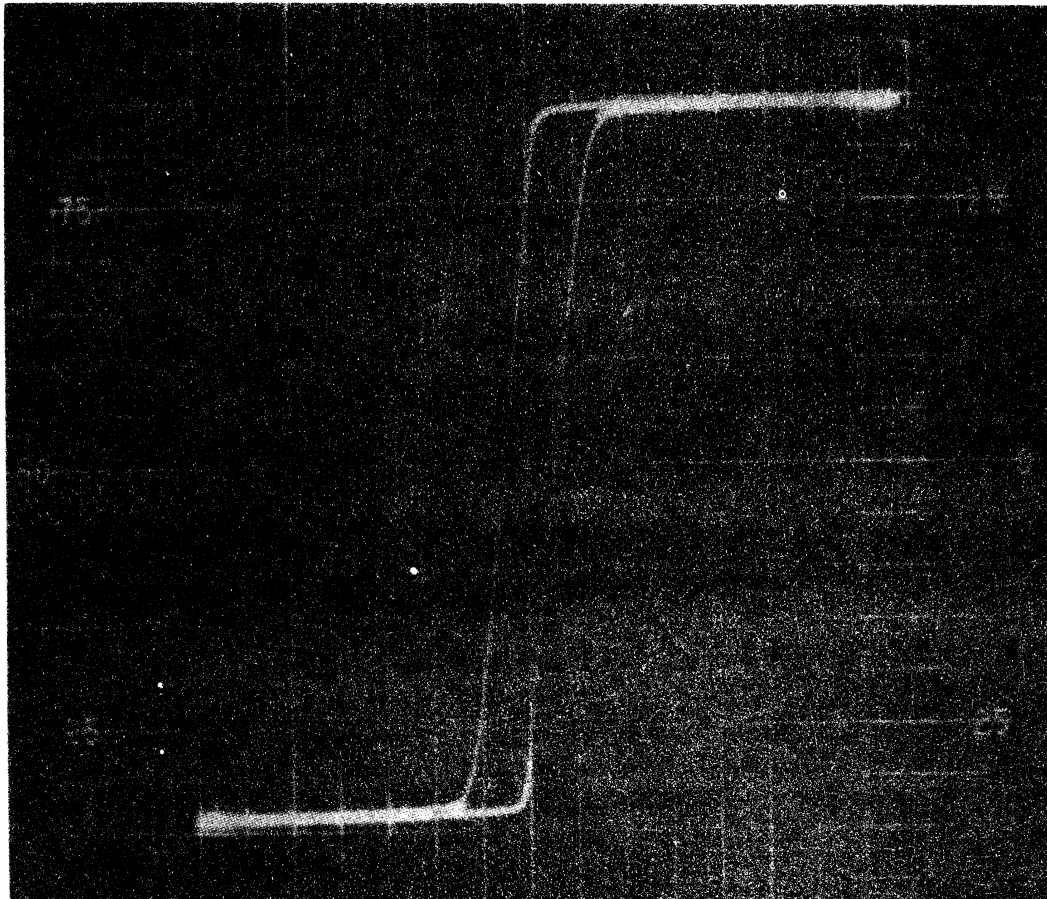
FIG. 14

HYSTERESIS LOOP FOR C-ORIENTED BARIUM TITANATE SINGLE CRYSTAL

of saturation polarization is produced at relatively small fields, indicated by the horizontal portions, or horns of the loop. Since the dielectric constant does not go to unity but has a value of about 200 at saturation, these horns are not truly horizontal. This loop is analogous to the rectangular B-H loop for a gain oriented magnetic material such as Orthonik when the field is applied in the easy direction of magnetization.

Ferroelectric ceramics having random orientation, do not show saturation even at fields sufficiently large to produce electric breakdown. The rounded P-E loops of such ceramics are analogous to B-H loops for unoriented magnetic materials.

2.5 Effects of Surface Plating

As was mentioned previously, much better results were obtained for the single crystals when the electrodes were vacuum plated. That is, this technique resulted in steeper sided P-E loops with lower losses. Several samples of the ceramic materials have also been provided with vacuum deposited electrodes. The usual commercial method of providing electrodes for ceramic capacitors is to silk screen a silver conducting paint onto the surface. In determining the effect of the plating method for the ceramic materials, a series of materials each with three separate types of electrodes, were compared. The three types of electrodes that have been used are:

(a) commercially silk screened

(b) a painted-on silver paste

(c) high vacuum deposited pure silver electrodes

In this investigation twenty-five samples were measured at frequencies ranging from 60 cycles to 1 mc. The data is still incomplete, but it was found

that for every material tested, the losses for the vacuum deposited specimens were the least, while the hand painted specimens had the greatest losses. This is dramatically displayed by the 60 cycle hysteresis loops shown in Fig. 15.* In the case where the dielectric constant is very high and the sample is very thin, then the effect of any "dead space" between the dielectric and the electrode is quite serious in terms of net reduction in the effective capacity. That is, there is a depolarizing effect due to the effect of the greatest portion of the field appearing across the region of lowest dielectric constant. This effect has been observed in the test specimens. The samples with the vacuum deposited electrodes show the highest dielectric constant (for the low frequency tests).

All of this explains very well the observed reduction in the effective capacity of the sample but does not account for the greater losses in the materials which have been provided with silk screened or hand painted electrodes. We may attribute·the losses in these latter samples to the losses in the electrodes themselves. All paints contain fluxes which remain with the paint after it dries; and even though in the case of the commercial capacitors, a special heat treatment is applied in order to remove the organic material from the conducting paints, it is very doubtful whether the organic binders can be removed completely.

At the time that this report is being prepared, the measurements are being continued along the line of determining the effect of the electrode plating

---

* Here the vacuum plated samples have the thinnest loops, and the hand painted samples have the fattest loops.
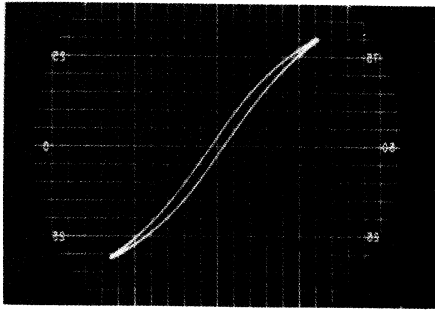
BRUSH PAINTED SILVER CONDUCTING
PAINT
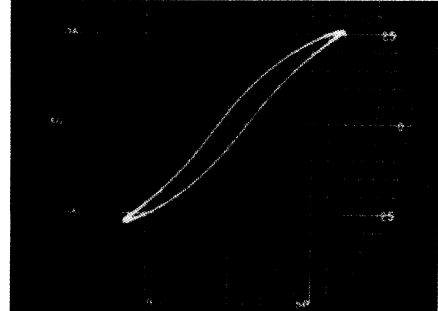
BRUSH PAINTED SILVER CONDUCTING
PAINT
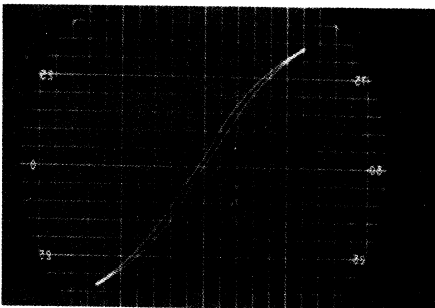
SILK SCREENED SILVER CONDUCTING
PAINT
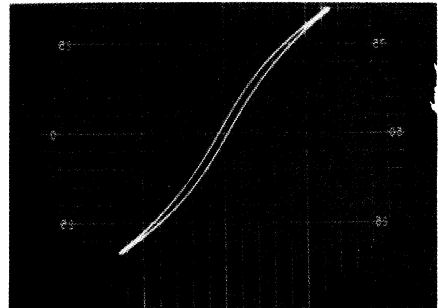
SILK SCREENED SILVER CONDUCTING
PAINT
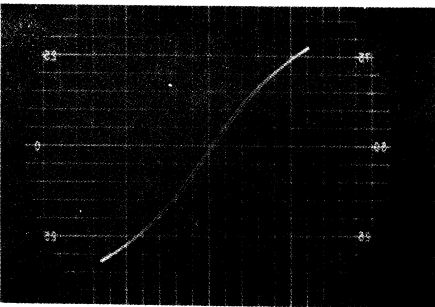
HIGH VACUUM DEPOSITED PURE SILVER

A. AEROVOX HI-Q 41
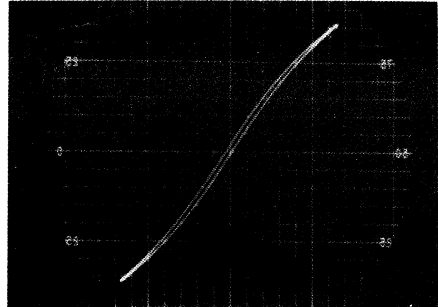
HIGH VACUUM DEPOSITED PURE SILVER

B. GLENCO K-3300

FIG. 15

THE EFFECT OF THE TYPE OF ELECTRODE
ON THE 60 CYCLE HYSTERESIS LOOP FOR
TWO FERRO-ELECTRIC CERAMICS

32

methods on the incremental dielectric constant and the losses in the high frequency and the very high frequency ranges. The results of these measurements will be reported upon as soon as sufficient data becomes available.

2.6 Double Hysteresis In Barium Titanate

2.6.1 Double Hysteresis Loops for Single Crystals.

It is known that for single crystals of barium titanate the Curie temperature shifts to higher temperatures upon the application of an electric field. If the crystals are subjected to a cyclic field at a temperature just slightly higher than the Curie temperature, then one would expect that the crystal can be made alternately ferroelectric and paraelectric. Such behavior has been recently reported by several investigators and has been duplicated by us; the best results being obtained by using fairly good crystals having only parallel and anti-parallel domains. Figs. 16 and 17 show the double loops as a result of the Curie temperature shift with field. It can be seen that the crystal used for the series of oscillographs shown in Fig. 16 contains a rather large proportion of domains aligned perpendicularly to the applied field causing the rounding of the shoulders of the hysteresis loop, whereas the crystal used for the series shown in Fig. 17 contained only parallel and anti-parallel domains so that the corners of the hysteresis loops and the Curie point transitions are sharp and distinct. The crystal used for the first series shown was rather lossy. This can be implied from the fact that the central portions of the double loop do not become a straight line as is expected for paraelectric barium titanate. For the latter series, the central portion of the double loop does become a straight line. (The small minor loops seen are produced by the sudden transitions causing the inductive drive circuit to "ring". A damping resistor was later added to the drive circuit.)
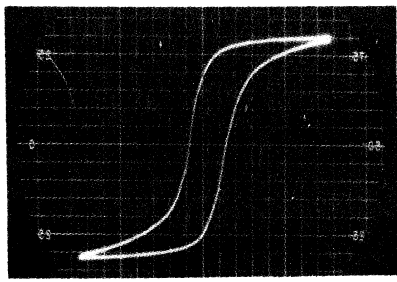
100°C
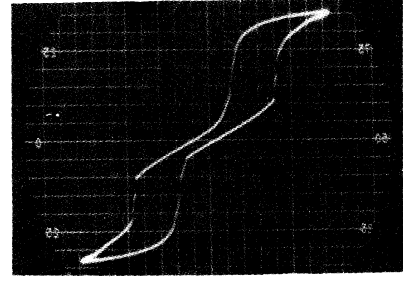
114.5°C
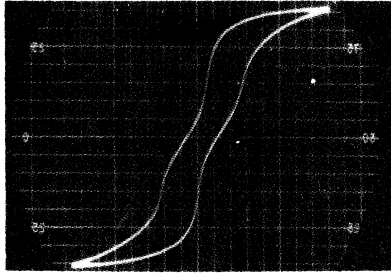
112°C

115°C

113°C

115.5°C
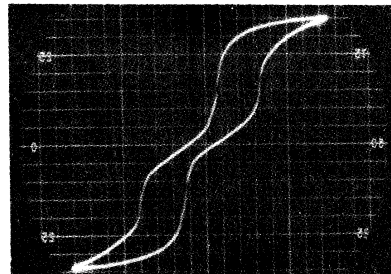
113.5°C
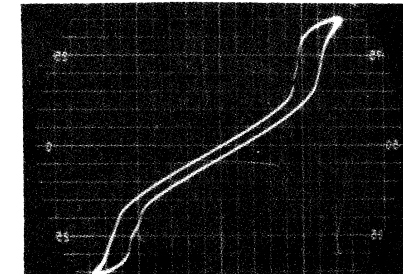
117°C
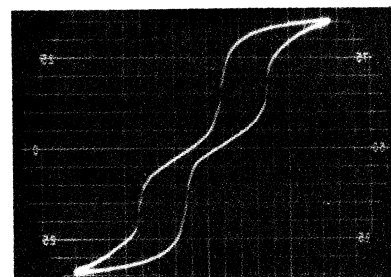
114°C
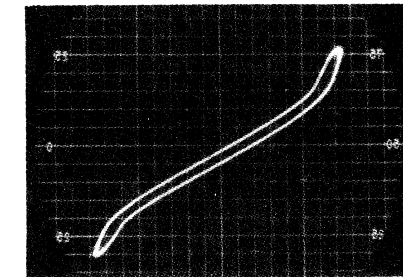
118°C

FIG. 16   DOUBLE HYSTERESIS LOOPS IN CRYSTALLINE BARIUM TITANATE
HAVING BOTH PARALLEL AND PERPENDICULARLY ORIENTED DOMAINS

34
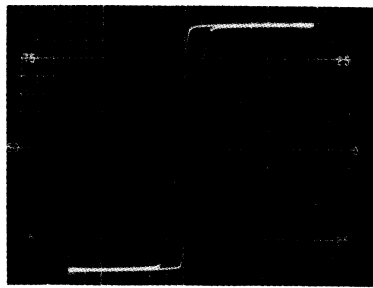
25°C
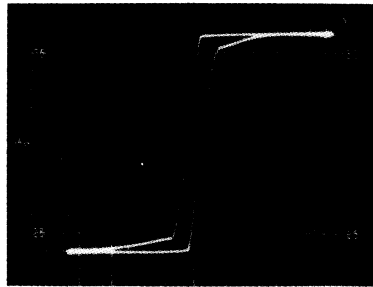
85°C
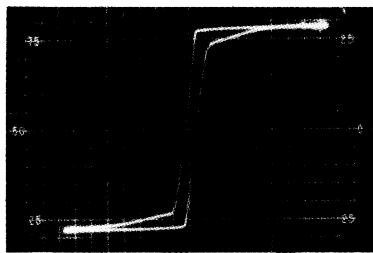
100°C
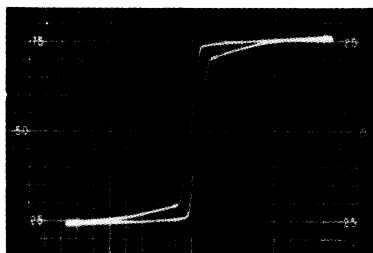
110°C
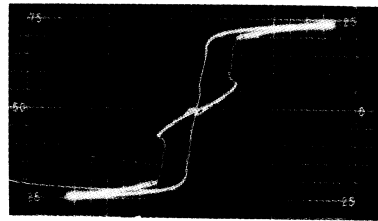
115°C
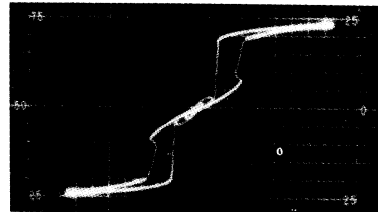
116°C
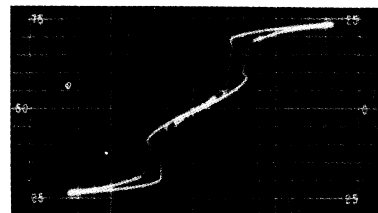
117°C

118°C
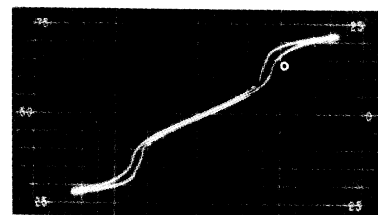
119°C

FIG. 17

DOUBLE HYSTERESIS LOOPS
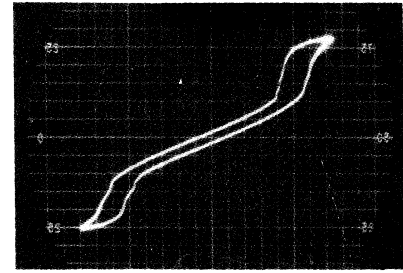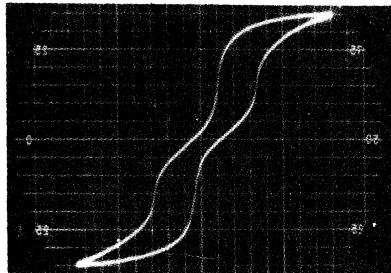IN A C-ORIENTED BARIUM TITANATE CRYSTAL

The field applied to the sample is a 60 cycle sine wave. The maximum value of field was 20 volts per mil in Fig. 16, and 30 volts per mil in Fig. 17.

For each temperature above the Curie, there is a critical electric field where the crystal just becomes ferroelectric. This field is observed on each oscillogram where the double loop occurs. By plotting the temperature against this critical field, we obtain a Curie shift curve. Such a curve for the series of oscillograms in Fig. 16 was plotted, and is shown in Fig. 18. Over the range plotted, the Curie shift is linear, having a slope of 0.5°C per volt per mil. This value confirms the results of Merz[1] (0.57°C per volt per mil).

2.6.2 Double Hysteresis Loops in Ceramic Materials. An effect which is masked when the samples are provided with conductive-paint electrodes but which becomes apparent when vacuum plated electrodes are used, is the double hysteresis loop phenomena observed in certain ferroelectric ceramic materials. In this case the double hysteresis loop, in contrast to the double loops observed for the single crystals of barium titanate, occurs over a rather large temperature range. As has been previously pointed out for the case of crystalline barium titanate, the double loop is caused by a transition from a non-ferroelectric state to a ferroelectric state via a shift in the Curie temperature with applied field.

Fig. 19 shows the results for a Centralab K-3100 body. The loop just doubles at about 10°C and completely closes to a straight line at about 50°C.

---

[1]W. J. Merz, "Double Hysteresis Loop of BaTiO$_3$ at the Curie Point", Phys. Rev. Vol. 91, p. 513. (Aug. 1, 1953).
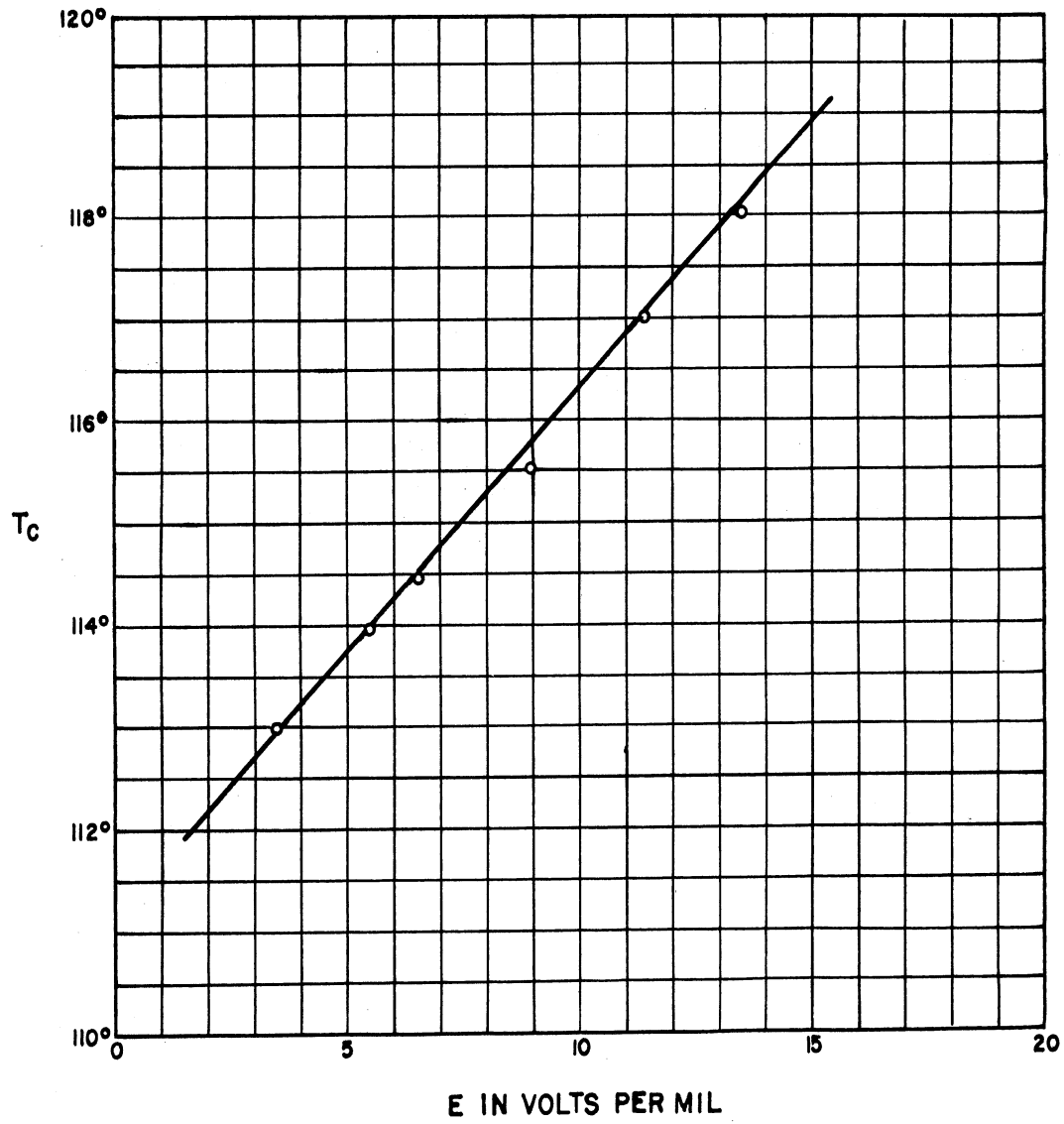
FIGURE 18

THE CURIE TEMPERATURE OF BARIUM TITANATE
AS A FUNCTION OF FIELD
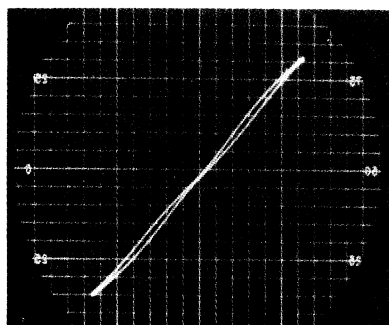
10° C
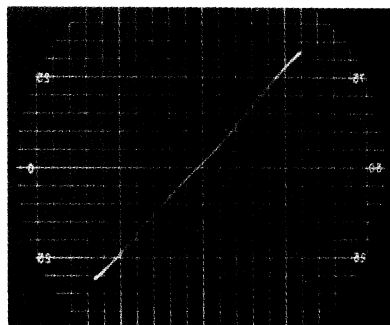
35° C
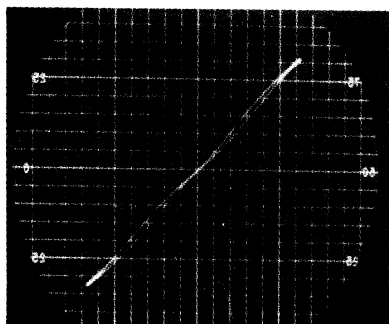
15° C
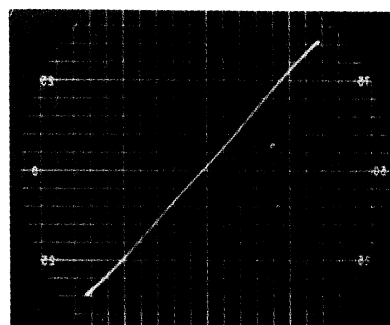
45°C
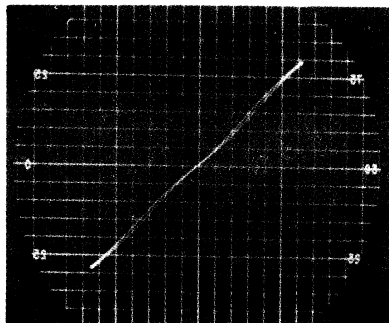
26°C
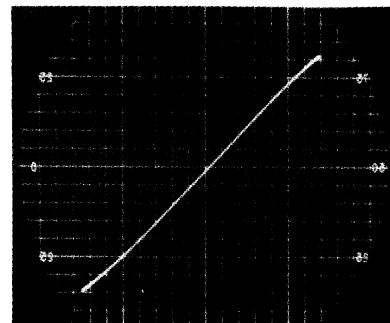
56°C

FIG. 19

DOUBLE HYSTERESIS LOOPS
FOR CENTRALAB D-31

(VACUUM DEPOSITED ELECTRODES)

It is noticed that the two halves of the double loop approach the straight-line central portion quite gradually in comparison with the pure barium titanate crystal which has very steep sided double loops. Also as the temperature is increased the area of the double loops becomes smaller until at around 50°C the loops degenerate into a line. This behavior can be expected of a multi-crystal-line material the particles of which have a wide temperature distribution of transitions from the ferroelectric to the non-ferroelectric state.

There are, however, certain peculiarities about this double loop. The loop just closes at the origin at about 10°C. This means that at this temperature, for no field, none, or at best very few, of the constituent particles in the sample are ferroelectric. At 35°C, the field required to cause the loop to just start to open is about 5 volts per mil. Thus, a five volt per mil field shifts the Curie point by 25°C (the interval between 10°C and 35°C). This means that the Curie temperature shift is of the order of 5°C per volt per mil -- a value ten times as great as for the case of pure barium titanate.

The Curie temperature for this sample is taken to be the temperature of the transition from the non-ferroelectric to the ferroelectric phases as determined by the hysteresis loop. As has been noted this is at about 10°C for zero field. The temperature - capacity curve, A, shown in Fig. 20, shows a peak in capacity at 5°C, which is approximately the temperature at which the double hysteresis loops begin to appear. Since it is assumed that the double hysteresis loop is caused by a change in phase of the crystalline aggregate, a rather sharp peak in the capacity - temperature curve is expected. However, it is noticed that this peak is not nearly as sharp as are the Curie temperature
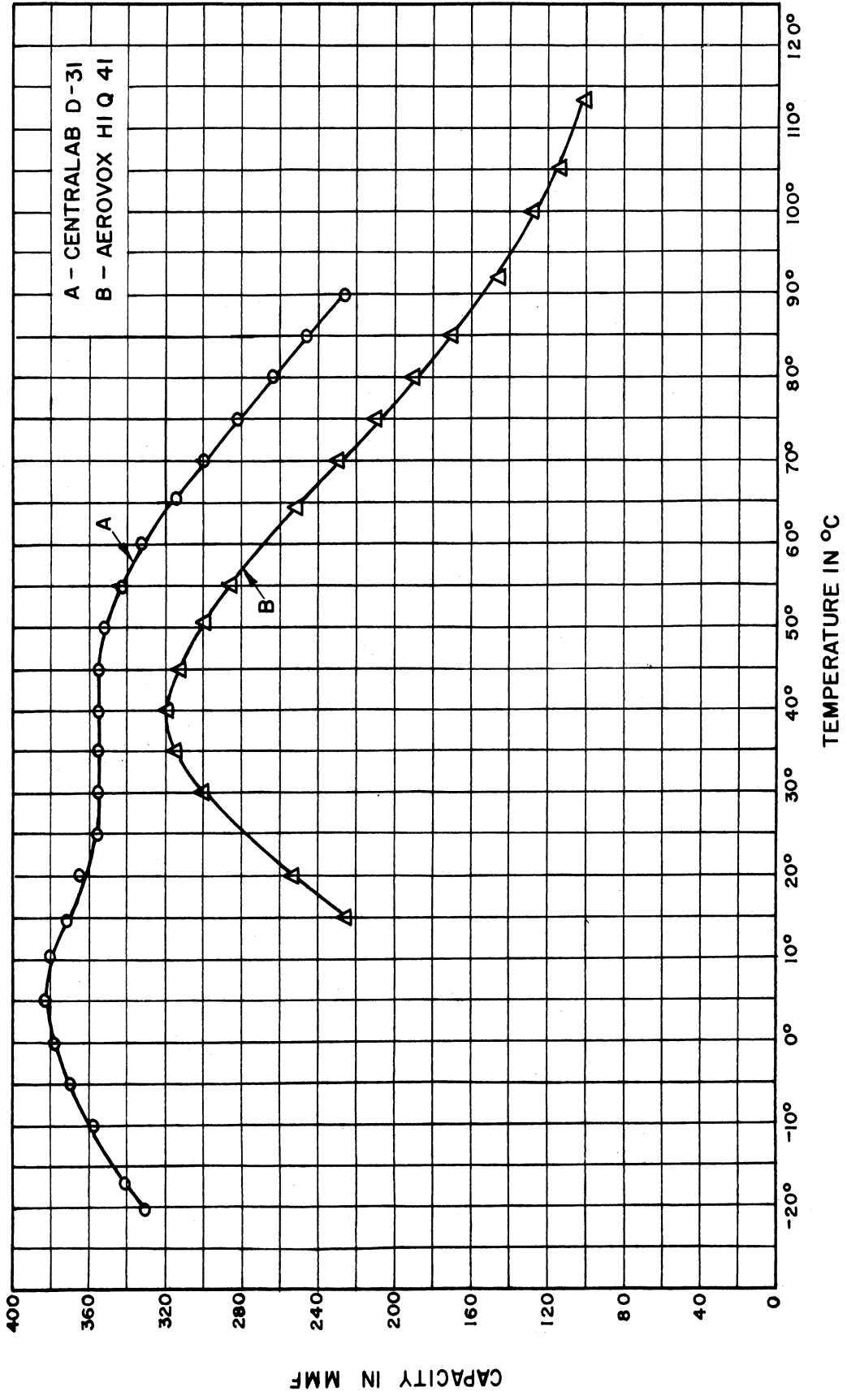
CAPACITY VS TEMPERATURE FOR TWO FERROELECTRIC CAPACITORS

FIG. 20

A – CENTRALAB D-31
B – AEROVOX HI Q 41

TEMPERATURE IN °C

CAPACITY IN MMF

peaks of the ceramic ferroelectric materials which do not show the double loop phenomenon (Curve B in Fig. 20). Thus it would seem that an explanation of the double loop phenomenon based solely on the ferroelectric-paraelectric transition with field is really not adequate for the D 31 material.

2.7 Butterfly Loops for Ferroelectric Materials

The results of the preceeding section can be at least qualitatively corroborated by "butterfly loop" data taken for the same sample. The butterfly loop is a plot of ϵ_Δ as a function of the applied field, E, when the specimen is in the "cyclic electric state." (This is analogous to the magnetic butterfly loop in which case μ_Δ is plotted against the magnetic driving field, H, while the magnetic specimen is in the cyclic magnetic state.)

The incremental dielectric constant, ϵ_Δ , is defined as:

$$\epsilon_\Delta = 1 + 4\pi \frac{\Delta P}{\Delta E}$$

or

$$\epsilon_\Delta \cong 4\pi \frac{\Delta P}{\Delta E} \qquad \text{in esu,}$$

(6)

when $\epsilon_\Delta \gg 1$ as in the case for ferroelectric materials. It must be clearly understood that the quantities ΔP and ΔE are small incremental quantities and are not to be confused with the reversable polarizations and field; nor in the strictest sense is the ratio $\frac{\Delta P}{\Delta E}$ to be considered the slope of the hysteresis loop at any point. However, in the case of the very thin loops, as are observed for the double looped ceramic material, we may treat the incremental quantities as reversible. This approximation becomes good in the central portions and on the horns of the double hysteresis loops. Thus the approximation is

made by writing the incremental quantities of Eq. 6, as exact differentials. Thus:

$$\epsilon_\Delta \cong 4\pi \frac{dP}{dE} \qquad (7)$$

or by taking another derivative with respect to the field,

$$\frac{d\epsilon_\Delta}{dE} = 4\pi \frac{d^2P}{dE^2} \qquad (8)$$

Now for the parts of the butterfly loop for which $\frac{d\epsilon_\Delta}{dE}$ is positive, the second derivative of P is positive, so that the change in polarization with the applied field is concave upward on a very thin hysteresis loop. Similarly, if the second derivative were negative as it is for fields greater than that which produces the maximum ϵ_Δ, the trace on the hysteresis loop would be concave downward. The maximum and minimum points on the butterfly loop imply inflection points on the double hysteresis loop. This is actually observed in Fig. 21, where a dynamically plotted butterfly loop is shown with the very thin hysteresis hysteresis loop of a Centralab D-31 body. Note that the hysteresis for this sample as shown by the butterfly loop and the hysteresis loop is extremely small. The dynamic butterfly loop plotter, which is discussed in detail in the following section, presents an oscillographic display, the envelope of which is the butterfly loop.

The dynamic technique developed for presenting butterfly loop data serves as a convenient means of rapidly obtaining qualitative information such as comparisons of the field non linearily and hysteresis losses in the ferro-electric materials being tested. When more quantitative data is required, it
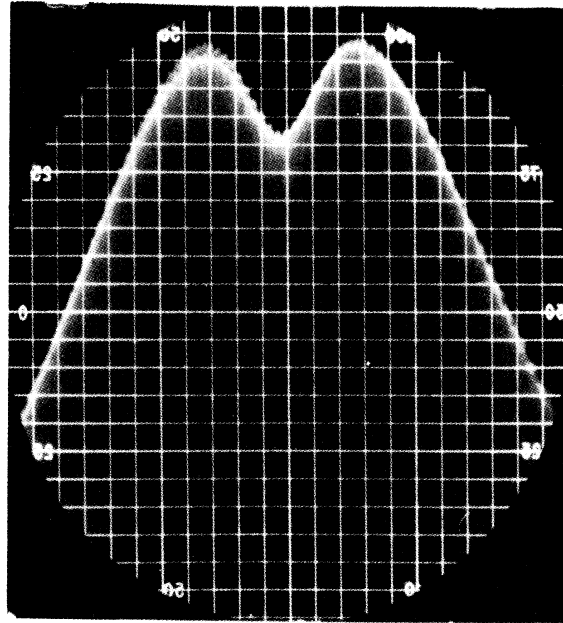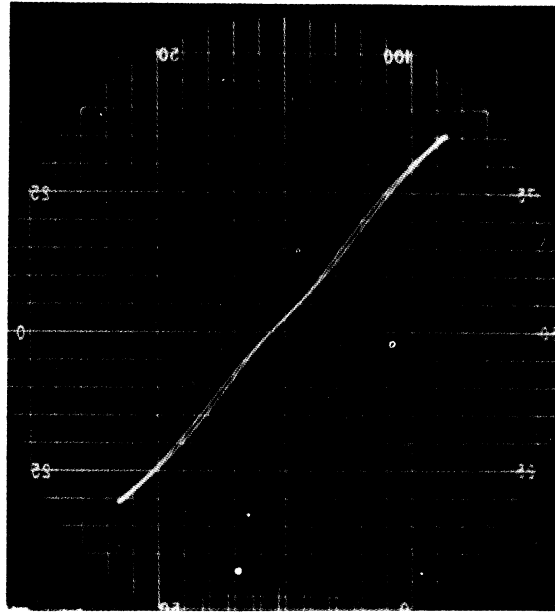
FIG. 21

THE P-E HYSTERESIS LOOP AND THE CORRESPONDING ϵ-E
BUTTERFLY LOOP IN THE CENTRALAB D-31 FERROELECTRIC CERAMIC

is necessary to use point by point plotting techniques. A butterfly loop obtained in this manner for the Centralab D-31 body is shown in Fig. 22. For convenience, the incremental capacity, which is proportional to the ϵ_Δ of the sample is plotted against the applied field. For this curve the details of the ϵ_Δ- E hysteresis are clearly seen.

2.8 The Dynamic Butterfly Loop Plotter

The complete circuit of the dynamic butterfly loop plotter, shown in Fig. 23, consists of three sections: (a) a free running multi-vibrator and integrator, (b) a high voltage amplifier, and (c) the display network. The square wave output from the multivibrator is integrated by the series resistance R, and the 1 mfd capacitor, C_i, producing a triangularly shaped wave. This triangle wave is fed to the grid of the Eimac 25T high voltage amplifier. The amplified wave is then placed across the capacitor, C, being tested, via the .5 megohm decoupling resistor. This high voltage triangle wave which serves as the polarizing voltage for the test capacitor, is sampled and fed to the X input of the oscilloscope. The circuit parameters shown in Fig. 23 are chosen to produce a low frequency triangle wave of about .5 cycles per second; higher frequency polarizing voltages may be obtained by changing the multivibrator and integrator time constants. To obtain the presentation of the incremental capacity, a low voltage audio frequency signal is also fed to the test capacitor through the .01 mfd 2000 v coupling capacitor. The audio frequency current through the test capacitor is essentially limited by its rather large capacitive reactance, the value of which changes over the long term[1] polarizing cycle.

---

[1] i.e. produced by the low frequency triangle wave
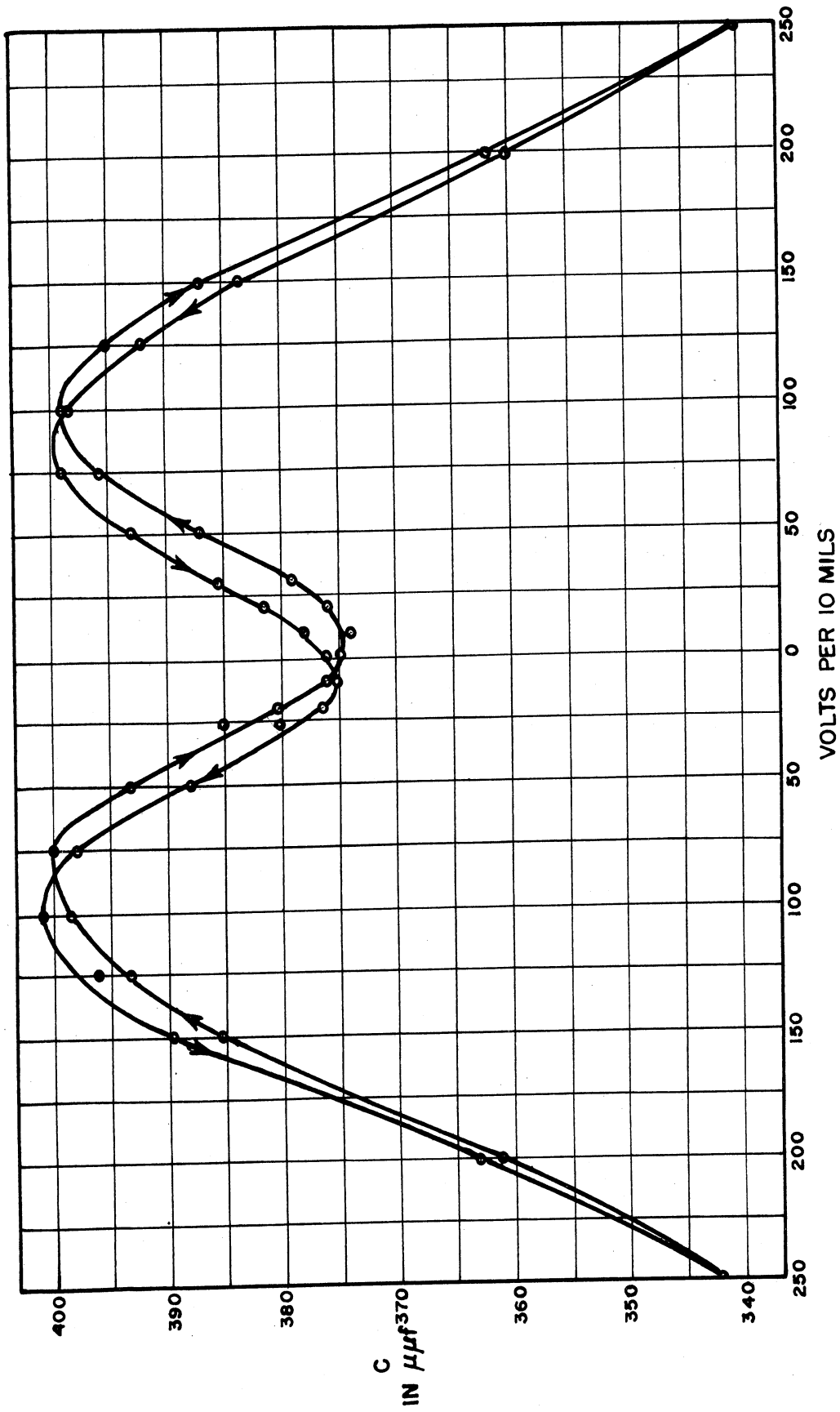
FIG. 22   THE STATIC CAPACITY-FIELD BUTTERFLY LOOP FOR THE CENTRALAB D-31
FERROELECTRIC CERAMIC

45

CRO
DISPLAY

VOLTAGE WAVEFORM
APPLIED TO SAMPLE C

D.C. BUCKING
ADJUST

HUM BUCKING
ADJUST

+500V

−500V

EIMAC
25T

VOLTAGE
AMPLIFIER

6.3V
60~

50ω

+2500V

200 K

−300 V

5 M

5 M

5 M

BIAS
ADJUST

5 M
R

5 M

C₁
1μf

INTEGRATOR

5 M

C

.01μf
2000 V

4.7 M

.33 M

1000ω

.05μf

10 V
1000~

S

+150 V

220K

220K

33 K

33 K

.2

.2

6J6

1

6

7

2

5

3.3 M

3.3 M

MULTIVIBRATOR
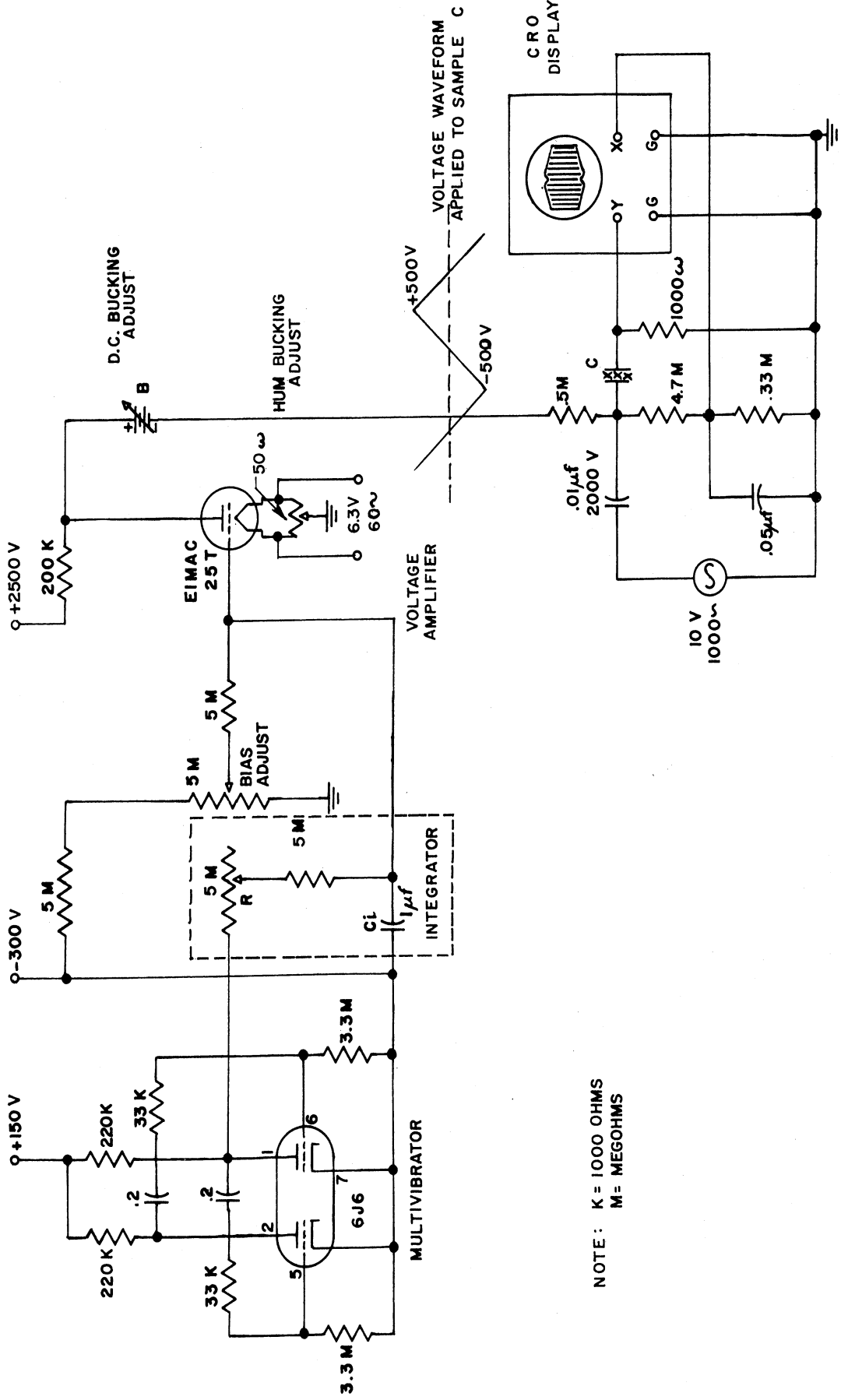
NOTE: K = 1000 OHMS
M = MEGOHMS

FIG. 23

CIRCUIT OF THE DYNAMIC BUTTERFLY-LOOP PLOTTER

46

The current is converted to a voltage drop across the 1000 ohm resistor, and

this voltage, which is proportional to the instantaneous value of capacity of C,

is fed to the Y terminal of the oscilloscope. The battery, B, is used to set the

center point for the excursion of the triangular wave polarizing field.

2.9 Barkhausen Noise Measurements

Measurements were made of the Barkhausen noise in ferroelectric

materials in order to determine its effect in low level tuned circuits employ-

ing these materials. To make these measurements an analyzer has been construct-

ed as shown by the block diagram of Fig. 24. The specimen is immersed in a

constant temperature oil bath, and a 60 cycle sinusoidal field is applied by

means of a high voltage transformer and a low pass filter which gives at least

70 db rejection of the line transients and other noise above 5 kc. The high

pass filter passes the Barkhausen noise unattenuated above 30 kc but offers

at least 70 db rejection of all power and noise voltage components below 10 kc.

The noise from the output of the high pass filter is amplifier by a low noise

battery operated preamplifier feeding a Tektronix model 512 oscilloscope.

Since the Barkhausen noise varies in a cyclic manner, depending upon

the phase of the applied cyclic field as shown in Fig. 25, a sampling technique

is required in making quantitative measurements. The block in Fig. 24 shown as

"Noise Measuring Equipment" consists of six sub-units:

      (a) Gate Generator

      (b) Gated Amplifier

      (c) Thermocouple

HIGH VOLTAGE XFMR — LOW PASS FILTER — SPECIMEN HOLDER — HIGH PASS FILTER — LOW NOISE PREAMP.

110V 60~

NOISE MEAS. EQUIPMENT — CRO
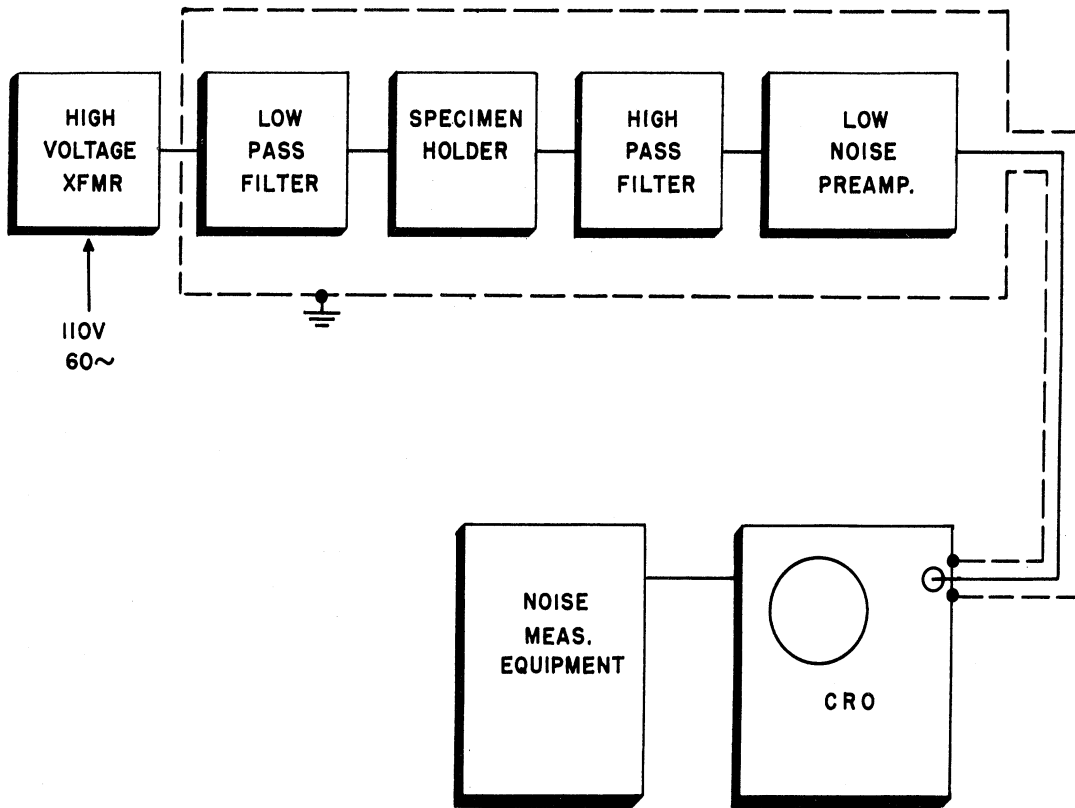
FIG. 24

BLOCK DIAGRAM
OF BARKHAUSEN NOISE ANALYSING EQUIPMENT.

48
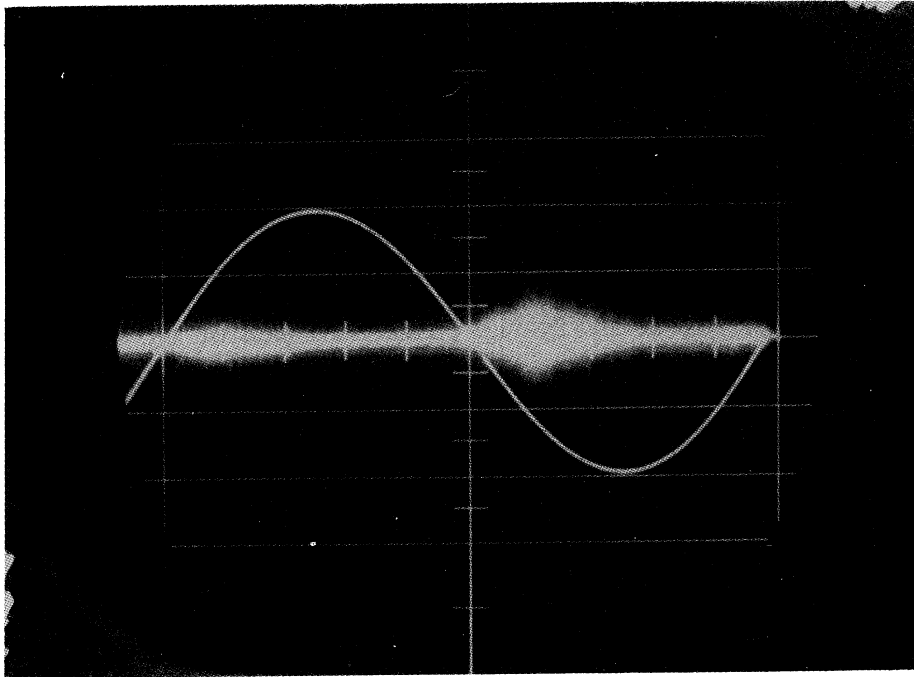
FIG. 25

BARKHAUSEN NOISE IN AEROVOX HI-Q 41
AT 27°C.

(d) Chopper

(e) Tuned Amplifier

(f) Detector and Meter Indicator

This equipment permits the measurement of noise output over any desired small

portion of the 60 cycle wave over a bandwidth of 30 kc to approximately 1 mc.

This is performed by taking a small sample of the noise from each cycle and

averaging the result. To identify the phase position of the sampling gate, a

portion of the gate voltage is used to intensify the trace on the oscilloscope.

The gate width for all measurements was 1.5 milliseconds.

Fig. 25 shows the qualitative display of the Barkhausen noise as a

function of the phase of the applied cyclic field. The phase of the 60 cycle

applied field is indicated on the oscillogram by superimposing sine wave

voltage on the same photograph as the noise. It is seen that the bulk of the

Barkhausen noise is produced just after the field passes through zero. These

regions correspond to the steep portion of the P - E loop where the number and

size of the Barkhausen jumps are both relatively large. As the temperature is

raised slightly above the Curie, the noise maximum is shifted to higher fields

because of the Curie shift with field.

The quantitative results of the Barkhausen noise as a function of the

maximum applied cyclic field, the phase of the applied field, and the tempera-

ture, are given in terms of noise currents. The actual measured quantity was

the RMS noise voltage across a 6600 ohm resistor in the detecting circuit.

Figs. 26A and B show the results for two samples of ferroelectric ceramic, Aerovox

Hi-Q body 41, and Glenco K-3300. Fig. 27 shows the corresponding capacitance vs.

temperature curves for these samples. The Barkausen noise current is shown as a

function of the phase of the applied field. The maximum field is used for
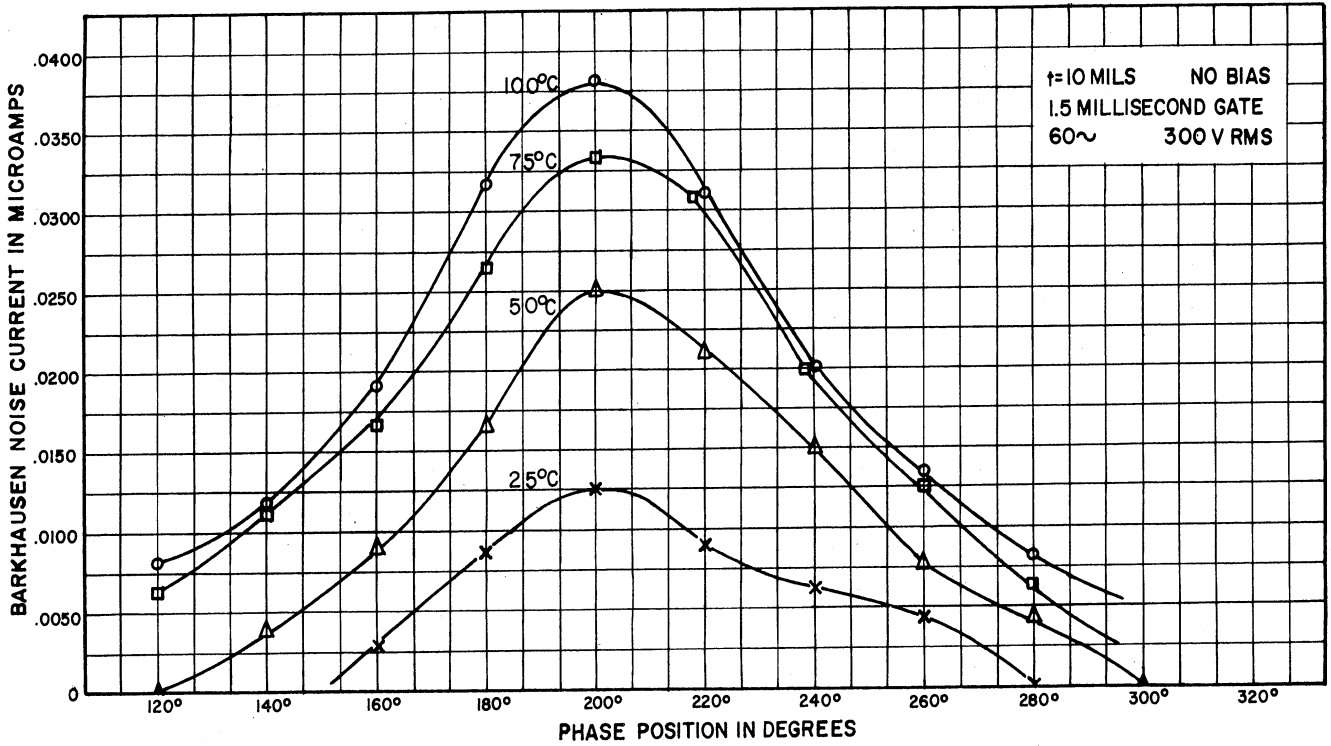
A. BARKHAUSEN NOISE IN A GLENCO K 3300 BODY
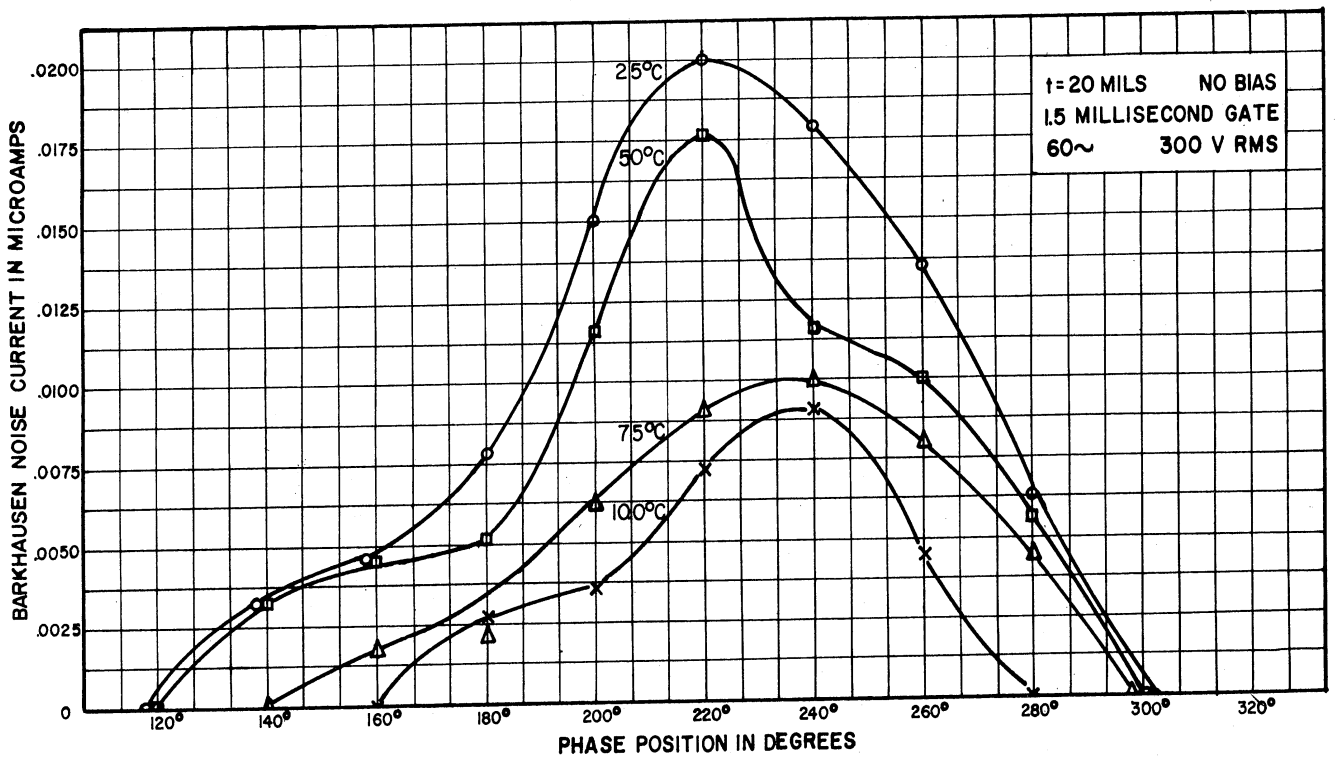
B. BARKHAUSEN NOISE IN AN AEROVOX HI Q 41 BODY

FIG. 26

BARKHAUSEN NOISE IN FERROELECTRIC CERAMICS
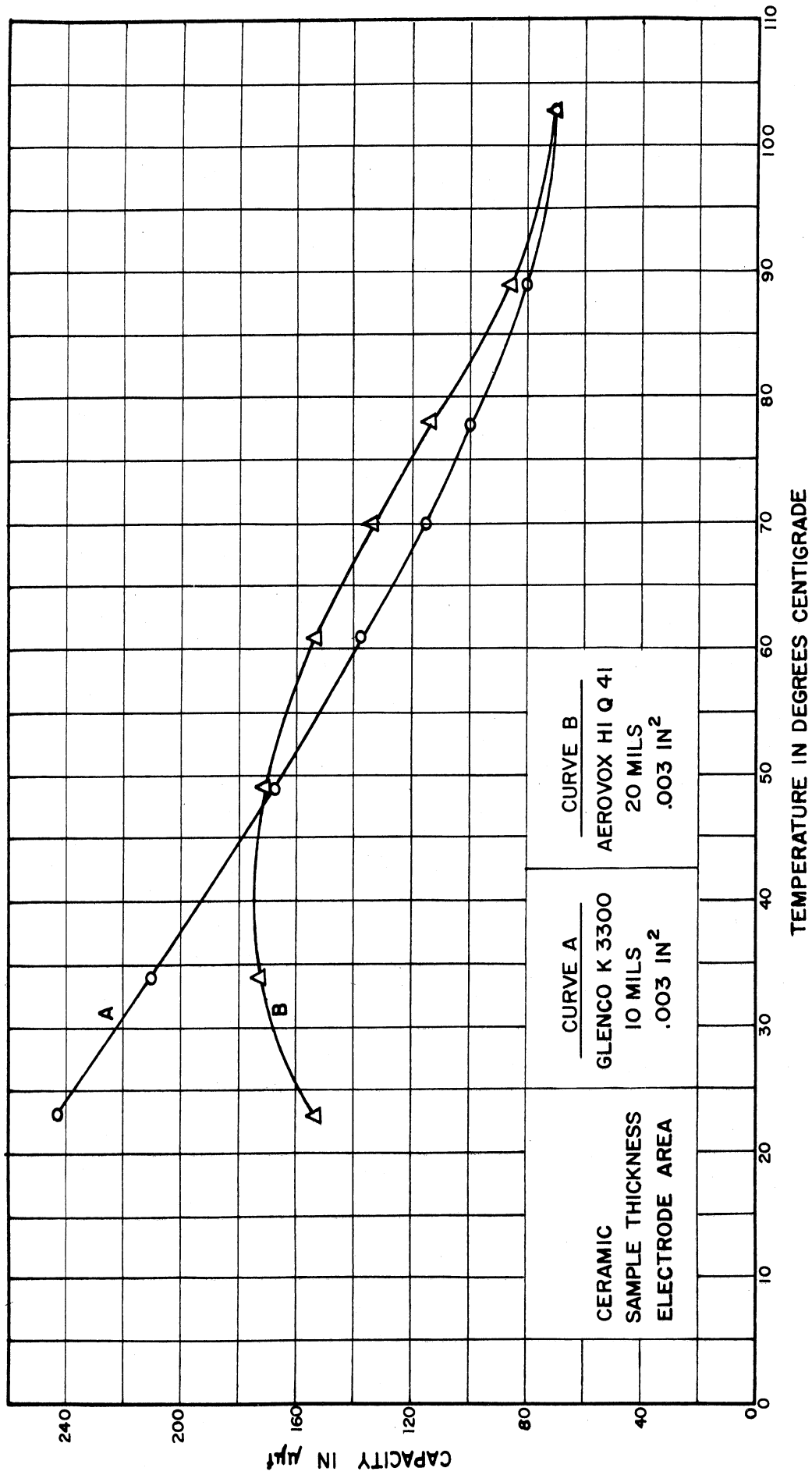
CAPACITANCE VS TEMPERATURE FOR CERAMIC BODIES OF FIG. 26

FIG. 27

TEMPERATURE IN DEGREES CENTIGRADE

CAPACITY IN µµf

	CURVE A	CURVE B
CERAMIC	GLENCO K 3300	AEROVOX HI Q 41
SAMPLE THICKNESS	10 MILS	20 MILS
ELECTRODE AREA	.003 IN^2	.003 IN^2

52

the samples was 40 volts per mil for the K-3300 body and 20 volts per mil for the

Hi-Q 41 body. It is noticed that for the temperature range considered, the noise

for the K-3300 body increases with temperature while the noise for the Hi-Q 41

body is reduced with an increasing temperature. The total noise (ungated noise)

current dependence on driving field is shown for the K-3300 body in Fig. 28.

As is expected, the total noise increases with the driving field since the net

number of domains that are switched increases with an increasing field.

Fig. 29 shows the realative phase and the comparative magnitudes of the

Barkhausen noise currents and the ferroelectric capacitor changing current with

an applied 60 cycle driving field of 40 volts per mil. This is for the K-3300

body.

When this particular ferroelectric sample was charged by a 60 cycle cur-

rent, the largest observed value of gated RMS noise current (in a frequency band

30 kc to 1 mc) was .013 x 10^{-6} amperes when the instantaneous value of charging

current to 45 x 10^{-6} amperes. Thus the ratio of gated RMS noise current to

instantaneous charging current is of the order of 10^{-3}.

The upper figure in the oscillograph shown in Fig. 30 is a display of

the charging current super-imposed upon the 60 cycle sine wave drive. The

lower figure of the oscillograph is the P-E hysteresis loop for this material.

It is noticed from Fig. 29 and Fig. 30 that the maximum charging

current does not quite coincide with the maximum noise current. This is, how-

ever, to be expected since the maximum noise current is found where the polari-

zation goes through zero but the charging current per unit area is given as

$$\frac{dP}{dt} = \frac{dP}{dE} \cdot \frac{dE}{dt} \qquad ,$$
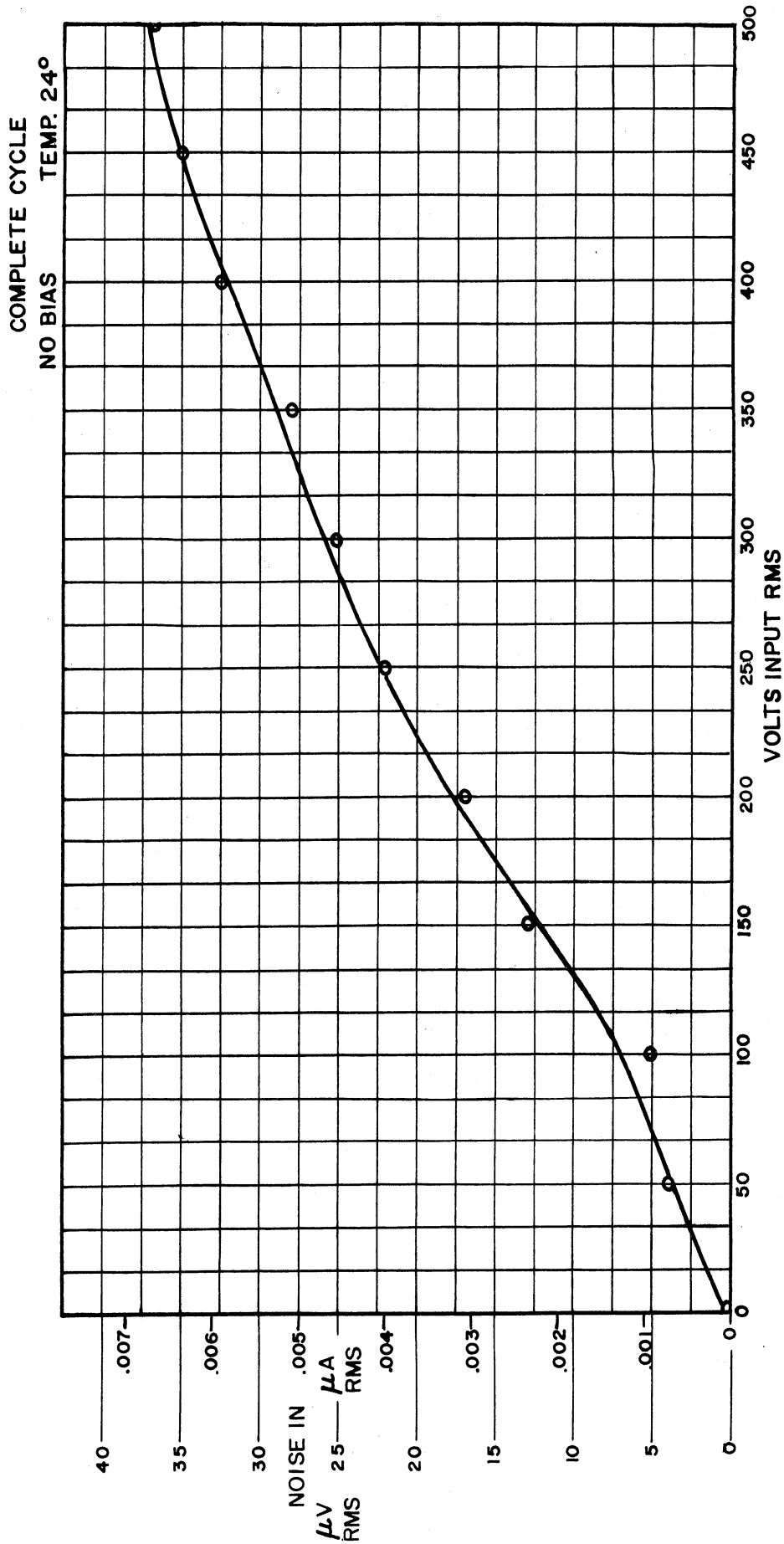
FIG. 28 TOTAL BARKHAUSEN NOISE DEPENDENCE UPON THE AMPLITUDE
OF AN APPLIED CYCLIC FIELD FOR THE GLENCO K 3300 FERROELECTRIC
CERAMIC

54
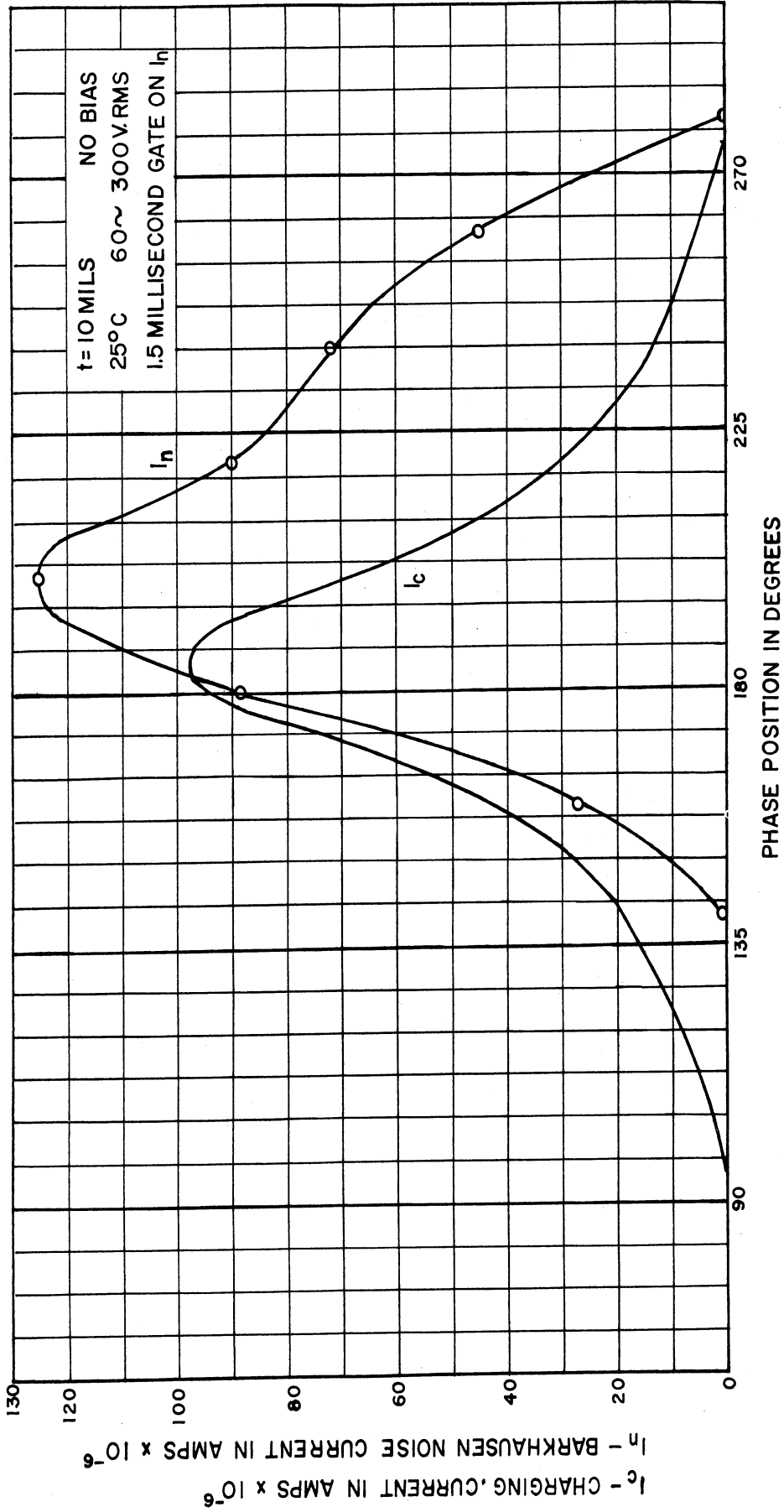
FIG. 29

BARKHAUSEN NOISE AND CHARGING CURRENT
IN A GLENCO K 3300 FERROELECTRIC CERAMIC

t = 10 MILS   NO BIAS
25°C   60~ 300 V.RMS
1.5 MILLISECOND GATE ON I_n

I_n

I_c

PHASE POSITION IN DEGREES

I_n – BARKHAUSEN NOISE CURRENT IN AMPS x 10^{-6}

I_c – CHARGING CURRENT IN AMPS x 10^{-6}
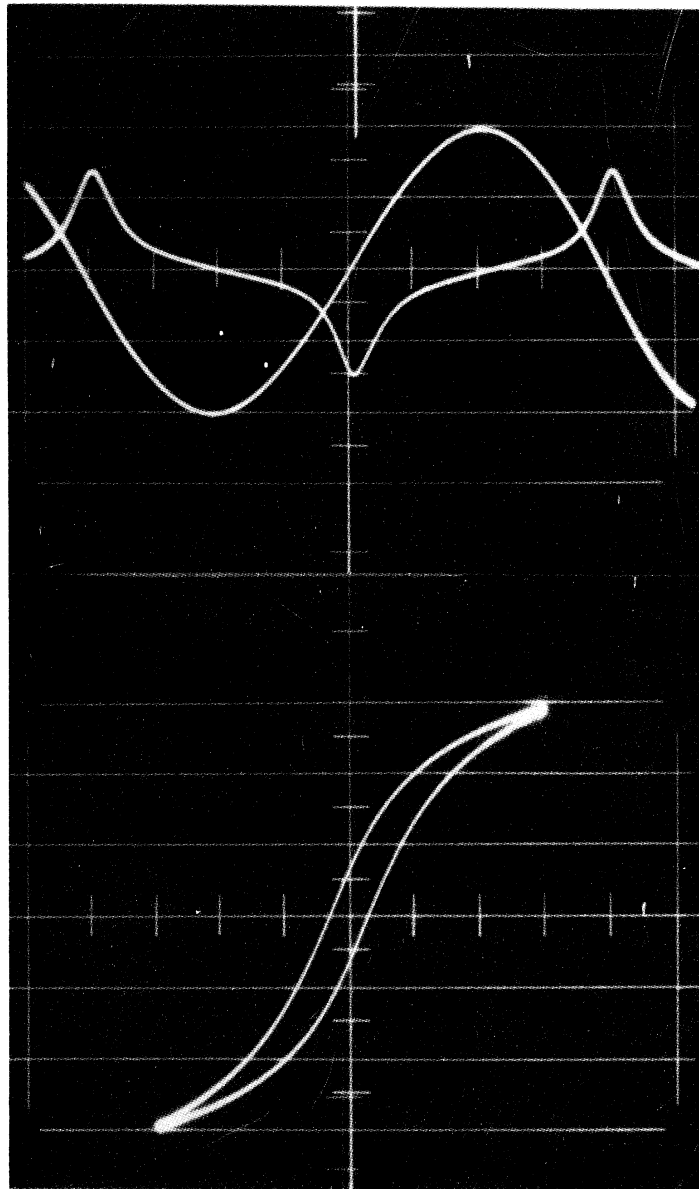
FIG. 30

ABOVE: CHARGING CURRENT WAVEFORM SUPERIMPOSED ON
THE 60 CYCLE DRIVING FIELD FOR THE GLENCO
K-3300 FERROELECTRIC CERAMIC

BELOW: P-E HYSTERESIS LOOP FOR THE SAME MATERIAL

and $\left[\dfrac{dE}{dt}\right]$ is maximum where the 60 cycle field goes through zero but $\left[\dfrac{dP}{dE}\right]$ is

usually maximum where the polarization is zero. Thus the maximum charging

current per unit area, $\left[\dfrac{dP}{dt}\right]_{max}$ is somewhere in between $\left[\dfrac{dP}{dE}\right]_{max}$ and $\left[\dfrac{dE}{dt}\right]_{max}$.

A more detailed presentation of the data and a complete description

of the measuring circuits will be covered in a separate Technical Report;

Electronic Defense Group Technical Report No. 34, entitled "Barkhausen Noise

Measurements in Titanate Ceramics", to be issued.

2.10 The Effect of Frequency on Dielectric Constant and Q

High frequency measurements were made of the dielectric constant and

Q on several typical ferroelectric ceramics. The capacitors used for the

measurement were the low capacity units described earlier in this report. The

high frequency measurements were made with a Boonton 190A high frequency Q

meter. In order to minimize the effect of the lead inductance, the samples were

mounted as close as possible to the Q-meter terminals. (Only one centimeter

of total lead length was used.)

Kittel[1] indicates that the dielectric constant of pure barium titanate

decreases gradually with frequency until about 1000 mc where there is a sharp

decrease to about 10 per cent of the low frequency value. Our results on the

ceramics confirm this behavior within the frequency ranges of our tests, and

as expected, the losses become greater as the frequency increased. The behavior

for typical samples is shown in Figs. 31 and 32.

It is seen that the Q of the better material at 200 mc is around 5,

---

[1]Kittel, Charles, Intro. to Solid State Physics, John Wiley and Son, New York, 1953, Fig. 2-11, p. 130.
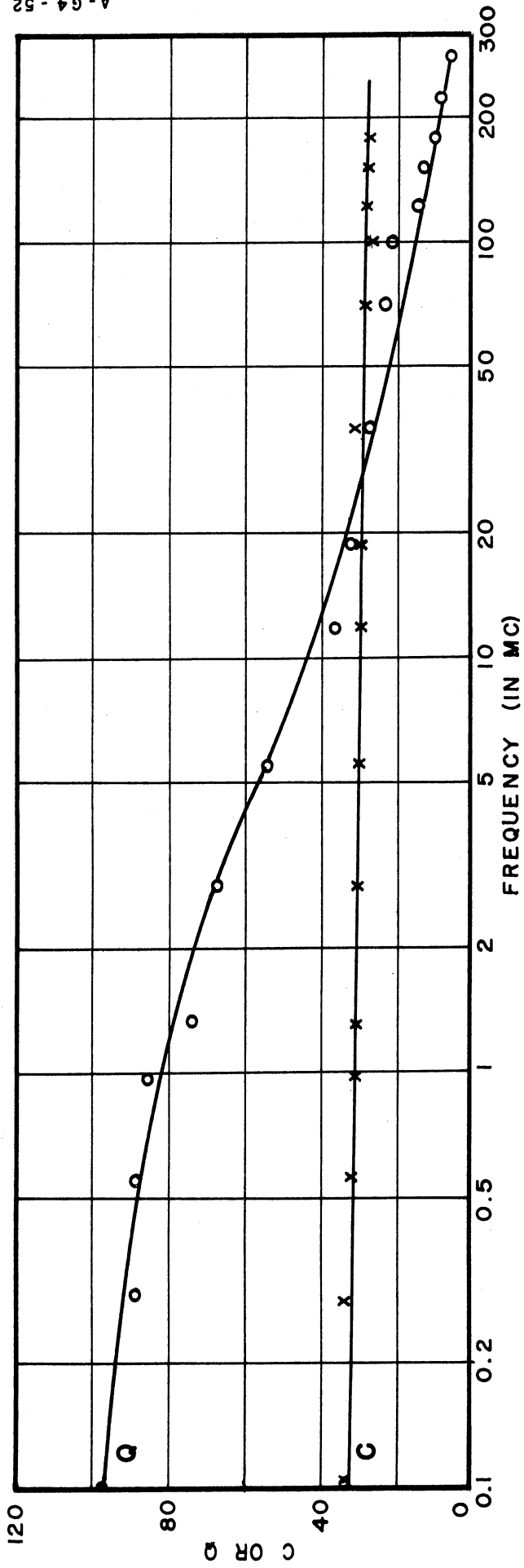
EFFECTIVE AC CAPACITY & Q VS FREQUENCY.
AEROVOX "HI-Q" BODY NO 40 DIELECTRIC WITH
SMALL AC FIELD UNDER CONDITIONS OF ZERO
DC BIAS FIELD.

FIGURE 31

58
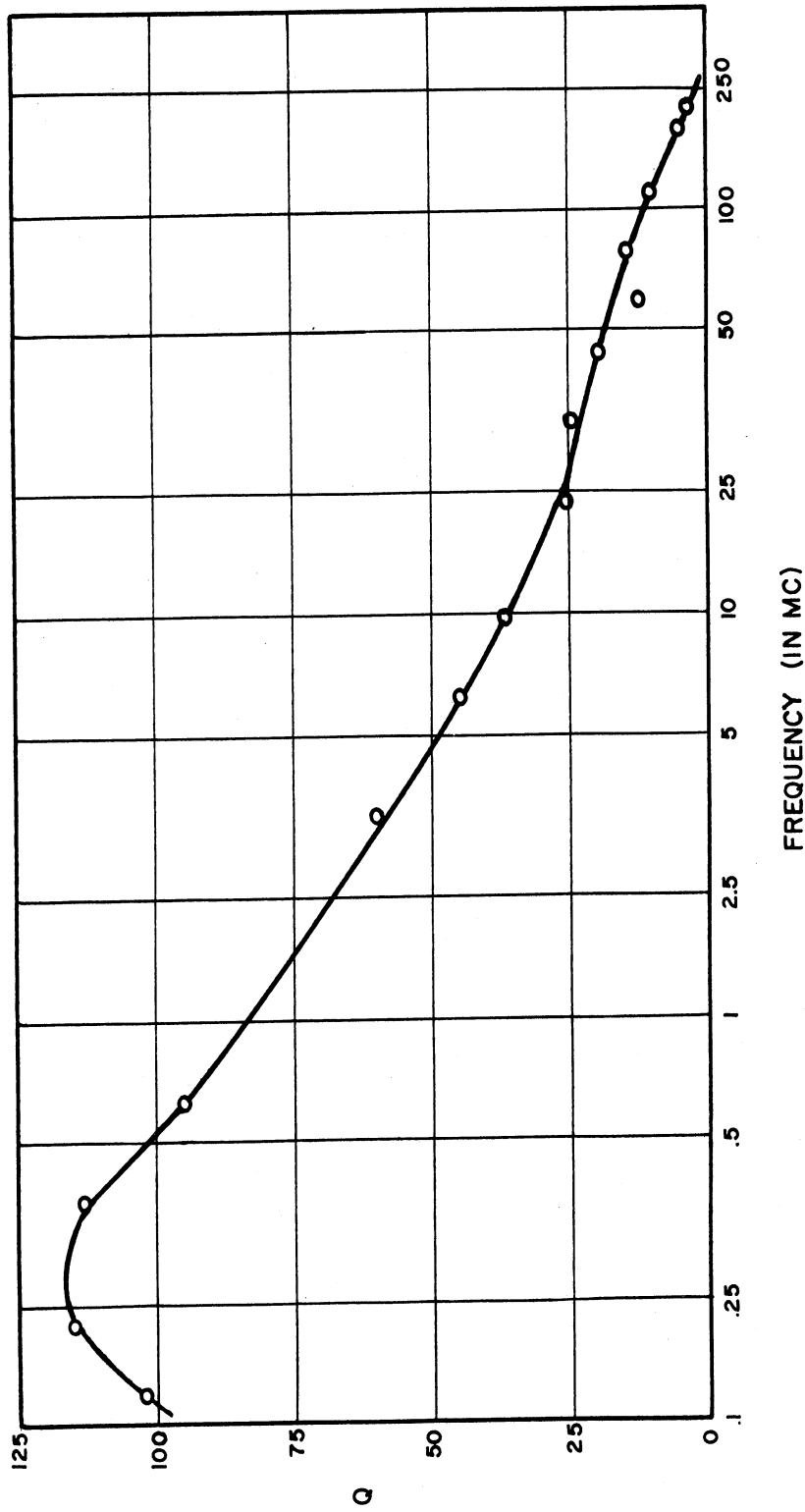
FIG. 32

Q VS FREQUENCY FOR AEROVOX "HI-Q" BODY
NO. 41 DIELECTRIC WITH SMALL AC FIELD
UNDER CONDITIONS OF ZERO DC BIAS FIELD

dropping to about 2 at 300 mc suggesting that the latter frequency may serve as more or less the upper limit for applications of the particular sample in a tuned local oscillator.

To date the measurements of the losses as a function of frequency have been made under conditions of zero DC bias field. However, it has been our experience that the application of a DC bias field has the effect of raising the Q, as measured at low frequencies. A measurement of this effect at very high frequencies is now under consideration.

3. APPLICATIONS OF FERROELECTRIC MATERIALS AS TUNED CIRCUIT ELEMENTS

3.1 Ferroelectric Tuning of a Broadcast Receiver

In order to investigate the tuning capabilities of the titanate capacitors at the lower frequencies, a broadcast band search receiver has been designed and constructed, using the ferroelectric ceramics as tuning elements. This receiver uses a standard superhetrodyne circuit with three ferroelectric tuned stages.

The complete circuit of the broadcast receiver is shown in Fig. 33. It was found necessary to load the radio frequency tanks to increase the bandwidth and hence improve the tracking. The resistor marked R* in the diagram was introduced to achieve oscillator tracking. The decoupling resistors in the polarizing circuit were used to isolate this circuit from the rest of the receiver. A value of 120k ohms was found to be satisfactory in providing decoupling and in giving a sufficiently low time constant in the charging circuit.

In the following sections, each part of the receiver circuit will be discussed in detail.

VARIABLE POLARIZING VOLTAGE INPUT

+200V D.C.

68K

120K

.01 μμf

75 μμf

R*

270K

150 μμf

22K

OSC. TANK

6BE6

NOTE:

TITANATE CAPACITOR

6AL5

150 μμf

150 μμf

1 MEG

.01

IF. TRANS. 460 KC

100K

DET. A.F. OUTPUTS

2.7 MEG

A.V.C.

1 MEG

200 μμf

120K

1 MEG

50K

DET. TANK

.01 μf

.01 μf

6AH6

220K

120K

100K

.01

6BA6

120

.05 μf

IF. TRANS. 460 KC

50K

R.F. TANK

HEATERS OF ALL TUBES

6.3V
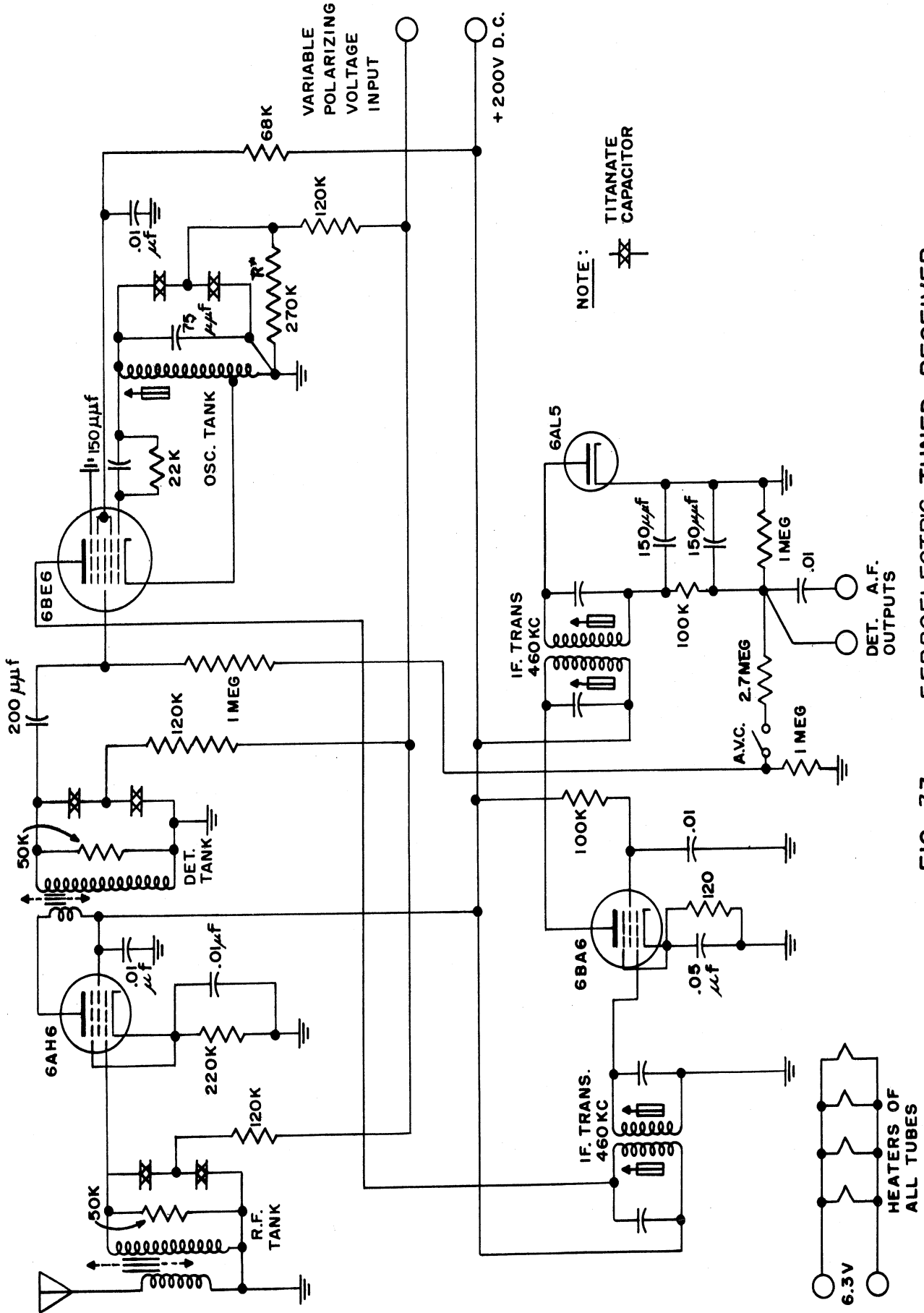
FIG. 33.   FERROELECTRIC-TUNED RECEIVER.

3.1.1 Oscillator Unit. The circuit diagram of the oscillator-mixer stage is shown in Fig. 34.

The oscillator frequency is varied by varying the DC bias applied to the titanate capacitors. Fig. 35 is a tuning curve showing the relationship between the biasing voltage and frequency throughout one cycle of the biasing voltage. It was found that the hysteresis, seen in the figure, increased with the cycling rate.

3.1.2 Polarization Lag. The increase in hysteresis with cycling rate is believed due to the polarization lagging behind the applied electric field. This time lag is considerable for a decreasing voltage, and somewhat shorter for an increasing voltage. To demonstrate the effect, switch S, in Fig 34, was switched from position 1 to position 2, and f_t/f_∞ was plotted as a function of time, t, after the switching. f_t is the oscillator frequency at the time, t, and f_∞ is the ultimate frequency. Frequencies were measured by detecting the oscillator signal with a broadcast receiver. There was no noticeable difference in the data between continuous or intermittent oscillator operation in these tests.

Curve (1) of Fig. 36 shows the ratio f_t/f_∞ for a Centralab k-3500 body, 6 mils thick previously charged at 1000 volts for 10 minutes. Curve (2) is for the same unit charged at 1000 volts for 5 minutes and curve (3) for the same unit charged at 1000 volts for 1 minute. Curve (4) shows the ratio f_t/f_∞ after the polarizing voltage was changed from 1000 volts to 500 volts. Curve (5) shows the response after 1000 volts of polarizing the field is suddenly applied, showing that the response is more rapid on applying the electric field than on removing it.

Fig. 37 shows the polarization lag for the Centralab K-7000, K-6000,
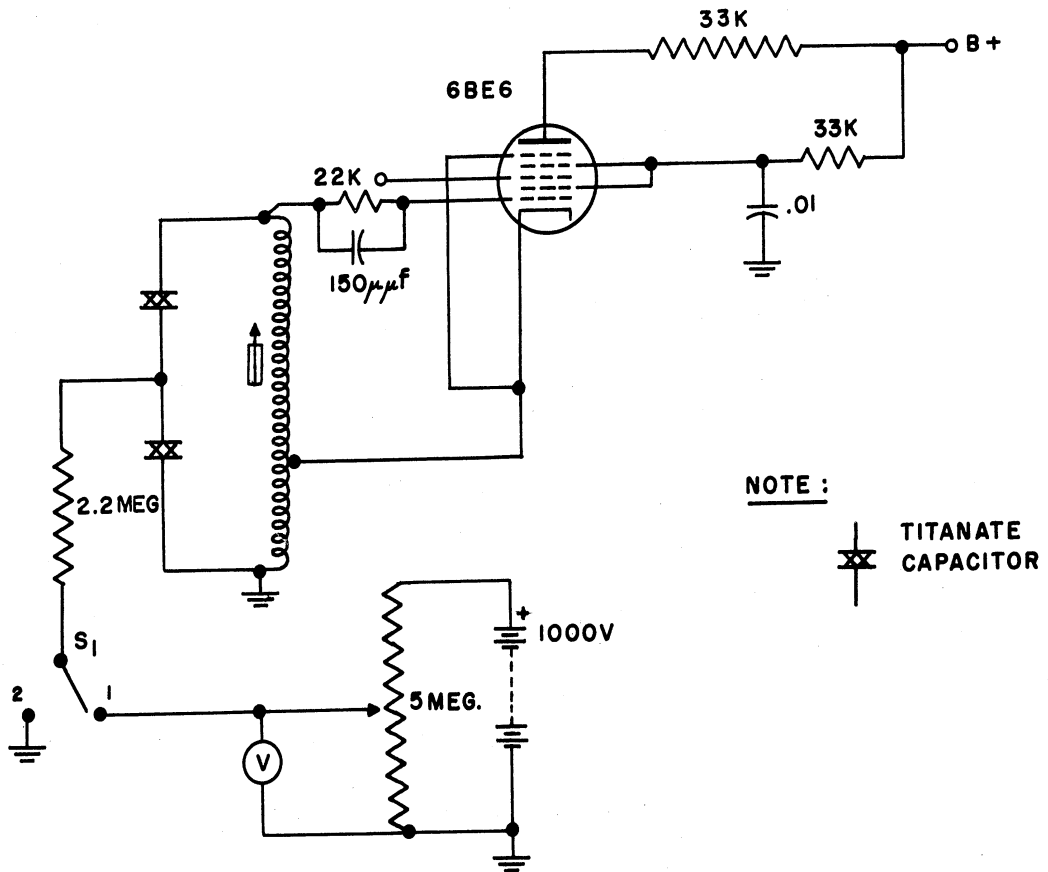
FIG. 34

MIXER – OSCILLATOR
CIRCUIT FOR CHECKING OSCILLATOR PERFORMANCE

THICKNESS OF SAMPLE — 6 MILS.
CENTRALAB K3500.
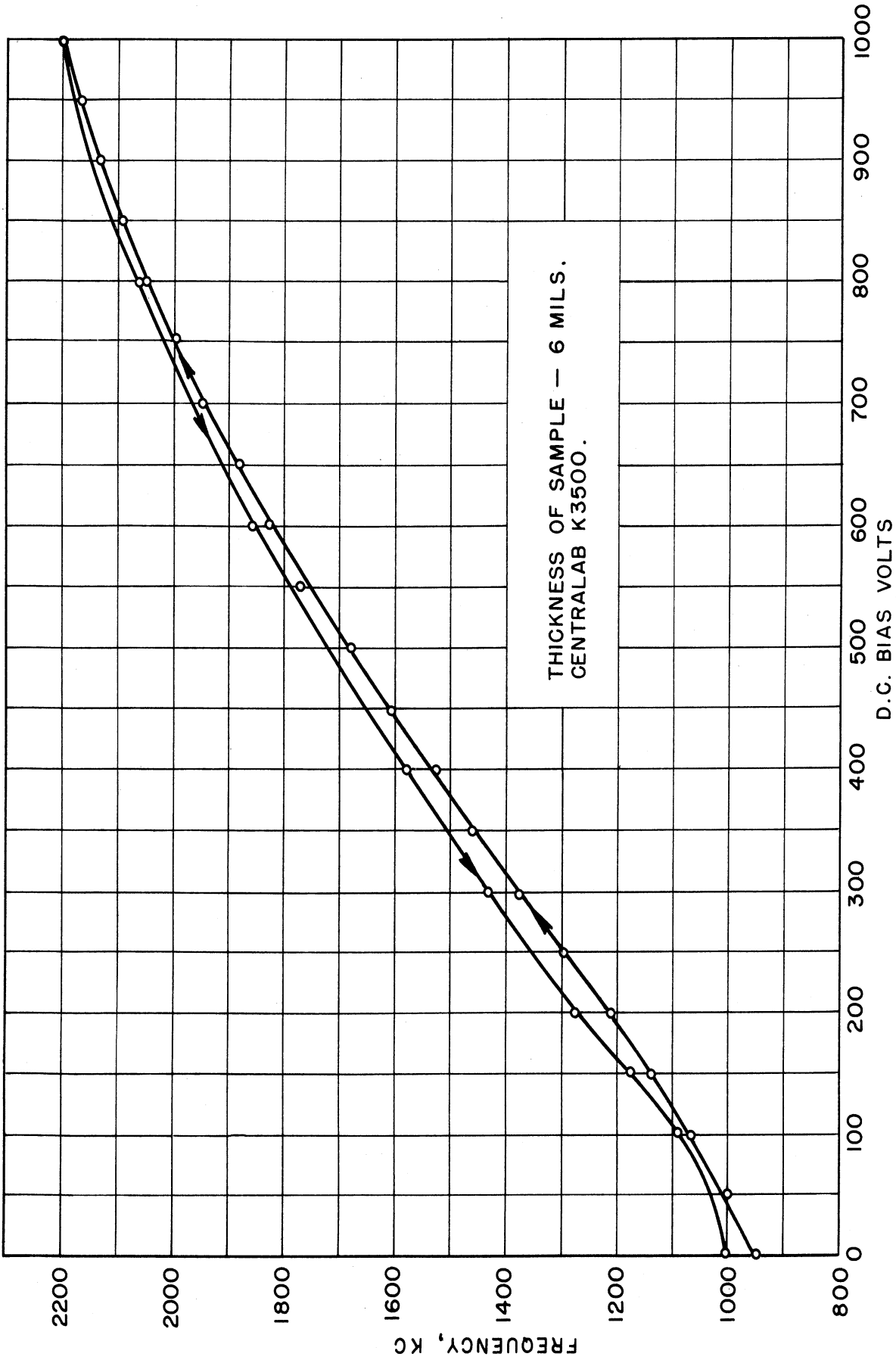
FIG. 35
OSCILLATOR TUNING CURVE.

D.C. BIAS VOLTS

FREQUENCY, KC

CURVE	f_0/f_∞
2	2.2
3	2.2
4	2.2
5	0.45

STARTING FREQUENCY
RATIOS
$t=0$

TIME IN SEC.

f_t/f_∞
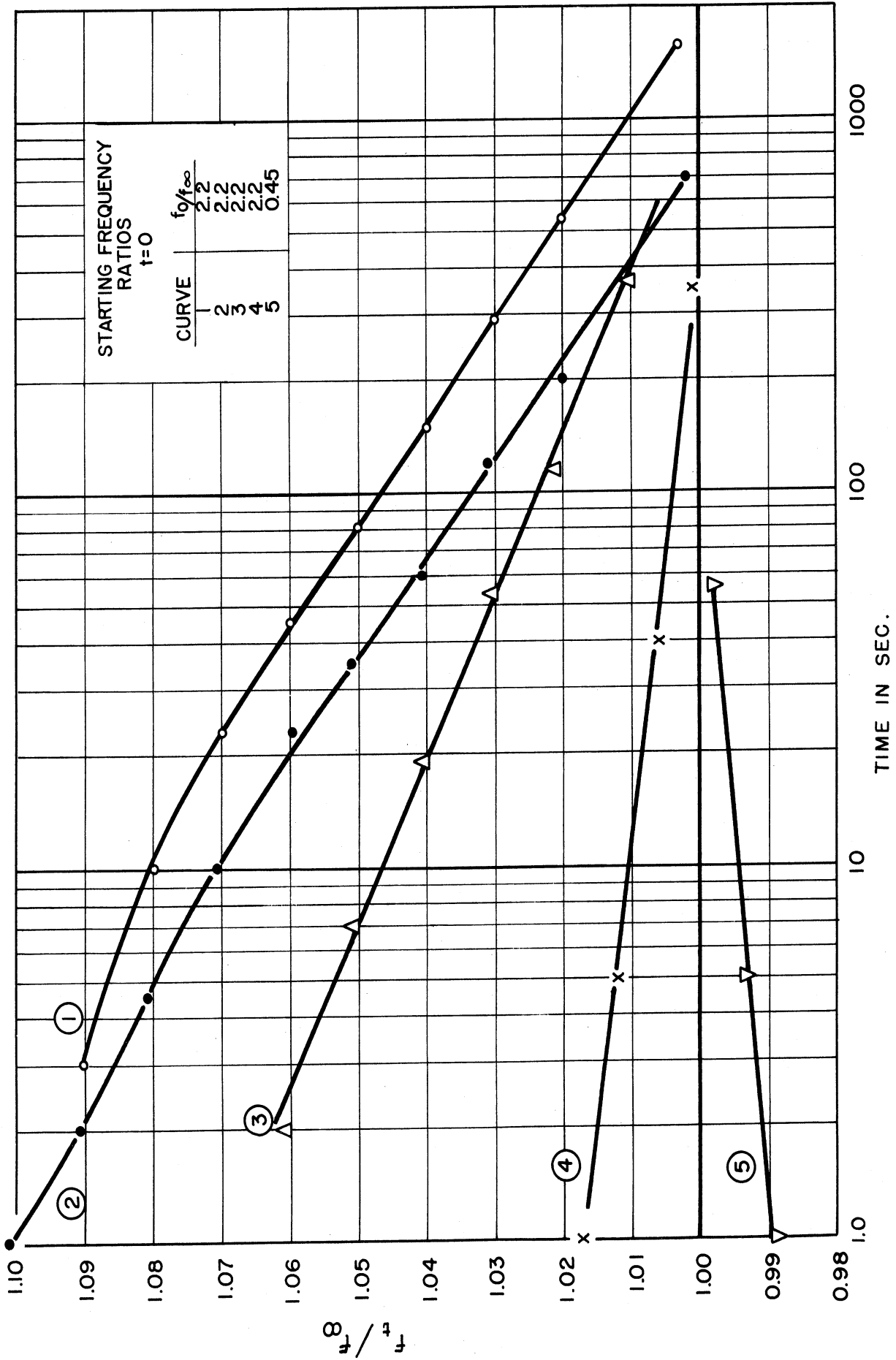
FIG. 36

POLARIZATION LAG FOR CENTRALAB K3500 BODY.
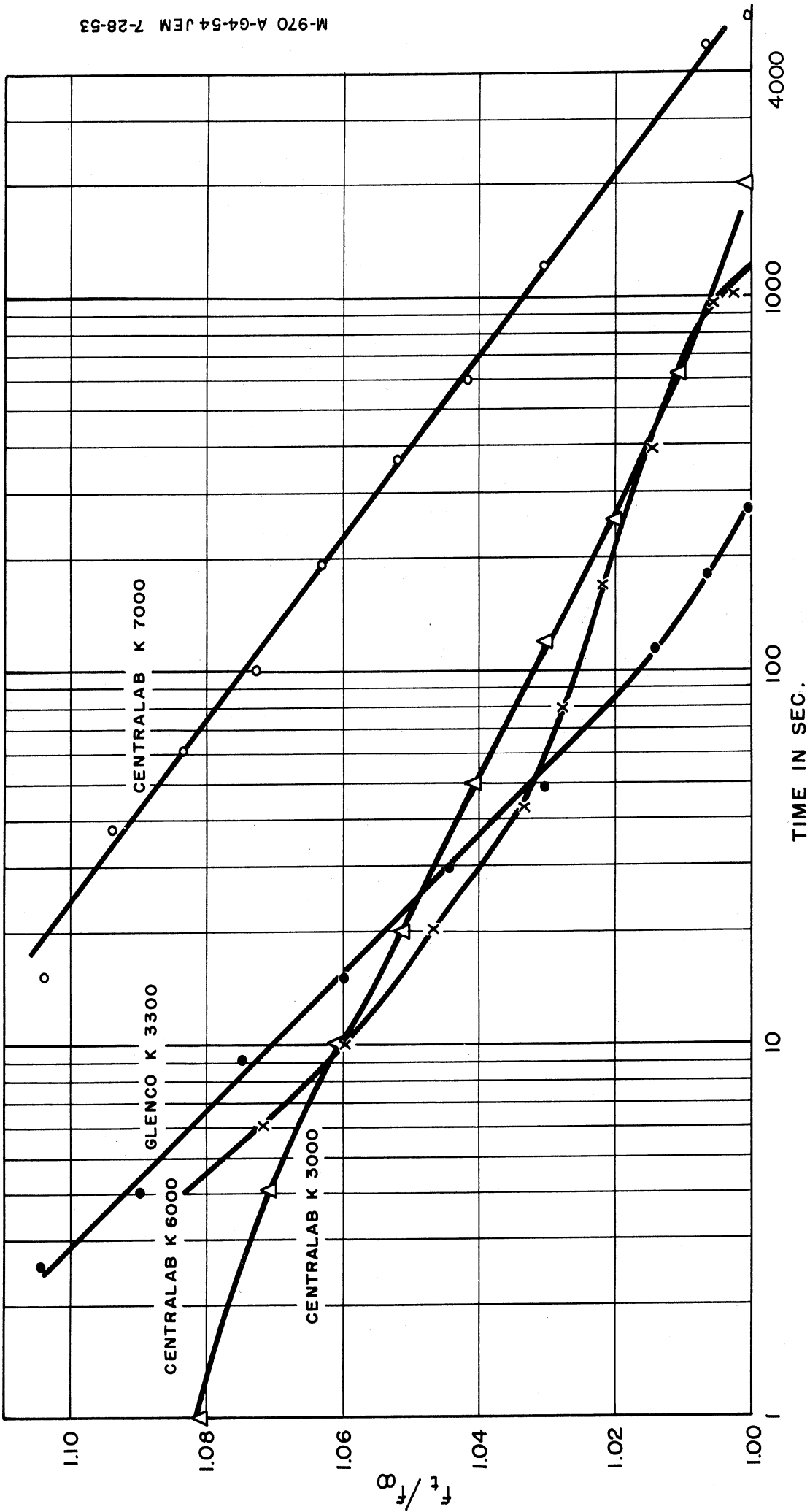
POLARIZATION LAG FOR VARIOUS TITANATE BODIES.

SAMPLES CHARGED TO 100V/MIL FOR 10 MINUTES.

FIG. 37

and K-3500 bodies, and also for the Glenco K-3300 body. The k-6000 body has a large temperature coefficient of capacity and as a result, the accuracy of the measurement suffered. There were also variations from sample to sample. However with the exception of two different samples of the K-6000 body, it was noted that the frequency ratio decayed approximately as a logrithmic function with time.

3.1.3 Temperature Effects. Fig. 38 shows the effect of capacitor temperature on the frequency of the oscillator of Fig. 34. Using two tank capacitors made from a Centralab K-6000 body 10 mils thick, the figure shows curves of frequency vs. polarizing voltage, with temperature as a parameter. For dielectric tuning, materials of dielectric constant in the range 3000-4000 appear to be the most desirable due to their higher temperature stability, and they also seem to withstand a larger polarizing potential than the higher K bodies.

3.1.4 Electronic Sweep Circuit. A sawtooth wave generator was built to impress a 1000 volt sawtooth wave on the polarizing circuit of the receiver. The circuit of this generator is shown in Fig. 39. The sawtooth has a fast rise time and then a nearly linear decreasing voltage. This was employed because of the slower depolarizing described earlier in Section 3.1.2. The sweep rate could be varied from about 10 cps to about 60 cps. The 1000 volt change swept the receiver from 1380 to 1010 k.c. using commercial 400 $\mu\mu$f Glenco type K-3300 capacitors with .010 inch thick dielectric as the tunable elements.

3.1.5 Receiver Output. The output voltage from the receiver was taken from the detector stage and applied to a cathode ray oscilloscope. Fig. 40 shows the local radio spectrum when the polarizing voltage is impressed on the horizontal axis and the detector output on the verticle axis of the
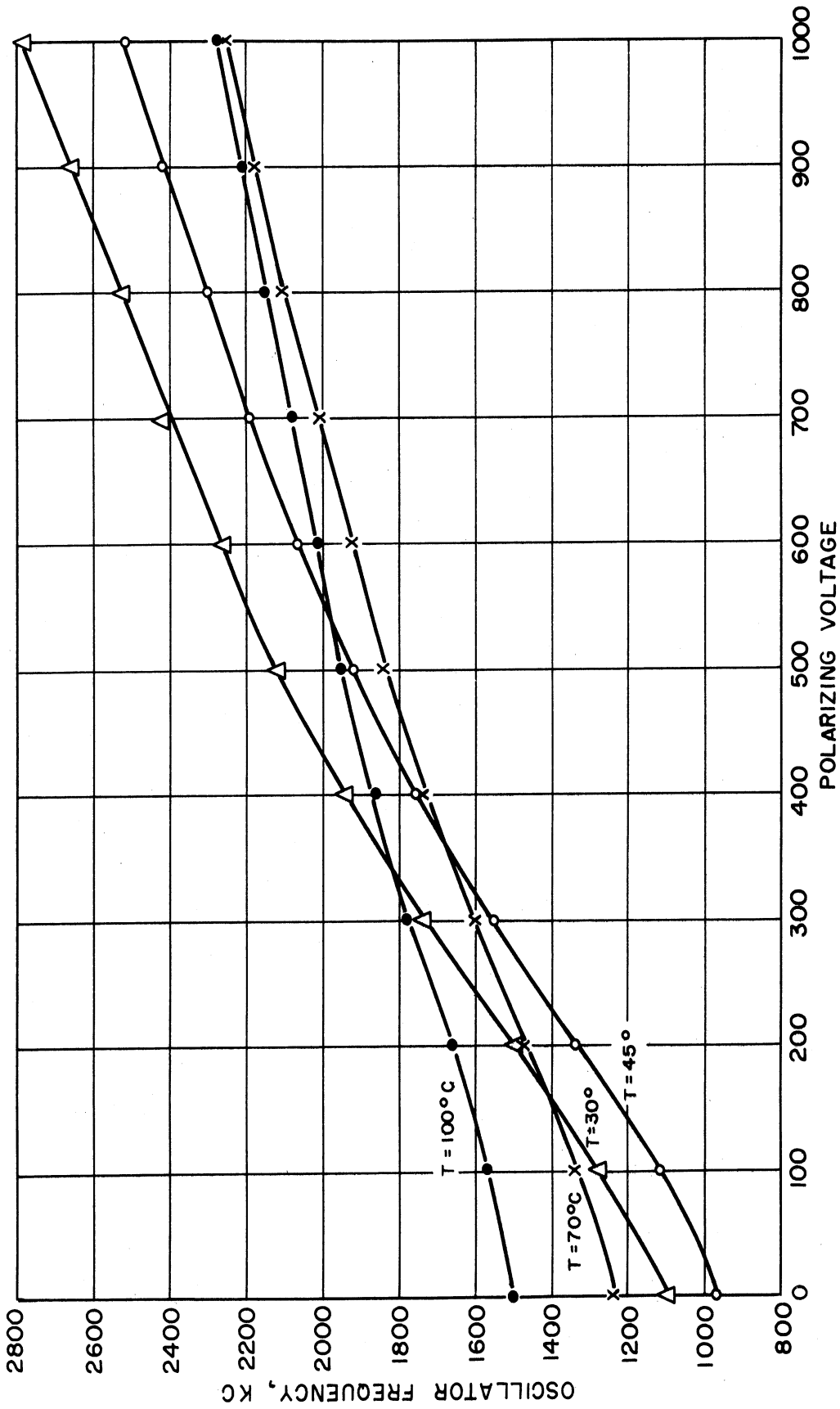
FIG. 38

TEMPERATURE EFFECT ON TUNING.

CENTRALAB K6000. THICKNESS OF SAMPLE = 6 MILS.

OUT PUT

EIMAC 25T

5MEG ③

200K

0.25 μf

5 MEG

100 Ω
884

5MEG

5MEG

5MEG

②

5MEG

2MEG

5 MEG

2MEG

①

0.5 μf

25K 10W

8 μf

1.0 μf

68K

30μf

10K

30μf

1K

6X5

REVERSED HEATER TRANS.

115V

6.3V

HEATER TRANS.

115V

7.5V

HIGH VOLTAGE TRANS. 1500V

81

115V

HEATER TRANS.

115V

6.3V

HUM ADJ. 15Ω 20W OHMITE DIVIDOHM

15Ω

6.3 V

2 AMP FUSE

S₂

2 AMP FUSE

S₁

115 V
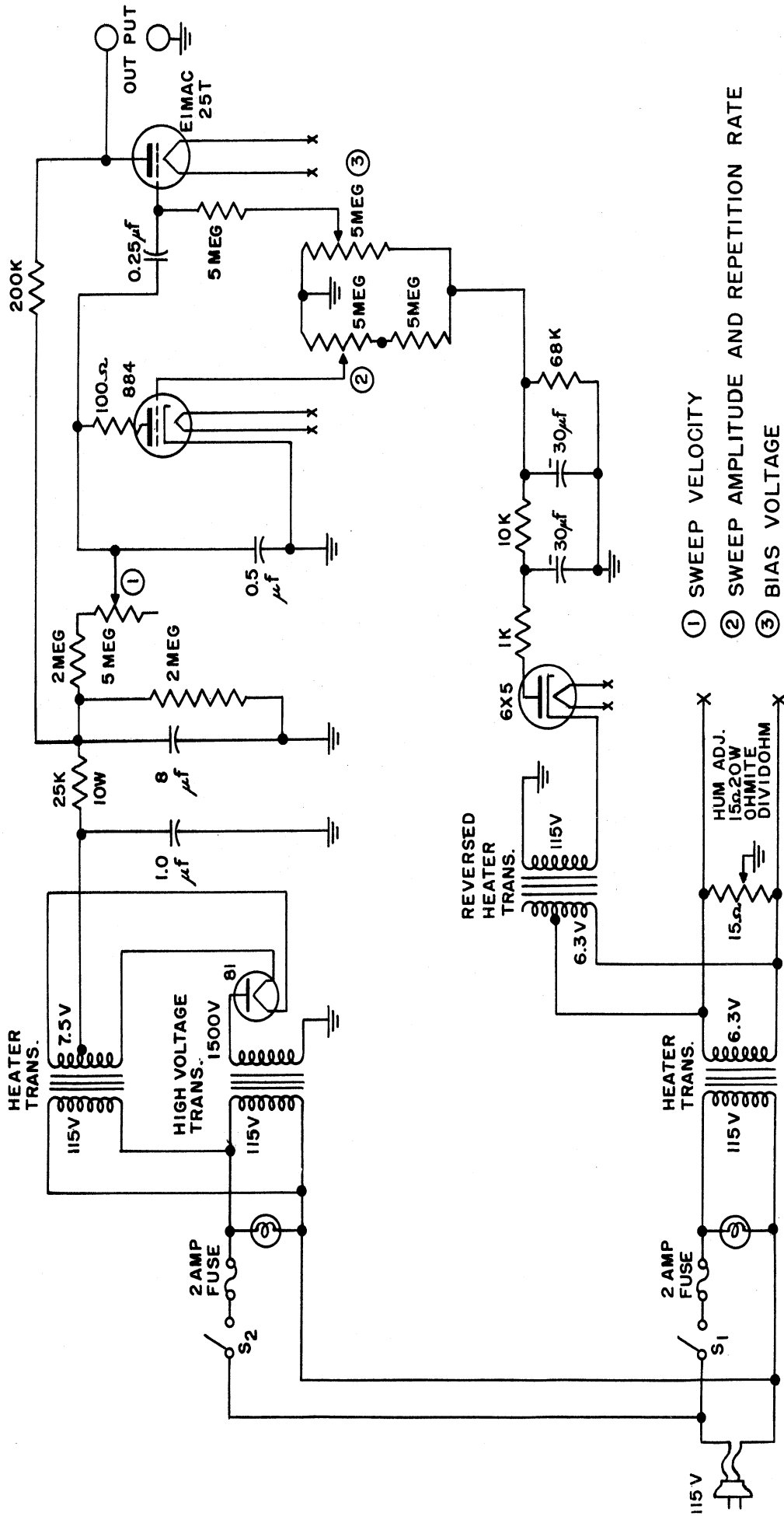
① SWEEP VELOCITY

② SWEEP AMPLITUDE AND REPETITION RATE

③ BIAS VOLTAGE

S₁-HEATER POWER, AND BIAS SWITCH

S₂-HIGH VOLTAGE POWER SWITCH

FIG. 39

SAWTOOTH GENERATOR.
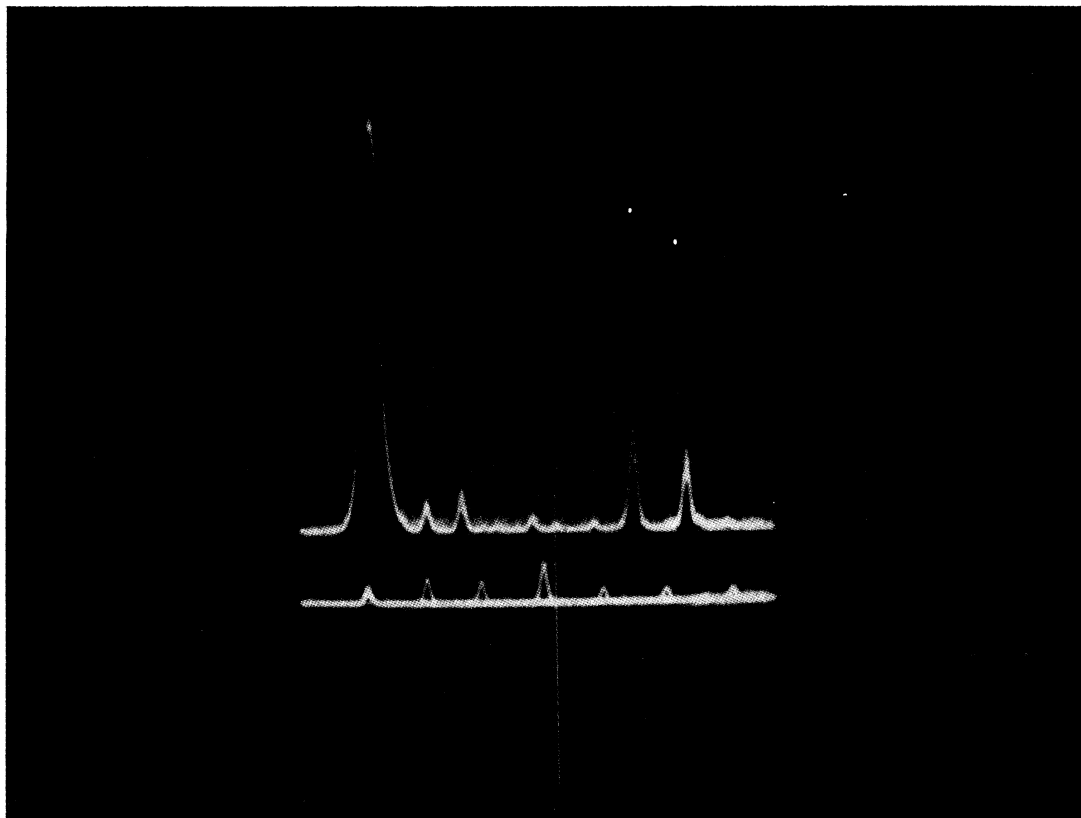
FIG. 40

PANORAMIC DISPLAY OF
RECEIVER OUTPUT.

SWEEP WIDTH = 370 KC
CENTER FREQUENCY = 1200 KC
MARKER SPACING = 50 KC

display oscilloscope. The strong station at the left is WPAG (1050 kc.)
Frequency markers (lower trace) were obtained by multiple exposure and an external signal generator. The markers are separated by 50 kc., the central one
being 1200 kc. These show the frequency sweep to be fairly linear with sweep
voltage. The results obtained are by no means the ultimate that could be attained in sweep width since the latter has been sacrificed in this circuit to
improve the tracking. The circuit employed was designed with three tuned stages
in order to determine whether the tracking problem would be a serious one. With
a little care it was not difficult to obtain good tracking over the tuning
range indicated, and with a little more work it should be possible to track all
three stages over the entire broadcast band. The results obtained for this
receiver using ferroelectric tuning are considered very promising.

3.2 Very High Frequency Swept Oscillators

A survey of various lumped constant oscillator circuits suitable for
dielectric tuning in the high frequency and very high frequency ranges is being
made.

By employing the type of low capacity units that have been previously
described in this report (c.f. Section 2.1.2) in the tank circuit of the high
frequency oscillator shown in Fig. 41, successful operation could be obtained
in most cases for frequencies up to about 110 mc with the ceramics presently
available to us. For the circuit shown in Fig. 41, the frequency of the oscillator, which employs a triode connected 6AH6, could be varied from 50 to 100 mc
by changing the applied biasing field from 0 to 1000 volts when .010 inch thick
dielectric was used in the tank capacitors, C. These capacitors were made from
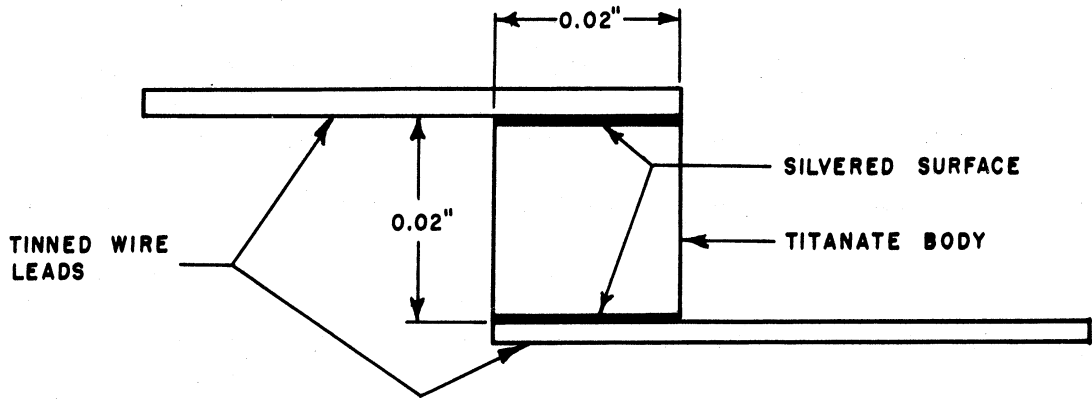
CONSTRUCTION OF THE LOW
VALUE TITANATE CAPACITORS

FIGURE 6

FIG. 41

VERY HIGH FREQUENCY
SWEPT OSCILLATOR CIRCUIT

72
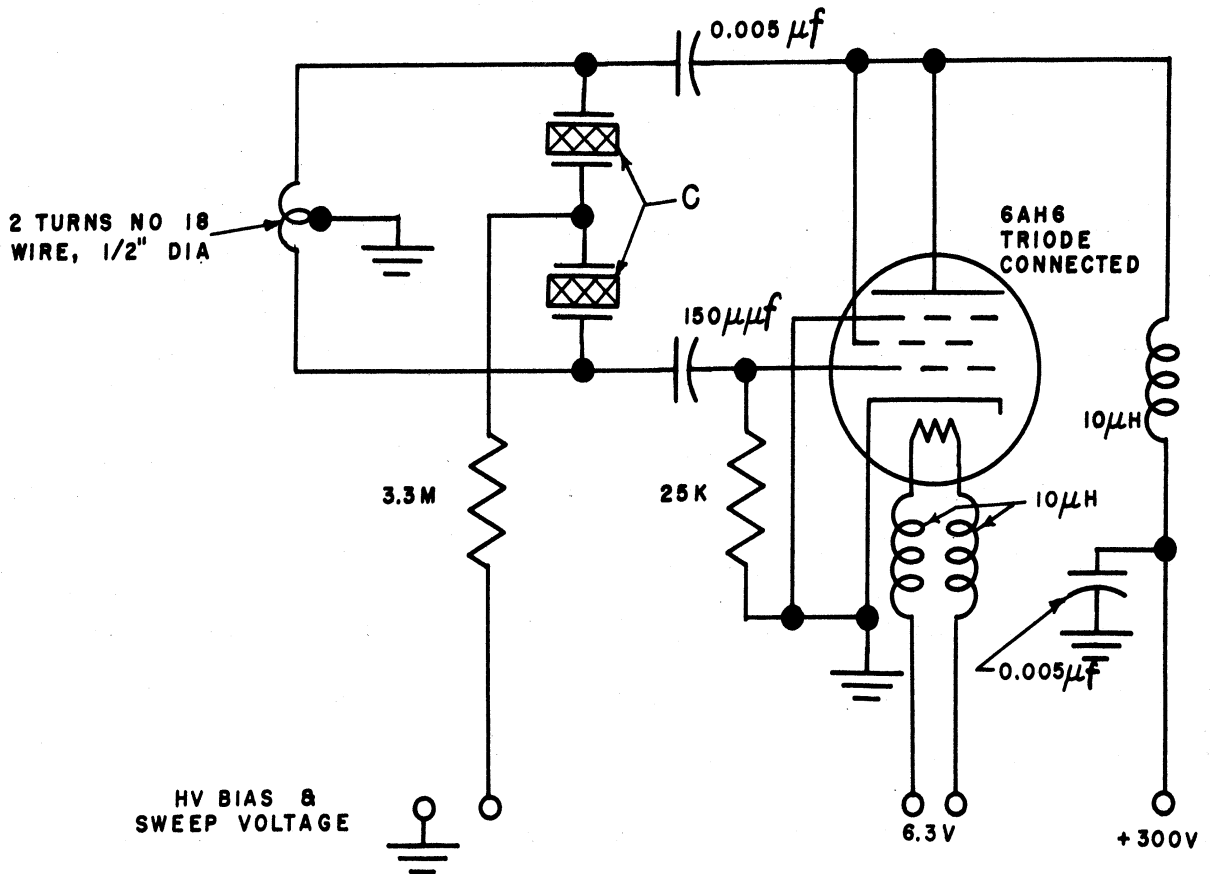
the Glenco K-3300 bodies and from the Aerovox Hi-Q 40 bodies. Each section of the tank capacitor is 120 $\mu\mu$f. Frequencies were measured on both a communications receiver and a grid dip meter using very loose coupling. Point by point techniques were used to obtain the frequency range.

Several other types of circuits have been examined in order to investigate the tunability of very high frequency oscillators using ferroelectric tank elements. Representative results are shown in Table III.

In order to obtain a low rf field across each ferroelectric capacitor and still have the required polarizing field held to resonable values, a low capacity stack was used in some of the VHF oscillators. This device is shown in Fig. 42.

The highest frequency so far observed in lumped-constant electric tuned oscillators was with the ultra audion circuit shown in Fig. 43. The ultra audion circuit utilizes the interelectrode capacitances and lead inductances in such a way that the equivalent circuit is really a Colpitts oscillator. The inductive part of the tank circuit is composed entirely of the grid and plate leads, L_i, while the variable capacitive element, C, is used to vary the resonant frequency of the tank.

The condition for oscillation in a Colpitts circuit may be shown to be approximately

$$ g_m' > \frac{4}{Q}\sqrt{\frac{C}{L}} + G_g \tag{7} $$

where

g_m' - is the effective tube transconductance.

Q   - is the total Q of the resonant circuit.

TABLE III

TUNABILITY OF VERY HIGH FREQUENCY OSCILLATORS USING
FERROELECTRIC TANK ELEMENTS

Frequency Range mc.	Tuning Range[1] in Percent	Range of Bias Field in volts/mil	Capacitive[2] Circuit Element	Type of Oscillator Circuit	Tube Type	g_m
38 - 80	110	0 - 120	C	Push-Pull	6J6	5,300
45 - 80	87	0 - 60	D	Push-Pull	6J4	12,000
50 - 100	100	0 - 100	A	Hartley	6AH6	11,000
95 - 115	21	0 - 60	B	Push-Pull	6J6	5,300
110 - 140	27	0 - 60	B	Colpitts	6J4	12,000
135 - 160	18.5	10 - 60	B	Push-Pull	6J6	5,300
285 - 295	3.6	0 - 50	B	Push-Pull	6J6	5,300
365 - 375	2.7	0 - 60	B	Ultra Audion	6J4	12,000

---

[1]The figure given is the increase in frequency as a percent of the lower frequency.

[2]Element A consists of two Glenco 120 $\mu\mu$f, K-3300 bodies in a series across the tank. Element B is a low capacity stack of six 200 $\mu\mu$f, Glenco K-3300 bodies in a series as shown in Fig. 42. Element C consists of two 400 $\mu\mu$f Glenco K-3300 bodies in series. Element D is two 600 $\mu\mu$f Aerovox Hi-Q body 40 (20 mil) capacitors in series.

FIG. 42

LOW CAPACITY STACK.

DC CONTROL VOLTAGE

NOTE :
R = 5 MEG.
= CERAMIC CAPACITOR

B+

RFC

RF BY-PASS

+ CONTROL VOLTAGE

−

C

RESONANT TANK

6J4

R_g 47K

B−

(a) ACTUAL CIRCUIT

C

C_{gp}

C_{pk}

C_{gk}

L_ℓ
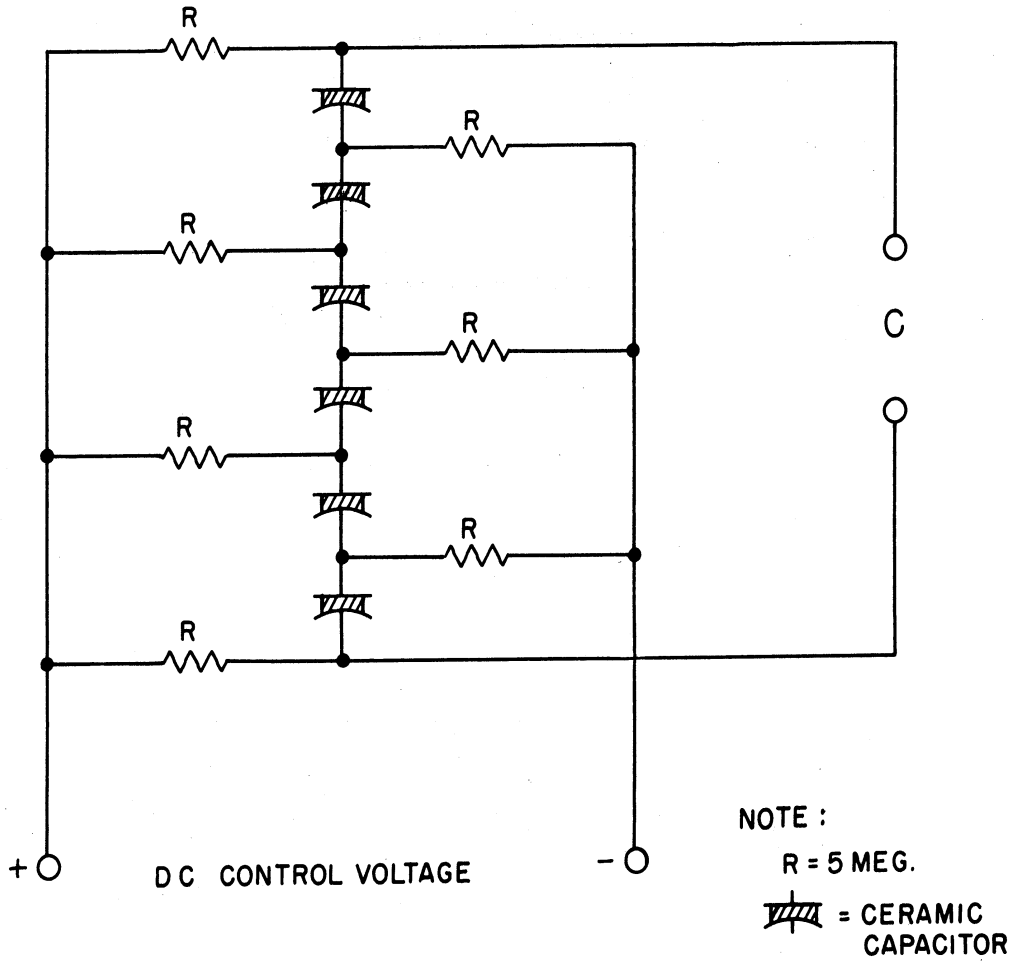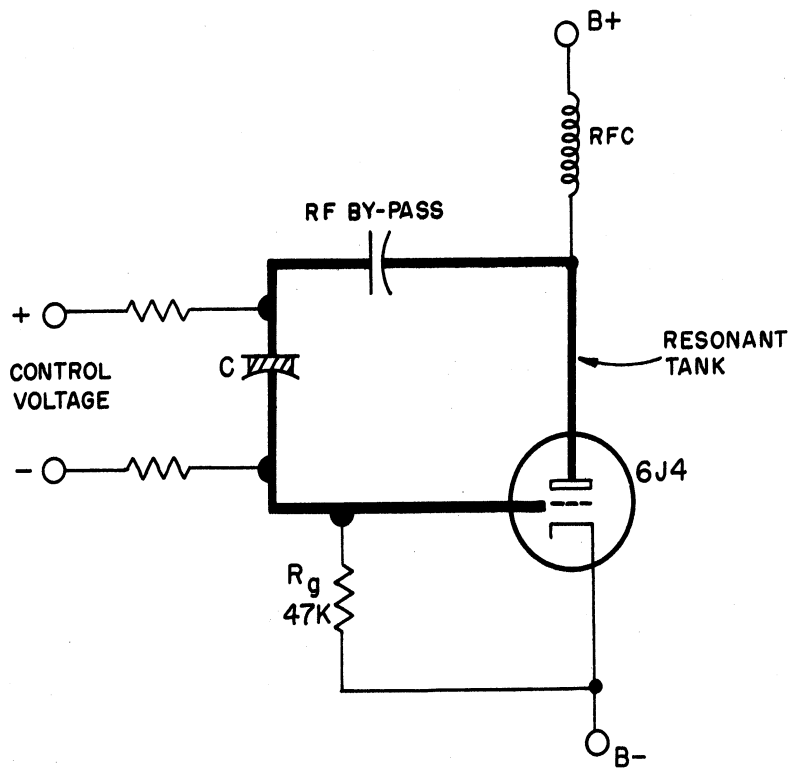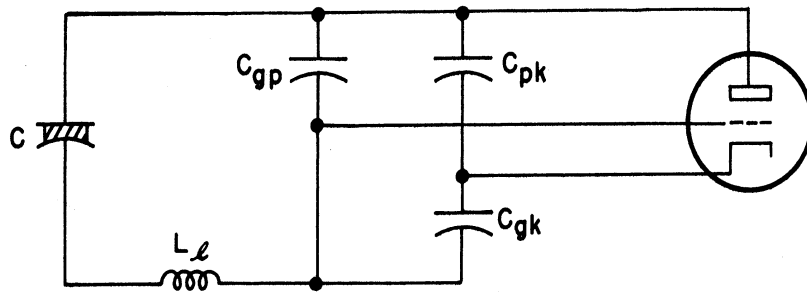
(b) EQUIVALENT CIRCUIT

FIG. 43

ULTRA-AUDION OSCILLATOR.

C and L - are the capacity and inductance of the resonant tank.

G_g - is the input conductance of the grid and grid circuit exclusive of the tank.

For the other oscillators tested, the condition for oscillation has the same general form as relation (7). It has been previously shown that the Q of the ferroelectric capacitors is greatly reduced at the higher frequencies, and for this reason it is necessary to use tubes of high transconductance and tank circuits of large L to C ratio for successful operation in this frequency region. Some of these circuits refuse to oscillate at very high frequencies because of this reduced Q; however, as a bias field is applied to the capacitors, the Q is often improved sufficiently to permit oscillation.[1] It has been observed while varying the field about the point where oscillations begin that the starting field (value at which oscillations start) is larger than the dropout field.

At resonance we find the relation for the circuit:

$$\omega^2 L = \frac{1}{C} + \frac{1}{C'}$$

where

$$C' = C_{gp} + \frac{C_{gk} \cdot C_{pk}}{C_{gk} + C_{pk}} + C_{wiring}$$

(8)

Then by differentiation it follows that:

$$\frac{\delta \omega}{\delta C} = \frac{1}{2C} \cdot \frac{C'}{LC \ (C+C')}$$

(9)

---

[1]See for instance Fig. 3, where it is seen that the Q rises as a polarizing field is applied.

which can be written in the form:

$$\frac{\Delta\omega}{\omega} = -\frac{C'}{2(C+C')} \cdot \frac{\Delta C}{C} \qquad (10)$$

which gives the relation for the percentage frequency change at a given frequency

as a function of the percent of the change in capacity. The latter formula also

shows that for this circuit the optimum tuning condition is for the case where

C, the ferroelectric capacitor, is kept small in relation to C', the circuit and

interelectrode capacities.

3.3 Dielectric Amplifiers

It is possible to build amplifiers with a limited voltage gain but

with high current gain by utilizing the non-linear characteristics of the

titanate dielectrics. The output of such a device is an audio frequency output

signal of higher current than that of the input signal. The dielectric

amplifier, unlike the conventional vacuum tube amplifier, uses an rf power

supply. The signal to be amplified must be lower in frequency than the supply

frequency.

3.3.1 Types of Dielectric Amplifiers. There are two general types

of dielectric amplifiers

(a) <u>Resonant Types</u> - those in which the resonant frequency of one

or more resonant circuits is varied by the input signal being applied to the

non-linear capacitive elements.

(b) <u>Non-Resonant Types</u> - those in which the loop impedence is varied,

but no resonance phenomena are employed.

The resonant type of amplifiers have· large power gain and relatively

large temperature coefficients. The non-resonant types have small power gain and smaller temperature coeffiecients than the resonant types. Despite the lower temperature stability of the resonant types, their large gain makes them attractive. The temperature instability can then be minimized by thermostating or by using temperature compensation in one or more circuit elements.

3.3.2 Tests on Dielectric Amplifiers. Examples of resonant type of dielectric amplifiers are shown in Figs. 44 and 45. Loops 1 and 2 are tuned to resonate at the same frequency for zero audio input, and feed a differential output transformer, T_1, The rf carrier power is applied at a frequency slightly different from the loop resonant frequency. The audio frequency signal alternately drives one loop closer and the other loop farther from resonance. The rf output voltage from the transformer is proportional to the vector difference in the loop currents, I_1 and I_2, and this voltage is demodulated by a diode circuit to produce the audio frequency output.

Sufficient DC bias is applied to the ferroelectric capacitors C_1 and C_2 to establish an operating point near the maximum slope of their C-E curve. Resistors R_1 and R_2 are made sufficiently large so that a negligible amount of audio-input power will be absorbed at the lowest operating frequency.

To prevent audio frequency doubling, the differential transformer is slightly unbalanced, giving some rf output for zero audio input. The adjustment is easily made with an oscilloscope to produce minimum distortion of the amplified signal.

Circuits corresponding to Figs. 44 and 45 were constructed and tested. The circuit of Fig. 45 employs for C_1 and C_2 a pair of 400 $\mu\mu$f Glenco K-3300 bodies as the non-linear elements. The rf power was supplied at a frequency

FIG. 44
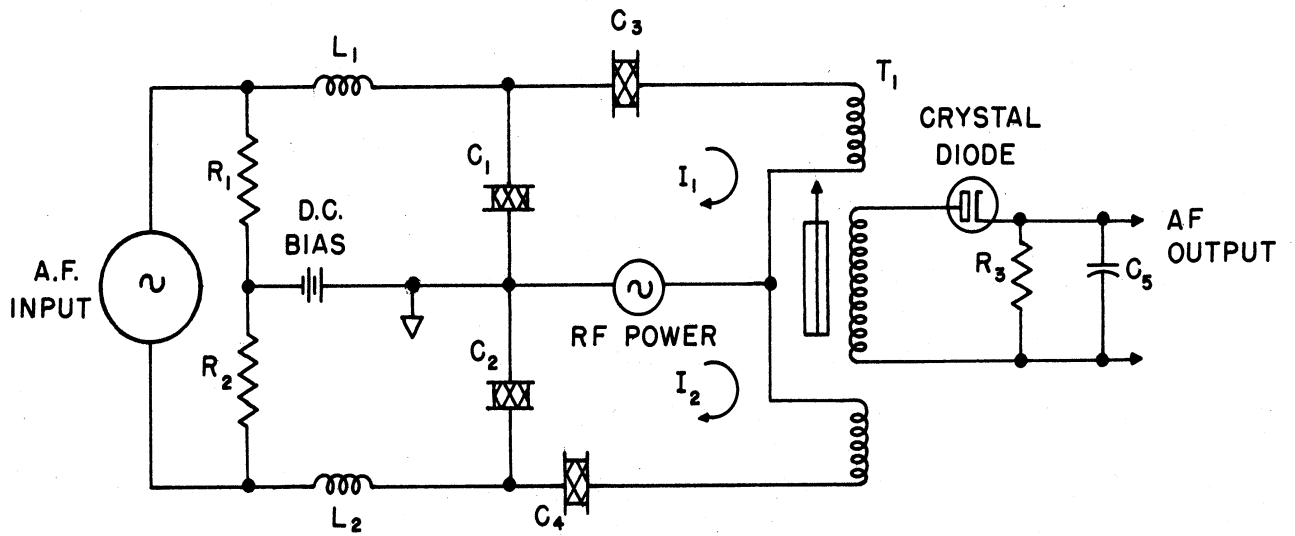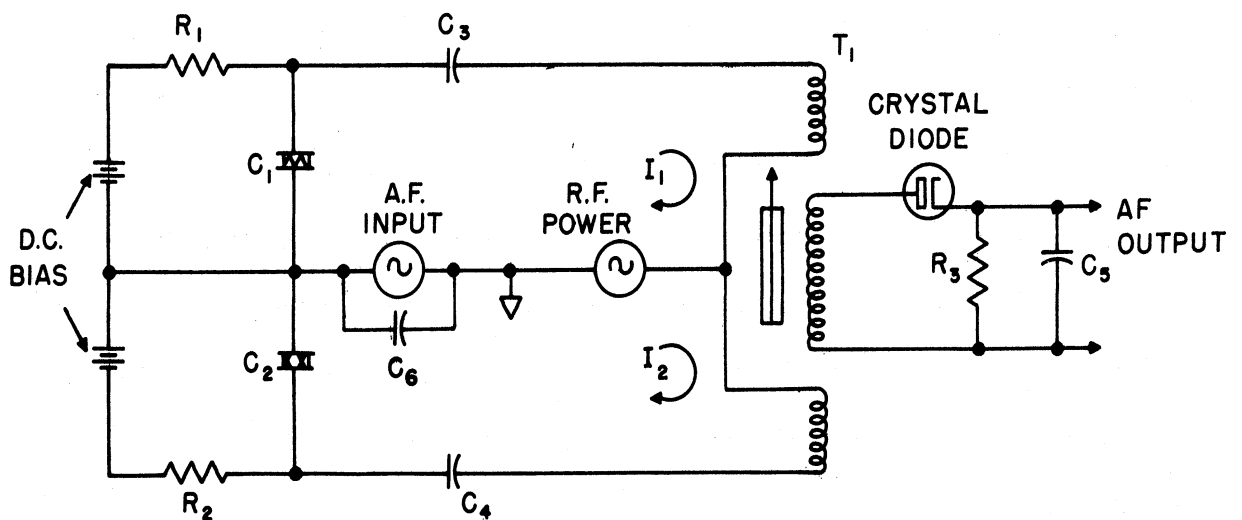
BRIDGE TYPE
RESONANT DIELECTRIC AMPLIFIER.

FIG. 45

SERIES FED
RESONANT DIELECTRIC AMPLIFIER.

80

of 4.5 mc. For this circuit the voltage gain is substantially flat from 20 cps to 20 kc and is about .5 over this range. The current gain is about 170 for low frequency operation.

The output impedence is essentially the resistance, R_3, and has the value of 10,000 ohms, while the input impedence is essentially 3.3 megohms (R_1 and R_2 in parallel) shunted by a capitance of roughly 1,000 $\mu\mu$f. Thus,

$$\text{current gain} = \text{voltage gain} \times \frac{1}{R_3 \ (G+jwC)} \tag{11}$$

where G is the input conductance and C is the input shunt capacitance. This shows the current gain to be essentially flat with a value of 170 up to about 30 cps., and falling off to a half power point of 120 at 50 cps.

Satisfactory results have also been obtained for the amplifier shown in Fig. 44. The values for the components used in this circuit are:

$$R_1 = R_2 = 10 \text{ meg.}$$

$$R_3 = 10 \text{ k}$$

$$L_1 = L_2 = 200 \text{ mhy.}$$

$$C_1 = C_2 = C_3 = C_4 = \text{Glenco K-3300 capacitors 10 mils thick}$$

$$\text{and } 400 \ \mu\mu\text{f at zero bias.}$$

A 1N34 diode was used as a detector. The carrier frequency for the rf supply was 4.5 mc. When the amplifier was operated under these conditions a voltage gain of 1/2 was obtained. The current gain was found to be 33 at 1,000 cps, and since the input is largely capacitive it can be seen that the current gain will increase at lower frequencies. As a DC amplifier with R_1 and R_2 very large, a

very large current gain may be obtained from this circuit.

Because of their high input impedance at low frequencies, dielectric amplifiers are well suited to a number of applications requiring very low level current amplifiers at low frequencies. Because of the small size of the components, they lend themselves well to programs of miniaturization.

It is noted that dielectric materials with large S values (see Table II) result in amplifiers with large power gain. However, large S values are usually associated with large temperature coefficients of capacity so that operation of high gain resonant dielectric amplifiers is quite sensitive to temperature changes. One trick which is very useful in compensating for the temperature effects is to introduce a capacitor with a similar temperature coefficient in the rf power generator so that its frequency is shifted with the temperature by an amount equal to the shift in the resonant frequency of the resonant loops in the amplifier.

A factor which limits the available power output is the rf power which must be dissipated by the non-linear capacitors. Large amounts of rf input power produce overheating of these elements, and the circuit then becomes detuned because of the temperature coefficient of the capacitors. The non-linear elements must therefore be designed for adequate power dissipation.

3.4 The FM Dielectric Amplifier

An interesting amplifier circuit, which also demonstrates the application of ferroelectric materials to comparitively narrow band FM devices is shown in Fig. 46. The unit consists of a variable frequency oscillator followed by a frequency discriminator. The oscillator is a twin triode in push-pull.
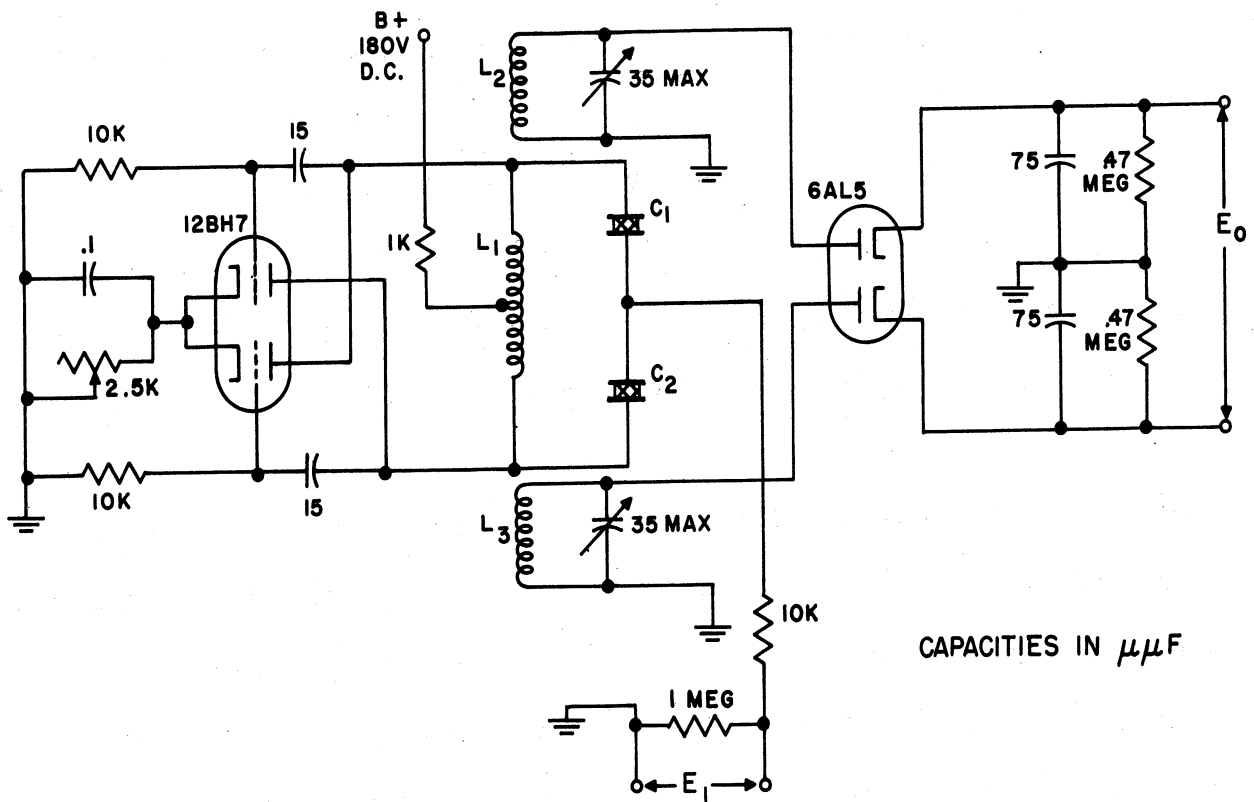
FIG. 46

FM DIELECTRIC AMPLIFIER CIRCUIT.

The oscillating tank L is tuned by a pair of ferroelectric ceramic capacitors, C_1 and C_2, capable of capacity variation with applied field. The capacity variation produced by the audio-frequency input modulates the oscillator. The FM output is discriminated by the high Q tuned circuits, L_2C_4, L_3C_3. The upper circuit is tuned slightly above the carrier center frequency, and the lower circuit, slightly below. The diodes are used to demodulate the signal to produce an audio output.

One model of this circuit was constructed using two pairs of Glenco type SSM capacitors and C_1 and C_2. These are rated at 50 WVc, and have a nominal capacity of 400 $\mu\mu$f each. They employ a 10 mil thick wafer of K-3300 ceramic. A photograph of the amplifier is shown in Fig. 47. The four small ferroelectric capacitors are visible above the coil in the upper center of the photograph.

TThe amplifier operates at a center (carrier) frequency of 5 mc, and gives a voltage gain of 9.0, flat to within one decibel up to 7 kc. An audio output voltage of 40 volts peak can be obtained with less than 5 percent harmonic distortion. The transient response for square wave inputs of 1 kc and 5 kc are shown in Figs. 48a and 48b respectively. Input and output waves are shown on each oscillogram with the same vertical calibration of 10 volts per division.

The amplifier requires a voltage regulated power supply for stable operation since the polarizing bias voltage for C_1 and C_2 is obtained from the B+ line.

The audio frequency response of this circuit is limited by the time constant of the discriminator circuit. It is possible to construct dielectric amplifiers having much wider frequency ranges by a suitable redesign of the circuit time constants. The voltage gain is controlled by the thickness of the dielectric in the oscillator tuning capacitors, and by the sensitivity of the FM discriminator. In addition a voltage gain of 40 to 50 is possible by using

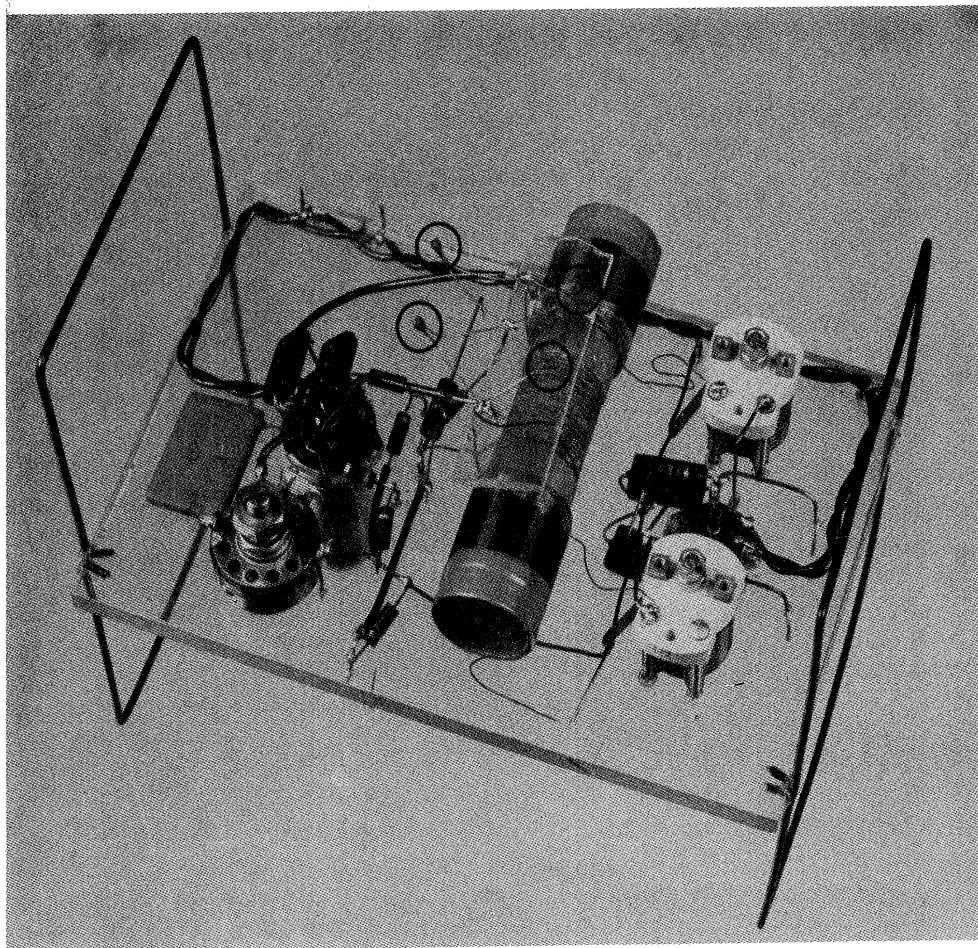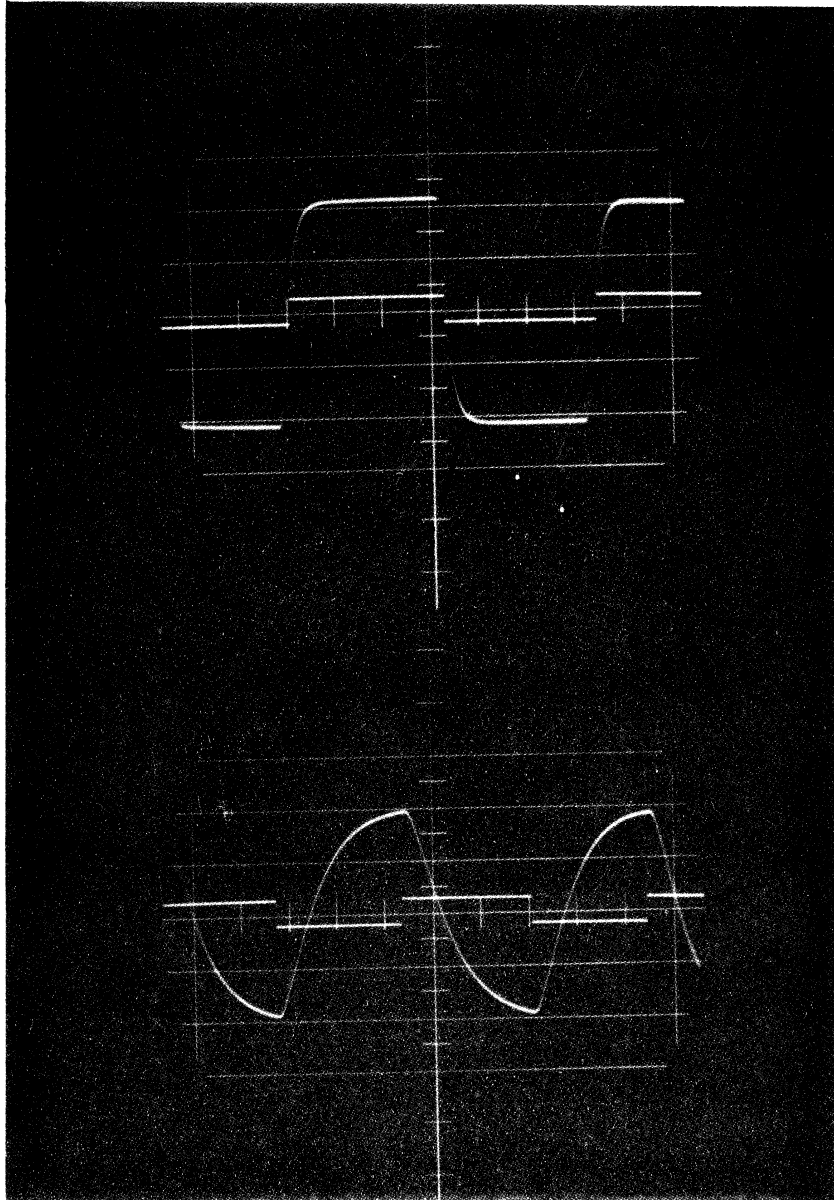FIG. 47

F-M DIELECTRIC AMPLIFIER SHOWING
LUCITE BREADBOARD CONSTRUCTION.

NOTE: DIELECTRIC UNITS SHOWN IN CIRCLES

A.

B.

FIG. 48

TRANSIENT RESPONSE
F - M DIELECTRIC AMPLIFIER.

SQUARE WAVE INPUT FREQUENCIES:
A = 1 KC
B = 5 KC

86

oscillator tuning capacitors made with a 2 mil thick dielectric of the same type. Such thin dielectrics are presently available from the Glenco Corporation.

4. THE NEGATIVE CAPACITY ELEMENT

The maximum range in dielectric tuning is limited by the ratio of the maximum to minimum capacity available from a particular ferroelectric capacitor. Since this ratio is at best of the order of 9, (and for material with this ratio, the temperature effect is quite severe) electric tuning cannot compete in tuning range with ferromagnetic tuning in the low and middle frequency ranges. However, if some method could be found to decrease both the maximum and the minimum capacity of a ferroelectric capacitor by an equal amount, the ratio of the maximum to minimum capacity could be greatly increased.

A negative capacity amplifier may be utilized to perform this service. The input capacitance of this amplifier is negative. If this negative capacity is used in conjunction with a ferroelectric tuned element it may be possible to make tuning elements which will compete with ferromagnetic tuning.

A typical circuit of the negative capacity amplifier is shown in Fig. 49. This is a two stage amplifier with combined positive and negative feedback. The circuit constants are adjusted to produce a negative capacity in the input terminal.

Investigation of the negative capacity circuit alone showed favorable operation up to about 2 mc. At frequencies above 3 mc the input conductance tuned negative, and the unit tended to oscillate strongly.

When the negative capacity amplifier was placed in parallel with a
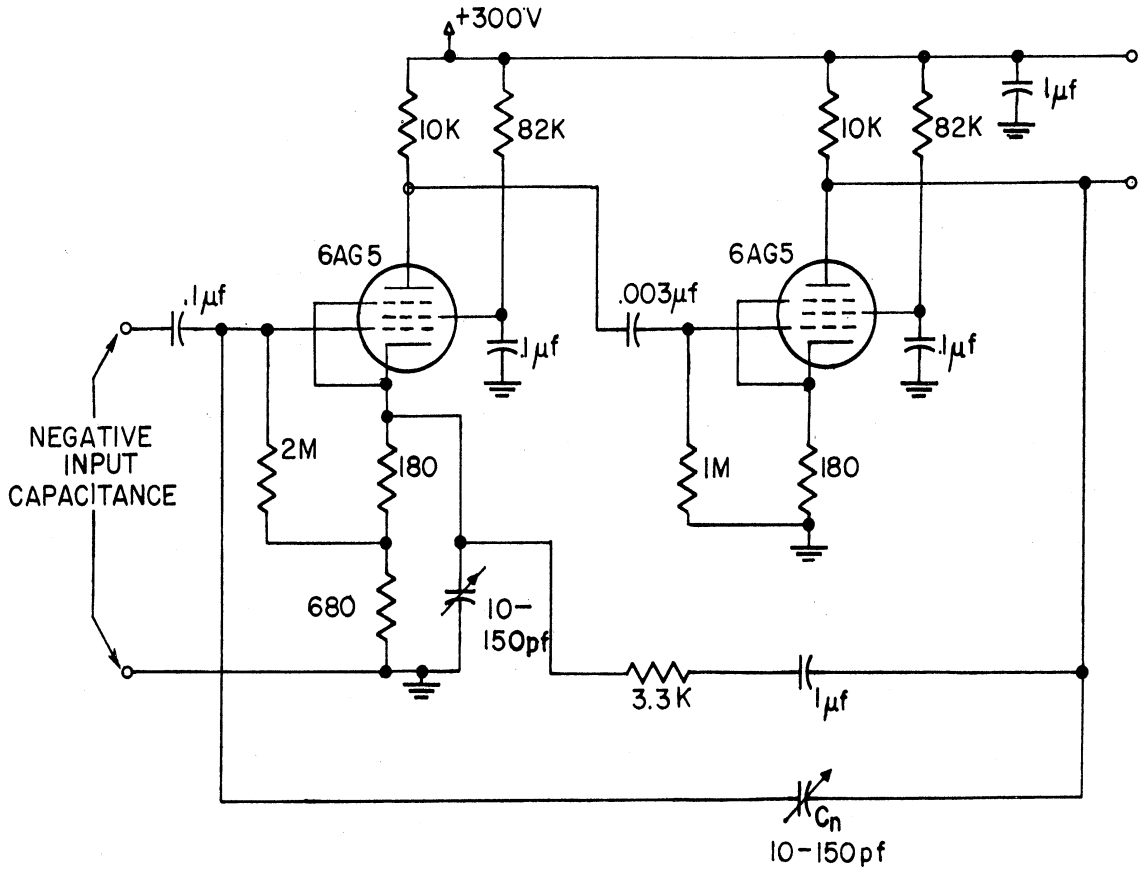
FIG. 49

THE NEGATIVE CAPACITY AMPLIFIER

tank circuit tuned with ferroelectric capacitors the tuning range was indeed

increased. Satisfactory operation was obtained at frequencies up to about 2

mc. However, when the negative capacity circuit was used as part of the tank

circuit of an oscillator, the rf tank voltage had to be limited to prevent over-

loading the input of the negative capacity circuit.

Full details regarding the negative capacity amplifier as a circuit

element will appear in Technical Report No. 33, which is now being prepared

This report will be published in the near future.

5. CONCLUSIONS

This report has summarized the work to date of a continuing investi-

gation of basic properties and applications of ferroelectric materials with

particular emphasis on electric tuning of rf components.

Measured properties of ceramic and single crystal materials confirm

those found by the other investigators, and a number of other important effects,

such as Barkhausen noise, polarization lag, and double hysteresis loops in

titanate ceramics are discussed.

An important effect is obtained when silver electrodes are applied by

vacuum evaporation. This results in reduced losses both in titanate ceramic

specimens and single crystals.

The variations of dielectric constant are shown for a number of repre-

sentative materials by the use of epsilon-temperature surfaces, butterfly loops

and tuning curves. Such plots are extremely useful in the design of ferroelectric

devices. The devices described show that ferroelectric materials have practical

applications at all frequencies up to at least 375 mc.

Because of temperature sensitivity of these materials, some form of temperature control is considered essential in most applications, but because of the very small size of the capacitor units, this is not considered a major difficulty.

DISTRIBUTION LIST

1 copy	Director, Electronic Research Laboratory Stanford University Stanford, California Attn: Dean Fred Terman
1 copy	Commanding Officer Signal Corps Electronic Warfare Center Fort Monmouth, New Jersey
1 copy	Chief, Engineering and Technical Division Office of the Chief Signal Officer Department of the Army Washington 25, D. C. Attn: SIGJM
1 copy	Chief, Plans and Operations Division Office of the Chief Signal Officer Washington 25, D. C. Attn: SIGOP-5
1 copy	Countermeasures Laboratory Gilfillan Brothers, Inc. 1815 Venice Blvd. Los Angeles 6, California
1 copy	Commanding Officer White Sands Signal Corps Agency White Sands Proving Ground Las Cruces, New Mexico Attn: SIGWS-CM
1 copy	Commanding Officer Signal Corps Electronics Research Unit 9560th TSU Mountain View, California
75 copies	Transportation Officer, SCEL Evans Signal Laboratory Building No. 42, Belmar, New Jersey **FOR - SCEL Accountable Officer** **Inspect at Destination** **File No. 22824-PH-54-91(1701)**

1 copy	H. W. Welch, Jr Engineering Research Institute University of Michigan Ann Arbor, Michigan
1 copy	Document Room Willow Run Research Center University of Michigan Willow Run, Michigan
10 copies	Electronic Defense Group Project File University of Michigan Ann Arbor, Michigan
1 copy	Engineering Research Institute Project File University of Michigan Ann Arbor, Michigan